BIOSYNTHETIC MECHANISMS OF LTA-TYPE EPOXIDES AND NOVEL BIOACTIVE LIPID MEDIATORS

By

Jing Jin

Dissertation

Submitted to the Faculty of the

Graduate School of Vanderbilt University

in partial fulfillment of the requirements

for the degree of

DOCTOR OF PHILOSOPHY

in

Pharmacology

December, 2013

Nashville, Tennessee

Approved:

Professor Alan R. Brash

Professor Claus Schneider

Professor Sean S. Davies

Professor David L. Hachey

Professor Ned A. Porter

ACKNOWLEDGMENTS

I am especially grateful to my professor, Dr. Alan Brash, who has provided exceptional mentoring through my Ph.D. study. He has incomparable knowledge in the research field and pays close attention to important experimental details, setting a high standard of being an excellent scientist in my mind. Without his consistent guidance, this dissertation would not have become possible.

I would like to thank my committee members, Dr. Claus Schneider, Dr. Sean Davies, Dr. David Hachey and Dr. Ned Porter, for their excellent suggestions over the years. Many thanks go to William Boeglin in the lab who provided countless technical support in protein expression and NMR analysis. I am thankful to Dr. Yuxiang Zheng for her insightful comments on the projects as well as her help in my adapting to the lab during the very beginning period.

Nobody has been more important in my pursuit of Ph.D. degree than the members of my family. I wish to thank my parents who provide selfless support through every stage of my career. Most importantly, I would like to thank my loving and supportive wife Danye, and my wonderful daughter Lingxi who provided me courage and motivation.

TABLE OF CONTENTS

ACKNOWLEDGEMENTS ii

LIST OF FIGURES v

LIST OF ABBREVATIONS ix

Chapter

I INTRODUCTION 1

Lipoxygenase catalysis 1
Secondary metabolism of fatty acid hydroperoxides by lipoxygenases 3
Leukotriene biosynthesis 6
Lipoxygenase and LTA-type epoxides 9
Dual role of lipoxygenase iron in LTA biosynthesis 12
Anti-inflammatory and pro-resolution lipid mediators 15
Our hypotheses about LTA-type epoxide formation 17
Overall objectives of the dissertation study 20

II BIOSYNTHESIS, ISOLATION, AND NMR ANALYSIS OF LEUKOTRIENE A EPOXIDE 21

Introduction 21
Experimental procedures 24
Results 26
Discussion 38

III BIOSYNTHETIC MECHANISMS OF LEUKOTRIENE A EPOXIDE: DUAL ROLE OF LIPOXYGENASE IRON 41

Introduction 41
Experimental procedures 47
Results 50
Discussion 66

IV LTA-TYPE EPOXIDES IN RESOLVIN, PROTECTIN, AND MARESIN BIOSYNTHESIS 71

Introduction 71
Experimental procedures 79
Results 82
Discussion 97

V 8*R*-LIPOXYGENASE-CATALYZED SYNTHESIS OF A PROMINENT *CIS*-EPOXYALCOHOL 99

Introduction 99
Experimental procedures 101
Results 105
Discussion 115

VI A POTENTIAL ROUTE TO HNE-LIKE ALDEHYDES VIA LIPOXYGENASE-CATALYZED SYNTHESIS OF A BIS-ALLYLIC DIHYDROPEROXIDE INTERMEDIATE 118

Introduction 118
Experimental procedures 121
Results 124
Discussion 139

VII PARTIALLY RESOLVED ISSUES AND OPEN QUESTIONS 143

VIII SUMMARY 157

REFERENCES 161

LIST OF FIGURES

Figure Page

1. The catalytic cycle of lipoxygenase reaction 2

2. Leukotriene pathway....7

3. Formation of *trans*- or *cis*- LTA_4 by different lipoxygenases 12

4. Evidence for a dual role of lipoxygenase iron in epoxide synthesis 14

5. Bioactive lipid mediators derived from polyunsaturated fatty acids (PUFAs)....16

6. Hypothesis of the mechanistic basis for formation of *cis* or *trans* LTA epoxides 19

7. Coomassie Blue staining of cell homogenates and purified human 15-LOX-1 26

8. RP-HPLC of the reaction of arachidonic acid with human 15-LOX-1 28

9. UV analysis of LTA epoxide formation under biphasic reaction conditions 29

10. RP-HPLC analysis of the reaction of 15-LOX-1 with 15*S*-HPETE....31

11. SP-HPLC analysis of the reaction of 15-LOX-1 with 15*S*-HPETE 32

12. NMR analysis of 14,15-LTA_4 methyl ester 34

13. RP-HPLC analysis of the aqueous phase from the biphasic reaction between 15*S*-HPETE and human 15-LOX-1 36

14. RP-HPLC of the acid-induced hydrolysis of 14,15-LTA_4 methyl ester....37

15. Overview of the biphasic synthesis and simultaneous extraction methods....38

16. Summary of reactions of the enantiomeric fatty acid hydroperoxides with different lipoxygenases 43

17. RP-HPLC of reactions of 15*S*-HPETE with human 15-LOX-1 50

18. Chiral HPLC of purified 5*R*-HPETE 53

19. RP-HPLC of Arabidopsis AtLOX1 incubations with 5*S*-HPETE or 5*R*-HPETE 55

20. UV spectrum of 5*S*-HPETE and 5*R*-HPETE in hexane before and after vortex mixing with 5-LOX enzyme (AtLOX1) 56

21. RP-HPLC analyses of the product methyl esters from 5*S*-HPETE and 5*R*-HPETE ...57

22. GC/MS analysis of 5-oxo-ETE TMS ester methoxime derivative 58

23. Proton chemical shifts and coupling constants for LTA methyl ester and 5,6-*cis*-LTA methyl ester in C6D6 59

24. Partial ^{1}H-NMR spectrum (2.45 – 3.25 ppm) of the *trans*-LTA epoxide product from 5*S*-HPETE and the *cis*-LTA epoxide product from 5*R*-HPETE....60

25. Spectral comparison of LTA_4 and 5-*epi*-LTA_4....61

26. RP-HPLC of incubation of racemic 5-HPETE with 8*R*-LOX....62

27. RP-HPLC analysis of the product methyl esters from the biphasic reaction of 15*R*-HPETE with human 15-LOX-1 63

28. Dehydration of fatty acid hydroperoxide to keto derivative by lipoxygenase....67

29. Lipoxygenase-catalyzed transformations to LTA epoxides involve a dual role of the lipoxygenase non-heme iron....69

30. Biosynthesis of novel SPMs from EPA....73

31. Biosynthesis of novel SPMs from DHA....73

32. RP-HPLC analysis of the reaction of 17*S*-HP-DHA with human 15-LOX-1 82

33. RP-HPLC analysis of the reaction of 15*S*-HP-EPA with human 15- LOX-1 84

34. UV analysis of LTA epoxide formation from 17S-HP-DHA with human 15-LOX-1 under biphasic reaction conditions....86

35. RP-HPLC analysis of the reaction of 15-LOX-1 with 17*S*-HP-DHA 87

36. NMR analysis of 16,17-LTA_6 methyl ester 89

37. UV analysis of LTA epoxide formation from 15*S*-HP-EPA with human 15-LOX-1 under biphasic reaction conditions....90

38. SP-HPLC analysis of the reaction of 15-LOX-1 with 15*S*-HPETE 91

39. NMR analysis of 14,15-LTA_5 methyl ester 93

40. RP-HPLC analysis of the incubation of DHA and 17*S*-HP-DHA with mouse resident peritoneal macrophages....94

41. RP-HPLC analysis of the incubation of 15*S*-HP-EPA with mouse resident peritoneal macrophages 95

42. RP-HPLC analysis of products formed from 20:3ω6 and 20:4ω6 in homogenates of *P. homomalla* 105

43. GC-MS of the epoxyalcohol 8,9-epoxy-10-hydroxy-eicosadienoic acid 106

44. Partial ^{1}H-NMR spectra of the hydrogenated *P. homomalla* product from C20:3ω6 with *erythro* and *threo* fatty acid standards 109

45. Biosynthesis from 20:4ω6 and 20:3ω6 in *P. homomalla* 110

46. RP-HPLC analysis of products formed from 20:3ω6 and 20:4ω6 by two purified 8*R*-lipoxygenases 113

47. Mass spectrometric analysis of 8*R*-LOX-catalyzed transformation of [^{18}O]8*R*-HPETrE to epoxyalcohol 114

48. Mechanism of 8*R*-LOX-catalyzed epoxyalcohol synthesis from 8*R*-HPETrE 117

49. Bis-allylic fatty acid hydroperoxide and its cleavage to a 4-hydro(pero)xy-alkenal 119

50. RP-HPLC analysis of reaction of arachidonic acid with 8*R*-LOX 124

51. ^{1}H-NMR spectrum of 5-oxo-hept-6-enoic acid 125

52. COSY NMR spectrum of 7-oxo-hept-5*E*-enoic acid 126

53. GC-MS and NMR analyses of 8*R*-hydroperoxy-11-oxo-undeca-5*Z*,9*E*-dienoic acid 127

54. RP-HPLC analysis of on-ice incubation of arachidonic acid with 8*R*-LOX 130

55. Overlay of the UV spectra of 8*R*-HPETE and 8,11-diHPETE 131

56. GC-MS analysis of the TMS ester TMS ether derivative of the TPP-reduced hydrogenated 8,11-diHPETE 132

57. Conversion of purified 8,11-diHPETE to peaks 1 and 2 133

58. Scheme of 8*R*-LOX reactions with 9*E*,11*Z*,14*Z*-C20:3 134

59. GC-MS analysis of TMS ether TMS ester of TPP-reduced hydrogenated 11-hydroperoxy-C20:3 135

60. Chiral phase-HPLC analysis of PFB ester of TPP-reduced hydrogenated 11-hydroperoxyl C20:3 136

61. RP-HPLC analyses of room temperature reactions of 15*S*-HPETE with mouse platelet-type 12*S*-LOX (top) and human 15-LOX-1 (below) 137

62. Overlay of the UV spectra of 8*R*,11*R*-HPETE and 12*S*,15*S*-diHPETE.....138

63. Proposed routes of formation of compound **2**.....141

64. Reactive aldehyde formation in lipid peroxidation.....143

65. Dimer formation in lipid autoxidation.....144

66. LC-MS analysis of dimeric fractions before and after TPP treatment.....145

67. Standard curve of HNE/HPNE quantification by LC-MS.....147

68. H(P)NE production from autoxidation of dimers and pure 13*S*-HPODE.....148

69. H(P)NE production from autoxidation of dimers and pure 13*S*-HPODE in the presence of excess oleic acid.....149

70. HPNE and 13*S*-HPODE distribution on LH20 column.....150

71. LTA synthase activity of 15-LOX proposed by R. C. Murphy.....152

72. RP-HPLC analyses of the organic phase of biphasic reactions of enantiomeric 5-HPETEs with human 15-LOX-1.....155

LIST OF ABBREVIATIONS

AA	arachidonic acid
DHA	docosahexaenoic acid
diHP(E)TE	dihydro(pero)xyeicosatetraenoic acid
eLOX3	epidermal lipoxygenase-3
EPA	eicosapentaenoic acid
4-H(P)NE	4-hydro(pero)xy-2*E*-nonenal
GC-MS	gas chromatography mass spectrometry
H(P)ETE	hydro(pero)xyeicosatetraenoic acid
H(P)ODE	hydro(pero)xyoctadecadienoic acid
KETE	ketoeicosatetraenoic acid
LA	linoleic acid
LT	leukotriene
LX	lipoxin
FA	fatty acid
LC-MS	liquid chromatography mass spectrometry
LOX	lipoxygenase
NDGA	nordihydroguaiaretic acid
NMR	nuclear magnetic resonance
PD	protectin
PFB	pentafluorobenzyl
PG	prostaglandin

ROOH or LOOH	fatty acid hydroperoxide
RP-HPLC	reversed phase high pressure liquid chromatography
Rv	resolvin
SP-HPLC	straight phase high pressure liquid chromatography
TPP	triphenylphosphine
UV	ultraviolet

CHAPTER I

INTRODUCTION

Lipoxygenase catalysis

Widely expressed in plants, fungi, and animals, lipoxygenases (LOX) are a family of non-heme iron dioxygenases that catalyze the hydroperoxidation of polyunsaturated fatty acids (1). The hydroperoxide product (or its reduced hydroxy derivative) could be the end product in a pathway or act as an intermediate leading to the formation of other bioactive secondary metabolites (2-4).

All lipoxygenases are a single polypeptide of 75-105 kD with one iron atom. The hydroperoxidation reaction catalyzed by lipoxygenase depends on the presence of this non-heme iron. The ferric state of the non-heme iron Fe^{3+} accounts for the oxygenation activity, while as the lipoxygenase is isolated the enzyme contains predominantly the ferrous iron Fe^{2+}. It is the non-enzymatic oxidation of the substrate and the enzymatic oxidation catalyzed by a small amount of initially existing Fe^{3+} that forms fatty acid hydroperoxide which oxidizes the Fe^{2+} to Fe^{3+} and activates the enzyme (5,6). The same catalytic mechanism is proposed for all non-heme iron lipoxygenases (7). Briefly, the active form Fe^{3+}, covalently linked with one of its six ligands, a hydroxide ion, abstracts a hydrogen atom from the fatty acid substrate, forming a Fe^{2+}-H_2O complex and a fatty acid radical. The fatty acid radical then combines with a triplet O_2 to form a peroxy radical. Finally, the peroxy radical obtains the hydrogen atom back from the Fe^{2+}-H_2O

complex, forming the hydroperoxide product and regenerating the ferric enzyme, thus completing a catalytic cycle (**Figure 1**).

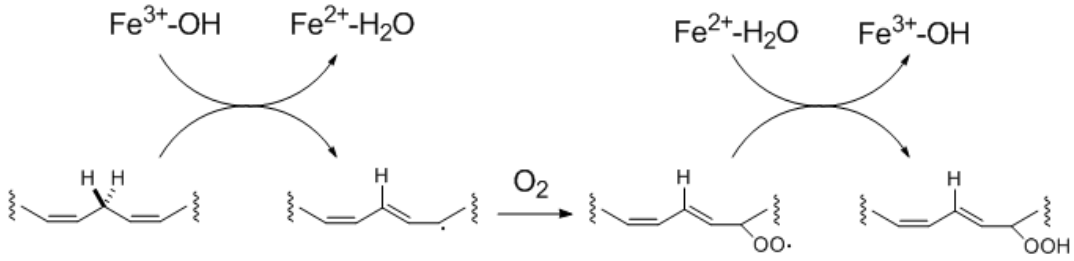

Figure 1: The catalytic cycle of lipoxygenase reaction

A remarkable feature of lipoxygenase catalysis is that the incorporation of molecular oxygen is regio- and stereo- specific (8). The suitable substrates for lipoxygenase catalysis contain at least one 1*Z*,4*Z*-pentadiene unit. Lipoxygenase initiates a stereoselective hydrogen abstraction from the methylene carbon of a selected 1*Z*,4*Z*-pentadiene unit (9). In the second step, out of the four available positions around the 1*Z*,4*Z*-pentadiene, region-selective oxygen addition occurs on the opposite face of the substrate (relative to the abstracted hydrogen), thus forming a single optically active hydroperoxide product after acceptance of a hydrogen. To accomplish these catalytic specificities, lipoxygenase has two levels of control: (1) Lipoxygenase-substrate interaction holds the substrate in a position that only one selected bis-allylic hydrogen is in proximity to the non-heme iron and thus accessible for abstraction. In this respect, soybean lipoxygenase-1 is a "clean" 15-lipoxygenase, which, at low enzyme concentrations, only abstracts 13L hydrogen and forms 15*S*-HPETE from arachidonic acid. By contrast, human reticulocyte 15-LOX (15-LOX-1) is not a "pure" 15-

lipoxygenase. It forms a mixture of 12*S*-HPETE and 15*S*-HPETE after abstracting the 10L and 13L hydrogen respectively (10). In the case of human 15-LOX-1, a carbon chain frame shift is allowed within the enzyme active site. (2) Lipoxygenase controls the molecular oxygen to the one of four available carbon positions (8,11,12). There are debates on how molecular oxygen access is controlled. Different mechanisms have been proposed, including steric shielding of oxygen by amino acid residues that ensures only one of the active pentadienyl radical is accessible and oxygen channeling that directs the molecular oxygen to the desired position (8).

Secondary metabolism of fatty acid hydroperoxides by lipoxygenases

In addition to polyunsaturated fatty acids, lipoxygenase enzymes also react with fatty acid hydroperoxides, the products from their own oxygenation reactions. Secondary conversion of fatty acid hydroperoxide is initiated by either the ferric or ferrous enzyme. Ferric enzyme starts the secondary oxygenation on the mono-hydroperoxide product by abstracting a different methylene hydrogen in a different 1*Z*,4*Z*-pentadiene unit. Ferrous enzyme, by catalyzing the homolytic cleavage of the hydroperoxide group, initiates the reaction cycle acting as a hydroperoxide isomerase or a hydroperoxide peroxidase. In order for the secondary metabolites to be significantly formed, the secondary transformation needs to be a self-propagating catalytic reaction rather than a single turnover, i.e. the ferric and ferrous enzyme need to cycle between each other constantly. For example, the typical dioxygenase activity of lipoxygenase enzymes involves activation of the resting ferrous enzyme to the ferric form. The ferrous enzyme is activated by a trace amount of fatty acid hydroperoxides present in the starting substrate.

Once the ferrous enzyme is oxidized to the ferric form, it will no longer react with the fatty acid hydroperoxide. Due to this single turnover nature of the reaction, the product during this activation phase is not formed in sufficient amounts for detection and identification (13).

Possible secondary metabolic routes of fatty acid hydroperoxides by lipoxygenases include:

1) Leukotriene pathway: 5*S*-HPETE is transformed by 5-lipoxygenase to conjugated triene-containing allylic epoxide leukotriene A_4 which is further enzymatically converted to bioactive leukotriene family members (3).

2) Epoxyalcohol synthesis: the hydroperoxide isomerase (epoxyalcohol synthase) activity of epidermal lipoxygenase-3 (eLOX-3) converts 12*R*-HPETE (the natural product by 12*R*-LOX, another lipoxygenase expressed in skin) to 8*R*,11*R*,12*R*-epoxyalcohol (14). Epoxyalcohols are chemically unstable and will be hydrolyzed to trihydroxy hydrolysis products either non-enzymatically or by the epoxide hydrolase (15,16).

3) Short chain aldehyde formation: the secondary hydroperoxide cleavage is well investigated and occurs in higher plants and animals as well as in algae (2,17,18). Whereas in higher plants the formation of cleavage products requires the combined action of lipoxygenase and hydroperoxide lyases (HPL) (19,20), in animals and algae the specific lipoxygenase alone is sufficient (21).

4) Double oxygenation, i.e. a second oxygenation on the primary hydroperoxide product: the dihydroperoxide is readily reduced to the dihydroxide in a physiological environment in which the hydroperoxide peroxidases are abundant. The first identified

anti-inflammatory lipoxins also originate from the sequential oxygenation by two different lipoxygenase followed by LTA-type reaction (3,22).

5) Keto derivative formation: it is well established that 5-HETE (reduced form of 5-HPETE) is oxidized to 5-oxo-ETE (5-oxo-eicosatetraenoic acid) by 5-hydroxyeicosanoid dehydrogenase (23). Our studies show that keto derivative could be directly produced from fatty acid hydroperoxide by lipoxygenase. Instead of being involved in metabolic inactivation, the keto derivative of a fatty acid hydroperoxide could function as a highly potent chemoattractant (24) or an electrophile which is to adduct with the nucleophilic amino acid residues in the biologically important proteins (25,26).

There is competition between the different secondary metabolic routes of fatty acid hydroperoxide. Several lines of evidence suggest that access of molecular oxygen within the lipoxygenase active site is an important determinant of the metabolic fate of hydroperoxides (13). If present, molecular oxygen reacts readily with radical intermediates, thus intercepting and blocking hydroperoxide isomerase or hydroperoxide peroxidase cycling. Furthermore, molecular oxygen promotes enzyme activation to the ferric form, also inhibiting other metabolic routes initiated by the ferrous enzyme (27,28). Based on the product profiles with fatty acid and fatty acid hydroperoxides, it is proposed that epidermal lipoxygenase-3 (eLOX-3) represents one end of a spectrum among lipoxygenases where oxygen concentration within active site is low, favoring hydroperoxide isomerase cycling, with the opposite end represented by soybean LOX-1 which has high active site oxygen concentration and favors dioxygenation reactions. Following this line of thinking, it is possible to manipulate the lipoxygenase reaction outcome with fatty acid hydroperoxide substrates by controlling the molecular oxygen

concentration within the reaction environment. By making the reaction conditions anaerobic, soybean LOX-1, which mainly catalyzes dioxygenation reactions, will produce instead ketones, aldehydes, fatty acid dimers (29) and products formed through transformation to allylic epoxides (30).

Leukotriene biosynthesis

The leukotrienes (LTs) are a family of lipid mediators implicated in host defense and pathophysiological conditions such as inflammation and immediate hypersensitivity (31,32). The term "leukotriene" was chosen because they were first discovered in the incubation of arachidonic acid with rabbit peritoneal polymorphonuclear leukocytes (PMNL) and their common structural feature is a conjugated triene (33-36). Based on whether they are conjugated with a peptide as well as their biological effects, leukotrienes can be sub-divided to the dihydroxy leukotriene LTB_4 and the cysteinyl leukotrienes LTC_4, LTD_4 and LTE_4. Concerning their biological activity, LTB_4 specifically stimulates a number of leukocyte functions, including the adhesion of leukocytes to the endothelium in blood vessels and the infiltration of leukocytes to the tissue (3,37). Furthermore, LTB_4 increases microvascular permeability that facilities the emigration of leukocytes from the bloodstream (3). On the other hand, cysteinyl leukotrienes (LTC_4, LTD_4 and LTE_4), also known as slow-reacting substance of anaphylaxis (SRS-A), primarily target smooth muscle and other cells with contractile ability. When acting on airway smooth muscle, they potently induce airway constriction and cause asthma. When given systemically, they increase permeability in postcapillary venules (3,32).

Around 1980, extensive studies were performed on the structural elucidation of LTB_4 and LTC_4 as well as an appreciation of their formation through the epoxide LTA_4 (38-41). The biosynthetic pathway of leukotriene family is now well-established. Arachidonic acid is first released from membrane phospholipids by cytosolic phospholipase A_2 (cPLA2) upon cell stimulation. Once released, arachidonic acid is converted to an extremely short-lived intermediate LTA_4 which is enzymatically converted by hydration to the dihydroxy acid LTB_4 and by addition of glutathione to cysteinyl LTC_4 (**Figure 2**). LTC_4 is metabolized to LTD_4 and LTE_4 by successive elimination of a γ-glutamyl residue and glycine (3,4).

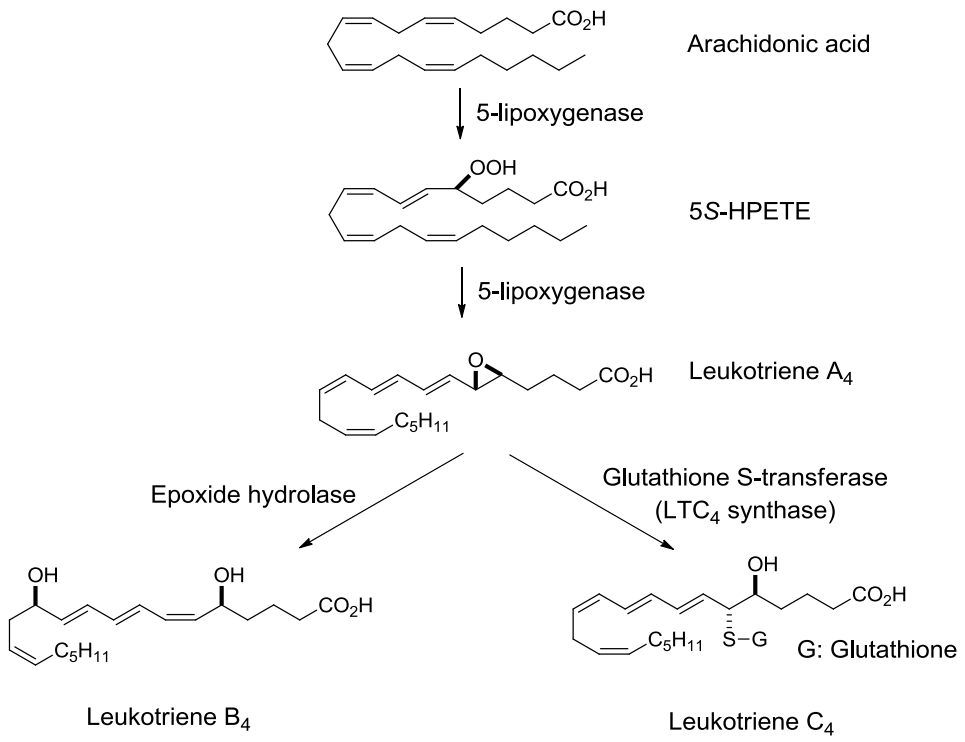

Figure 2: Leukotriene pathway

It was not self-evident that it is the unstable allylic epoxide LTA_4 that leads to the formation of stable bioactive lipids in the metabolism of arachidonic acid. First, an intermediate in the transformation was proposed with the aid of isotopic oxygen, and it was shown that the oxygen of the alcohol group at C5 of LTB_4 originated from molecular oxygen, whereas the oxygen of the alcohol group at C12 was derived from water (42). The epoxide identity of the intermediate was further established by trapping the intermediate with excess alcohol and analysis of the obtained derivatives showed that they carried hydroxyl groups at C5 and isomeric methoxy groups at C12 (42). It is now known that the enzymatic transformation from LTA_4 to stable end products bears the nature of nucleophilic attack on the unstable allylic epoxide by either the water or the cysteinyl group of a peptide.

The extreme instability in the aqueous solution at physiological pH is the major hurdle preventing studies on LTA_4. Its half-life in physiological buffer at pH 7.4 is estimated as approximately 3 s at 25 °C and 18 s at 4 °C (43). In the aqueous reaction systems especially those with an acidic pH, LTA_4, once formed, readily reacts with water and gives the formation of two 5*S*,12-dihydroxy-6,8,10-*trans*,14-*cis*-eicosatetraenoic acids, epimeric at C12 and two 5*S*,6-dihydroxy-7,9-*trans*-11,14-*cis*-eicosatetraenoic acids, epimeric at C6. Unlike the enzymatic conversion to LTB_4, the non-enzymatic hydrolysis of LTA_4 is through a common carbonium ion intermediate. These hydrolysis products have a characteristic UV chromophore which is distinct from that of LTB_4 (35). Even nowadays, due to the high instability of LTA epoxide, detection of its hydrolysis products becomes a reliable and acceptable way demonstrating the formation of LTA epoxide. Despite its instability, LTA_4 was still detected as an evanescent intermediate in

short-term incubations of arachidonic acid with human leukocytes (44). This was achieved by subjecting the isolation under alkaline conditions and in an aprotic solvent which were expected to increase the LTA epoxide stability. Furthermore, to explain its persistence as an intact allylic epoxide in a physiological environment, there were studies showing that albumin could stabilize LTA_4 by providing a hydrophobic and alkaline microenvironment (43).

Extensive efforts were directed towards the total synthesis of LTA_4 and its closely related 5,6-epoxide isomers after its pivotal role was realized (45,46). By comparison of the reactions of natural LTA_4 and synthetic LTA_4 and related isomers in transformation to the stable LTB_4 and LTC_4, the structure of LTA_4 was defined unequivocally as 5*S*,6*S*-trans-epoxy-eicosa-7*E*,9*E*,11*Z*,14*Z*-tetraenoic acid (40). It is important to recognize here that the stereochemistry of LTA epoxide has never been characterized directly from a natural LTA product. Performing comparison with synthetic standards is a classic approach, which researchers in the field still employ, to determine the stereoconfiguration of the natural eicosanoid product.

Lipoxygenase and LTA-type epoxides

The understanding of the leukotriene pathway took another leap forward when it was appreciated that 5-lipoxygenase (5-LOX) catalyzes not only the conversion of arachidonic acid to 5*S*-hydroperoxyeicosatetraenoic acid (5*S*-HPETE) but also the further transformation to the pivotal epoxide in the pathway LTA_4. Before 5-lipoxygenase was demonstrated to have LTA_4 synthase activity (epoxide synthase activity), it was noticed that LTA syntheses share some mechanistic features with lipoxygenase reactions (47,48).

1) Both reactions entail a stereospecific hydrogen removal. In the case of LTA_4 formation by human leukocytes, the D_R hydrogen is stereoselectively removed from the prochiral center at C10 of arachidonic acid (49). In the formation of 14,15-LTA_4, an analogue of LTA_4, the L_S hydrogen at C10 of arachidonic acid is abstracted (47). Importantly, the $10L_S$ hydrogen abstraction is also the initial event of the platelet 12-lipoxygenase catalysis that leads to the formation of 12*S*-HPETE with arachidonic acid as the substrate (50). 2) Both reactions entail a radical migration that leads to formation of new *trans* double bond(s). In the case of LTA formation, the radical, which is generated after hydrogen abstraction, undergoes a [1,5] migration which leads to the formation of two *trans* double bonds. In a lipoxygenase dioxygenation reaction, the radical undergoes a [1,3] migration that leads to the formation of one *trans* double bond. Based on these similarities, both this lab and the group from the Karolinska Institute made the assumption that leukotriene epoxide biosynthesis bears a lipoxygenase-like mechanism. The lipoxygenase nature of leukotriene epoxide synthase was finally established with the native 5-lipoxygenase isolated from potatoes, murine mast cells and human leukocytes as well as the expression of the recombinant 5-lipoxygenase in various biological systems (48,51-53).

With an appreciation of leukotriene biosynthesis as a model, several other pathways of leukotriene biosynthesis were established. The second leukotriene pathway was discovered in porcine leukocytes that proceeds from 15*S*-HPETE via an analogue of LTA_4 (54,55), 14,15-LTA_4 which is now named eoxin A_4, precursor of the proinflammatory eoxins (EXC_4, EXD_4, $EXE_{4)}$ of human eosinophils in asthma (56,57). Theoretically, a proper combination of fatty acid hydroperoxide substrate and

lipoxygenase catalyst could possibly generate a stereo- and regio- selective LTA epoxide product. However, in practice, whether such a reaction proceeds as expected depends on a number of factors that will be discussed in the later sections. Furthermore, testing reactions of different combinations of fatty acid hydroperoxides and lipoxygenase enzymes not only helps to identify novel bioactive lipid mediators but could further our understanding of LTA biosynthetic mechanism as well as the lipoxygenase biochemistry.

Since the epoxide configuration of LTA_4 derived from 5*S*-HPETE was established as *trans*, it has become one of the tenets of leukotriene biosynthesis that the *S*-configuration hydroperoxide substrate is converted to an LTA type *trans*-epoxide. Other possibilities, i.e. other combinations of fatty acid hydroperoxide and lipoxygenase enzyme might generate a *cis*-epoxy LTA product, have not been well studied. This is probably because that the *S*-configuration hydroperoxides are the dominant form occurring *in vivo* and the role of the three human lipoxygenases (5-LOX, 12-LOX and 15-LOX) in leukotriene pathways has been well established.

In the late 1980's, E.J. Corey's group investigated the reactions of 5*S*-HPETE with two different sources of lipoxygenase enzyme (58) (**Figure 3**). Importantly, the two lipoxygenase enzymes, potato "5-LOX" and coral "8*R*-LOX", abstract the different hydrogen at C10 from 5*S*-HPETE. It is predicted that potato "5-LOX" abstracts the 10*R* hydrogen (48) and coral "8*R*-LOX" removes the 10*S* hydrogen (59-61). They showed that potato "5-LOX" produced *trans*-epoxy LTA_4 and coral "8*R*-LOX" produced the *cis*-epoxide isomer of LTA_4 (6-*epi*-LTA_4). The epoxide structure was inferred indirectly based on the different pattern of hydrolysis products and comparison with that of synthetic standards. This important study, which has not been widely quoted, showed, for

the first time, the possible formation of *cis*- or *trans*- epoxy LTA product from a lipoxygenase reaction and demonstrated a relationship between the hydrogen abstraction, an inherent property of lipoxygenase catalysis, and the configuration of the resulting LTA epoxide.

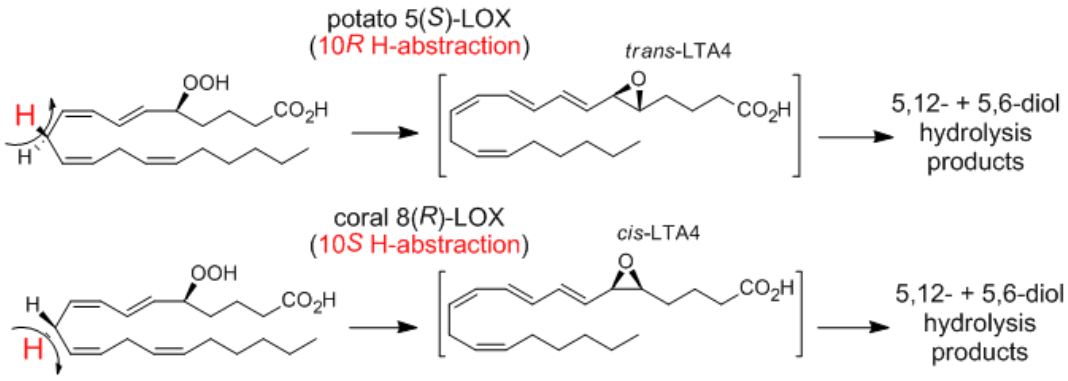

Figure 3: Formation of *trans*- or *cis*- LTA4 by different lipoxygenases

Dual role of lipoxygenase iron in LTA biosynthesis

The two oxidation states of the non-heme iron play different roles in lipoxygenase reactions and there are debates concerning their respective role in LTA epoxide biosynthesis. The transformation from fatty acid hydroperoxide to LTA epoxide involves two crucial steps, hydrogen abstraction and hydroperoxide cleavage. From a purely chemical perspective, either state of the LOX iron could initiate the LTA formation and the key difference of the two pathways is the order of those two steps. The pathway initiated by the ferric (Fe^{3+}) enzyme involves hydrogen abstraction followed by peroxide cleavage, while the ferrous (Fe^{2+}) pathway employs the same two steps in the reverse order. In practice, it is more conceivable and also widely accepted that the ferric iron accounts for the LTA formation. The ferrous iron pathway was originally proposed for

the leukotriene formation in fatty acid autoxidation (62) and in hemoglobin-catalyzed transformation of fatty acid hydroperoxide (63,64) and its actual involvement in lipoxygenase-catalyzed LTA formation is lacking experimental support.

Early studies in this lab showed that the conversion of [10*R*-^{3}H]5-HPETE to LTA_4 is associated with an enrichment in the specific activity of the unreacted substrate, interpreted as a primary isotope effect (49,65,66). This provides critical evidence identifying the 10*pro-R* hydrogen abstraction as the first irreversible step in leukotriene A_4 biosynthesis. In turn, this implicates the ferric iron (hydroxide) in 5-LOX as the active species catalyzing the first step of the transformation. Another piece of evidence comes from the use of lipoxygenase inhibitor in LT formation. Nordihydroguaiaretic acid (NDGA), an effective lipoxygenase inhibitor acting by reducing the active ferric iron to the ferrous form (67), blocks both the dioxygenase reaction and LTA synthesis from HPETEs (48,55). This provides further support for involvement of the ferric iron in catalyzing the initial hydrogen abstraction.

Recent results in this lab implicate that the ferrous iron of lipoxygenase is actively involved in the hydroperoxide cleavage step of LTA formation (30) (**Figure 4**). In the anaerobic reactions of 15*S*-HPETE with soybean LOX-1, a novel arachidonic acid epoxide with a cyclopropyl ring was produced, together with the 14,15-LTA_4 formation. To account for the formation of the cyclopropyl ring-containing epoxide, a dual role of the lipoxygenase iron was proposed. Key to the proposal is the involvement of first the ferric enzyme and then the ferrous species in activating the hydrogen abstraction and hydroperoxide homolytic cleavage sequentially, followed by intramolecular coupling of two radicals to give an unstable epoxide, in the case of 15*S*-HPETE with soybean LOX-1

the cyclopropyl ring-containing epoxide being formed. The mechanism entails a cycle between the two oxidation states of lipoxygenase iron. Testing this mechanism becomes the center of the thesis project.

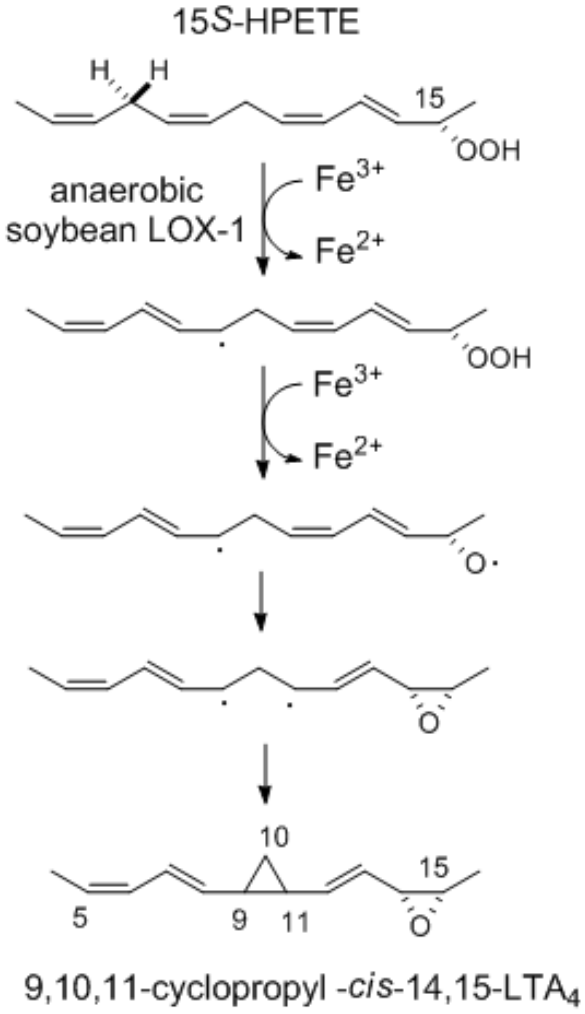

Figure 4: Evidence for a dual role of lipoxygenase iron in epoxide synthesis. Anaerobic reaction of soybean 15-LOX with 15*S*-HPETE produces a cyclopropyl-containing epoxide, which provides evidence for lipoxygenase iron-catalyzed H-abstraction and hydroperoxide O-O bond cleavage.

Anti-inflammatory and pro-resolution lipid mediators

Inflammation is a biological response and protective attempt by the host organism to remove harmful stimuli, such as pathogens, damaged cells, or irritants (68). The classical signs of inflammation are pain (dolor), heat (calor), redness (rubor), swelling (tumor), and loss of function (functio laesa) (68). Inflammation can be classified as either acute or chronic inflammation (69). Acute inflammation involves initial and local recruitment of leukocytes and maturation of immune response targeting the injurious stimuli within the damaged tissue. Two opposite outcomes might follow depending on whether acute inflammation is limited and timely resolved. The successful resolution of inflammation involves the exit of inflammatory machinery from the inflammatory site and leads to the healing and homeostasis of the tissue. On the other hand, if not terminated appropriately, acute inflammation develops to prolonged/chronic inflammation which causes chronic destruction of host tissue and finally results in chronic diseases including cardiovascular disease, cancer and Alzheimer's disease (70).

Just as acute inflammation requires constant stimulation to be sustained, the resolution phase of inflammation is also an active process which is promoted by a number of cellular and molecular factors. Different lipid mediators participate in either term of inflammation, with leukotriene family members being potent pro-inflammatory mediators (32) and several other similar lipid molecules acting with a dual role, anti-inflammation and pro-resolution, during the resolution phase of inflammation (69,71). Interestingly, those anti-inflammatory and pro-resolution lipid molecules share very similar structural features with leukotrienes (stereochemistry of conjugated double bond system and hydroxyl groups). In fact, the biosynthetic pathways leading to those novel-

functional lipid molecules were established based on the leukotriene pathway, with each step exactly parallel among each other. It is still an open question as to how the two kinds of molecules with similar structure play opposite roles. With identification of the corresponding G protein coupled receptor (GPCR) each lipid mediator acts on (72-76), the detailed investigation of lipid-receptor interaction could provide some clue to this question.

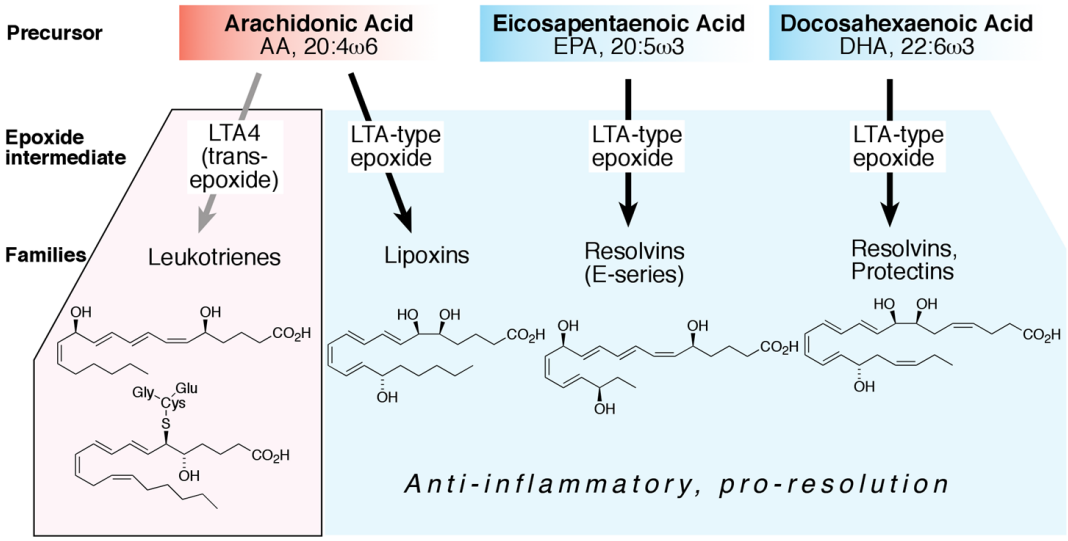

Figure 5: Bioactive lipid mediators derived from polyunsaturated fatty acids (PUFAs)

Lipoxins (lipoxin A_4 and lipoxin B_4) are the first group of lipids identified to be anti-inflammatory (3,22). They are a class of eicosanoids that are formed through the sequential metabolism of arachidonic acid by two different lipoxygenases, 5-LOX and 15-LOX. Different from LTB_4, lipoxins are trihydroxytetraene-containing structure. Other than lipoxins, other anti-inflammatory and pro-resolution lipids, resolvins (Rv) (77), protectins (PD) (78) and maresins (79), are derived from the essential omega-3 fatty

acids eicosapentaenoic acid (EPA) and docosahexaenoic acid (DHA). Previous studies have shown that administration of essential omega-3 fatty acids has beneficial effects in many inflammatory diseases, cancer and human health in general (80). The discovery of those novel anti-inflammatory and pro-resolution lipids partly explains the molecular basis of omega-3 fatty acid action (although how much those novel lipids account for the omega-3 fatty acid action is an open question). The biosyntheses of resolvins, protectins and maresins are proposed exactly based on the leukotriene and lipoxin pathways. The defining experimental data about the mechanism of the transformations and the enzymes involved are lacking.

Our hypotheses about LTA-type epoxide formation

Since the LTA-type epoxide was established as a lipoxygenase product, the possible formation of LTA epoxide was investigated from reactions of different combinations of lipoxygenases and fatty acid hydroperoxides. It is recognized that the ability to produce LTA-type epoxide varies among different lipoxygenases. For the same lipoxygenase, the reaction outcome varies towards different fatty acid hydroperoxide substrates as well as under different reaction conditions. On the other hand, although the leukotriene pathways originating from arachidonic acid were established decades ago, the novel bioactive lipids derived from omega-3 fatty acids (DHA and EPA) were discovered recently and are now receiving more and more research interest recently. Their formation was proposed with leukotriene biosynthesis as a model. Hence it becomes necessary to establish a coherent mechanism about LTA-type epoxide biosynthesis which encompasses different lipoxygenase reactions with fatty acid hydroperoxides.

We propose that the mechanism of LTA-type epoxide biosynthesis requires a combination of the following factors: alignment and orientation of the fatty acid hydroperoxide in the lipoxygenase active site, absolute configuration of the hydroperoxide group, stereospecificity of the H-abstraction, and exclusion of oxygen within the active site. With the role of active site molecular oxygen well established, we focus efforts to test the relationship between stereochemistry of LTA epoxide (product specificity) with absolute configuration of the hydroperoxide group (substrate property) and the H-abstraction (catalyst property).

The central hypothesis is that transformation of the fatty acid hydroperoxide to LTA epoxide depends on participation of the lipoxygenase non-heme iron in catalyzing both the initial hydrogen abstraction and in facilitating cleavage of the hydroperoxide moiety (dual role of lipoxygenase iron). This postulate implies that the hydrogen abstracted and the hydroperoxide lie in suprafacial relationship, which in turn, dictates that the *cis* or *trans* epoxide configuration of the LTA product depends on the pro-*R* or pro-*S* chirality of the H-abstraction (an inherent property of the specific lipoxygenase) and the R or S chirality of the HPETE substrate.

Figure 6 illustrates the established lipoxygenase-catalyzed LTA formation with the substrate-enzyme-product relationship explained by our hypothesis. In achieving the suprafacial relationship between the hydrogen abstraction and the hydroperoxide moiety, 5*S*-HPETE (the natural enantiomer) must assume the *transoid* conformation at the 5-carbon, thus dictating the natural *trans*-epoxy configuration of LTA_4 (the bottom reaction). With the *cisoid* conformation taken at the 5-carbon, 5*S*-HPETE is not converted to LTA-type product (the middle reaction). The top reaction illustrates the

result reported by E. J. Corey and coworkers (58), in which an 8*R*-LOX activity, which catalyzes *pro-S* hydrogen abstraction from C-10, converted 5*S*-HPETE to the *cis* epoxide, 6-*epi*-LTA_4. The deduced opposite tail-to-head orientation for 5S-HPETE binding in 8*R*-LOX (60,81) requires the *cisoid* conformation taken at the 5-carbon, thus dictating the *cis*-epoxy configuration of the resulting LTA product.

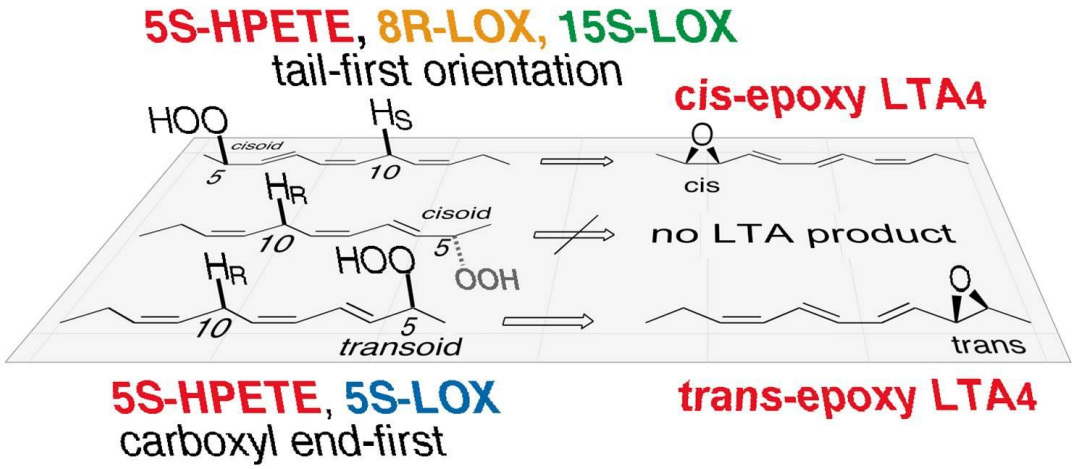

Figure 6: Hypothesis of the mechanistic basis for formation of *cis* or *trans* LTA epoxides

Overall objectives of the dissertation study

There are three overall objectives of this dissertation study:

1) Develop the methods in biosynthesis, isolation and direct structural analysis of the LTA-type epoxides from lipoxygenase reactions.

2) Utilize the methods developed in Objective 1 to investigate the reactions of different combinations of fatty acid hydroperoxides (*R* or *S* configuration) and lipoxygenase catalysts (which hydrogen is abstracted) and in turn to test our hypothesis about the LTA-type epoxide biosynthesis.

3) Investigate the novel bioactive lipid mediator biosynthetic pathways by conducting the *in vitro* enzymological studies and directly analyzing the LTA-type epoxides in these novel pathways.

CHAPTER II

BIOSYNTHESIS, ISOLATION, AND NMR ANALYSIS OF LEUKOTRIENE A EPOXIDE

Introduction

The leukotrienes are a family of lipid mediators derived from arachidonic acid and implicated in the pathogenesis of asthma and other inflammatory diseases (31,32). The biosynthetic pathway, unraveled three decades ago, is a model for related transformations to anti-inflammatory mediators, including the lipoxins, eoxins, resolvins, protectins and maresins (3,77-79). The establishment of leukotriene A_4 as the pivotal intermediate is a crucial event in the understanding of the leukotriene pathway. Since LTA_4 was first proposed and discovered in the early 1980s, extensive efforts were directed towards the determination of its exact chemical structure as well as its formation mechanism via a sequential lipoxygenase transformation (45-48).

LTA_4 is highly unstable in the physiological buffer at pH 7.4, with a half-life estimated as approximately 3 s at 25°C and 18 s at 4°C (43). Although LTA_4 was detected and isolated as an evanescent intermediate in short-term incubations of arachidonic acid with human leukocytes (44), the amount LTA_4 was isolated from a biological system is low and thus affords it impossible for a direct structural analysis. A smart, yet indirect, method was then developed to address the structural determination. Thanks to the contributions chemists made to the field, LTA_4 and closely related 5,6-epoxide isomers became available through total chemical synthesis. The stereochemistry

of the natural LTA_4 product was then deduced based on study of the reactions of synthetic LTA_4 and related isomers in transformations to the stable, bioactive leukotrienes, LTB_4 and LTC_4 (40).

The first aim of my thesis project is to develop methods to biosynthesize, isolate and directly NMR analyze leukotriene A epoxide from a lipoxygenase reaction. This fundamental issue has been rarely touched, not to say been achieved, with the leukotriene pathway having already been established for 3 decades. The successful fulfillment of this aim could not only fill a blank in the leukotriene study but also provide a strong tool for study of other leukotriene-related pathways.

The ability to isolate and structurally characterize the unstable epoxides by biosynthesis is a strength of Brash lab. Using the biphasic synthesis and simultaneous extraction methods which will be discussed in the later part of this chapter, the lab successfully isolated and achieved structural analyses of allene epoxides which have a half-life of 15~30 s at 0°C at pH 7.4 and are harder to handle than LTA epoxides because even the methyl esters are exceptionally unstable (82,83). Using the same approach, this lab has isolated and NMR analyzed LTA-type epoxides prepared by reactions of fatty acid hydroperoxides with a catalase/peroxidase-related hemoprotein (84,85). In this chapter I will apply the methods to the lipoxygenase reactions and aim to biosynthesize and isolate the LTA epoxides in sufficient amounts for NMR analysis.

I set out the project by testing human 15-LOX-1 in producing NMR-sufficient amount of LTA epoxide. For quite a long time, it was believed that LOXs in general and 15-LOX in particular might not occur in animal tissues. However, in 1975, a 15-LOX was discovered in rabbit reticulocytes, which was capable of oxidizing phospholipids and

biomembranes (86). Later the human orthologue of the rabbit 15-LOX was demonstrated and purified from human eosinophils (87). In mice (88) and other mammalian species, a leukocyte-type 12-LOX was identified and considered the functional equivalent of the reticulocyte-type 15-LOX in rabbits and human. Hence these enzymes are designated 12/15-LOXs. 12/15-LOXs from different origins share similar enzymatic properties, including the substrate specificity and the product profiles. The primary products of 12/15-LOX towards arachidonic acid are 15*S*-HPETE and 12*S*-HEPTE, with 15*S*-HPETE dominant by the rabbit and human enzyme (10) and 12*S*-HPETE by the mouse enzyme (88). Importantly, the dual positional specificity renders 12/15-LOX capable of producing the LTA-type epoxide as is discussed in Chapter I. In 1997, a second type of 15-LOX was cloned from human hair roots (89). This enzyme, which is now known as epidermis-type 15-LOX or 15-LOX-2 (with the reticulocyte-type 15-LOX named as 15-LOX-1), shares a low degree of homology with the reticulocyte-type 15-LOX and differs strongly with the latter isoform with respect to the enzymatic properties (90).

The methods developed in this chapter will be further applied to the reactions of other lipoxygenase enzymes and fatty acid hydroperoxides. By directly analyzing the structure of the LTA products from different reaction combinations, our hypothesis about the LTA-type epoxide biosynthetic mechanisms will be tested.

Experimental procedures

Materials

Arachidonic acid was purchased from NuChek Prep Inc. (Elysian, MN). Soybean LOX-1 (lipoxidase, type V) was purchased from Sigma. 15*S*-HPETE was synthesized by reacting soybean LOX-1 with arachidonic acid followed by SP-HPLC purification.

Biphasic reaction conditions for preparation of LTA epoxides

Enzyme reactions were performed at 0 °C, with the 15*S*-HPETE substrate initially in hexane (5 ml, bubbled for 30 min prior to use with argon to decrease the O_2 concentration, and containing ~200 μM 15*S*-HPETE) layered over the recombinant human 15-LOX-1 (1-2 mg, ~20 nmol) in 400 μl of Tris buffer (pH 7.5 optimal for human 15-LOX-1). The reaction was initiated by vigorous vortex mixing of the two phases. After 1.5 min, the hexane phase was collected and scanned from 200 to 350 nm in UV light by using a Perkin-Elmer Lambda-35 spectrophotometer. Then the hexane phase was evaporated to about 2 ml under a stream of nitrogen, treated with ethanol (20 μl) and ethereal diazomethane for 10 s at 0 °C and then rapidly blown to dryness and kept in hexane at -80 °C until further analysis.

Acid-induced hydrolysis of 14,15-LTA_4 methyl ester

Acid-induced hydrolysis was performed with the purified 14,15-LTA_4 methyl ester in a solvent of CH_3CN/H_2O/HAc (50/100/0.1, by volume) at room temperature for 2

hours. The hydrolysis products were extracted by methylene chloride and then analyzed by RP-HPLC.

HPLC analyses

Aliquots of the methylated hexane phase were analyzed by RP-HPLC using a Waters Symmetry column (25 x 0.46 cm), using a solvent of MeOH/20mM triethylamine pH 8.0 (90/10 by volume), at a flow rate of 1ml/min, with on-line UV detection (Agilent 1100 series diode array detector). Further purification was achieved by SP-HPLC with a silica guard column (0.46 × 4.5 cm) using a solvent of hexane/triethylamine (100/0.5) run at 0.5 ml/min.

NMR analysis

^{1}H NMR and ^{1}H,^{1}H COSY NMR spectra were recorded on a Bruker AV-III 600 MHz spectrometer at 283 K. The parts/million values are reported relative to the residual nondeuterated solvent (δ = 7.16 ppm for C_6H_6). Typically, 1024 scans were acquired for a 1-D spectrum on ~20 μg of the LTA epoxide.

Results

Expression and purification of human 15-LOX-1

The cDNA of human 15-LOX-1 was subcloned into the pET3a vector (with an N-terminal His6 tag) and the protein was expressed in BL21 cells. A typical preparation of a 100-ml culture was carried out as follows: 100 ml of 2XYT medium containing 100 μg/ml ampicillin was inoculated with a single colony of human 15-LOX-1-His in BL21 cells and grown at 37 °C at 250 rpm till OD600 reached 0.8. IPTG (0.5 mM) was then added to the culture which was grown at 16 °C, 220 rpm for 4 days.

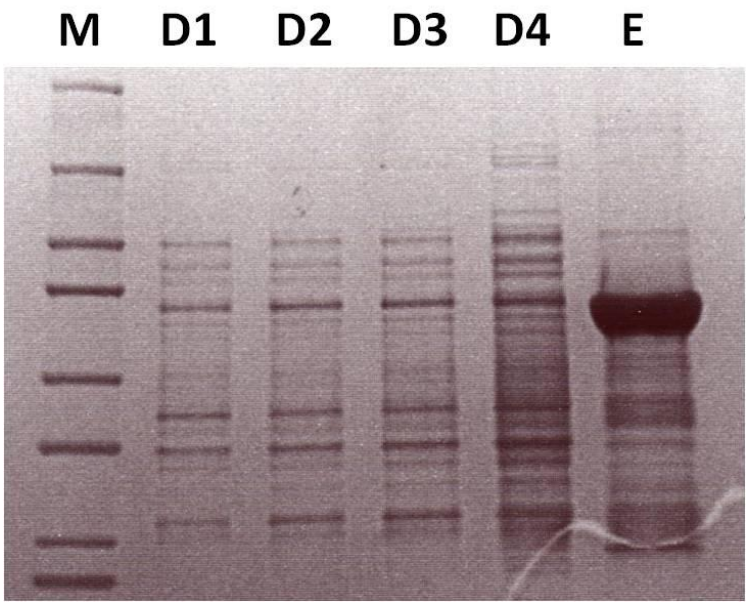

Figure 7: Coomassie Blue staining of cell homogenates and purified human 15-LOX-1. M, protein marker. D, cell homogenates at the different days of expression. E, purified human 15-LOX-1.

At Day 4, the cells were spun down at 5000 g for 20 min in a Beckman Avanti J-25I centrifuge, washed with 40 ml of 50 mM Tris, pH 7.9, pelleted again at 5000 g for 20 min, and resuspended in 10 ml of 50 mM Tris, pH 8.0, 500 mM NaCl, 20% glycerol and 100 μM PMSF. The spheroplasts were then sonicated 5 times for 10 s using a model 50 Sonic Dismembrator (Fisher Scientific) at a setting of 5. CHAPS detergent was added at a final concentration of 1% (w/w) and the sample kept on ice for 20 min. The resulting membranes were spun down at 5,000 × *g* for 20 min at 4 °C. The human 15-LOX-1 activity was present in the supernatant. The supernatant was loaded on a nickel-NTA column (0.5 ml bed volume, Qiagen) equilibrated with 50 mM Tris buffer, pH 8.0, 500 mM NaCl. The column was then washed with the equilibration buffer and the nonspecific bound proteins were eluted with 50 mM Tris buffer, pH 8.0, 500 mM NaCl, 50 mM imidazole. The human 15-LOX-1 was then eluted with 50 mM Tris buffer, pH 8.0, 500 mM NaCl, 250 mM imidazole. Fractions of 0.5 ml were collected and assayed for the LOX activity. The positive fractions were dialyzed against 50 mM Tris buffer, pH 7.5, 150 mM NaCl. The purity of the enzyme preparations was determined by SDS-PAGE and Coomassie Blue staining; the prominent band of h15-LOX-1 accounted for about 80% of the total protein (**Figure 7**).

RP-HPLC of reaction of arachidonic acid with human 15-LOX-1

To check the catalytic activity of the purified recombinant human 15-LOX-1 in producing 14,15-LTA$_4$, I incubated arachidonic acid with human 15-LOX-1 and analyzed the reaction by RP-HPLC (**Figure 8**).

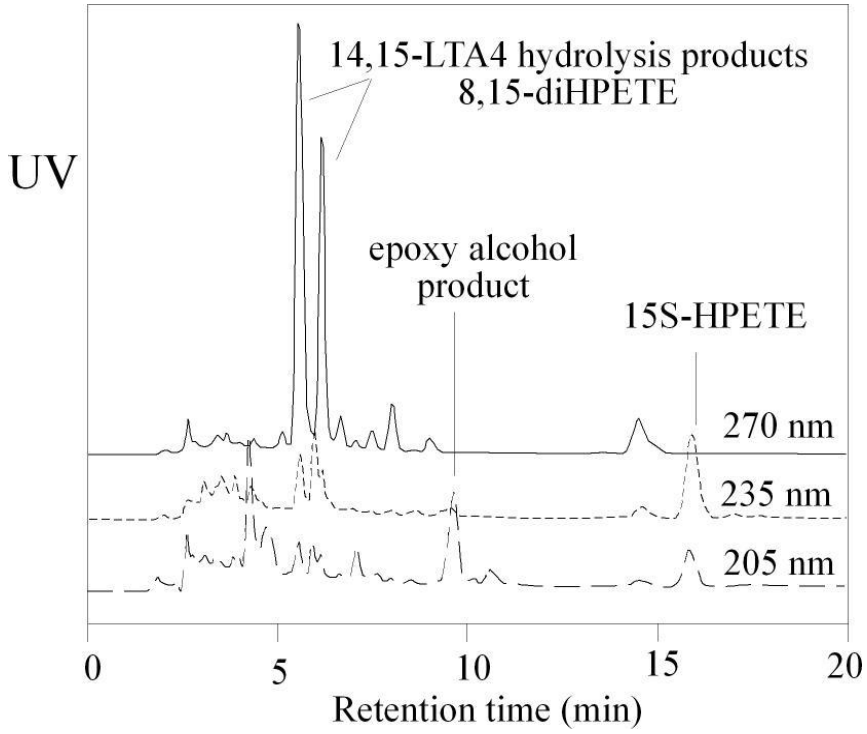

Figure 8: RP-HPLC of the reaction of arachidonic acid with human 15-LOX-1.
Arachidonic acid was incubated with human 15-LOX-1 at room temperature in 50 mM Tris buffer (pH 7.5) containing 150 mM NaCl. The sample was extracted using a C18 cartridge and analyzed by RP-HPLC using a Waters Symmetry column (25 × 0.46 cm), a solvent of MeOH/H2O/HAc (80/20/0.01, by volume), at a flow rate of 1 ml/min, with on-line UV detection.

RP-HPLC analysis demonstrated the formation of 8,15-diHETEs (14,15-LTA$_4$ hydrolysis products), 8,15-diHPETE (double oxygenation product) (8,15-diHETEs and 8,15-diHPETE eluted as a mixture at 5-7 min), epoxy alcohol product (with weak UV absorbance at 205 nm and eluted at 9.7 min) and the mono-oxygenation product 15*S*-

HPETE (eluted at 16.2 min with 12*S*-HPETE eluted just before it). 8,15-diHETEs and 8,15-diHPETE can be further resolved using a more polar mobile running solvent and be easily differentiated based on their characteristic UV chromophore (35).

Method development, preparation, and analysis of 14,15-LTA_4

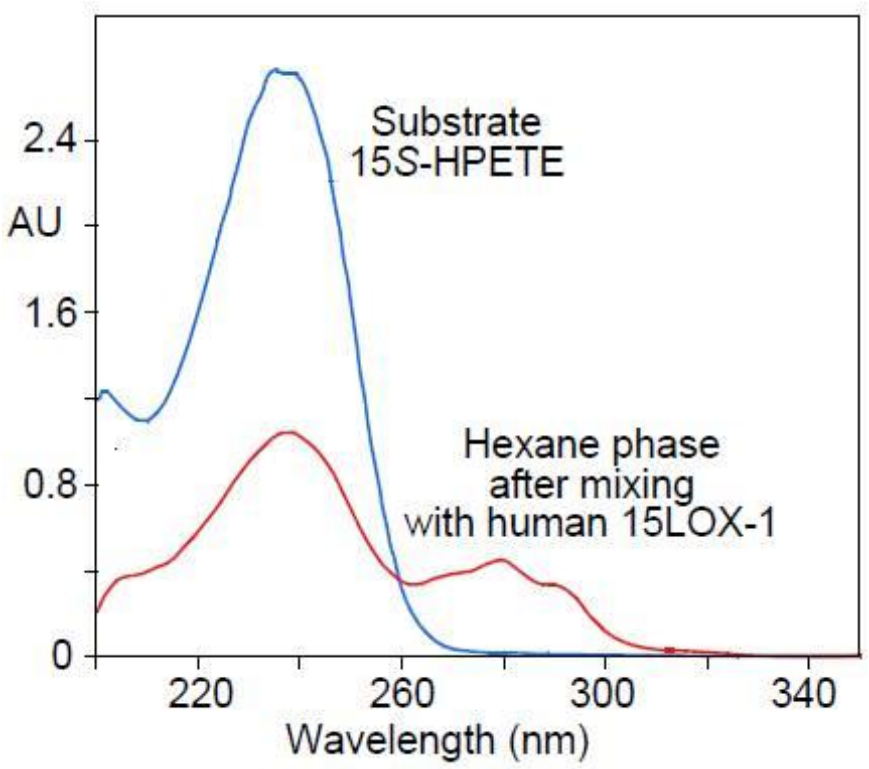

Figure 9: UV analysis of LTA epoxide formation under biphasic reaction conditions
The UV spectrum of 15*S*-HPETE substrate (40 µg/ml) in 5 ml hexane was recorded before reaction, and after vortex mixing for 90 s at 0 – 4 °C with 1.5 mg 15-LOX-1 enzyme in 400 µl 0.1 M Tris, pH 7.5.

To prepare and isolate 14,15-LTA_4 epoxide, I used the biphasic reaction system, kept at 0°C, with the 15*S*-HPETE substrate dissolved in hexane and the purified recombinant human 15-LOX-1 enzyme in aqueous buffer. Upon vigorous mixing, the more polar hydroperoxide will partition into the aqueous phase, react with enzyme, and

the less polar epoxide product will instantly back-extract into the hexane and thereby be protected from hydrolysis. In optimizing the conditions, I used a 12.5-fold excess of hexane over the aqueous phase (pH held at 7.5), and a mixing time of 90 s at 0 °C.

Comparison of the UV spectrum of the hexane phase before and after vortex mixing provided a quick feedback on the extent of reaction. In the example shown in **Figure 9**, a new conjugated triene chromophore typical of an LTA-type epoxide (λ_{max} 280 nm) is evident after mixing. The substrate concentration has diminished markedly and is only partially replaced by the conjugated triene. Hydrolysis of the epoxide will produce 8,15- and 14,15-dihydroxy derivatives that will not extract into hexane, especially at the elevated pH of 7.5, and the same applies to any dioxygenation products or epoxyalcohol derivatives (55). Overall, about 60% of the starting 15*S*-HPETE was consumed, with an estimated recovery of LTA-type epoxide under the above reaction conditions of 10-15% (taking into account the molar absorbance of the conjugated trienes is about 1.5 - 2 times the value for a conjugated diene), with the balance of products being accounted for mainly by the non-extractable more polar derivatives.

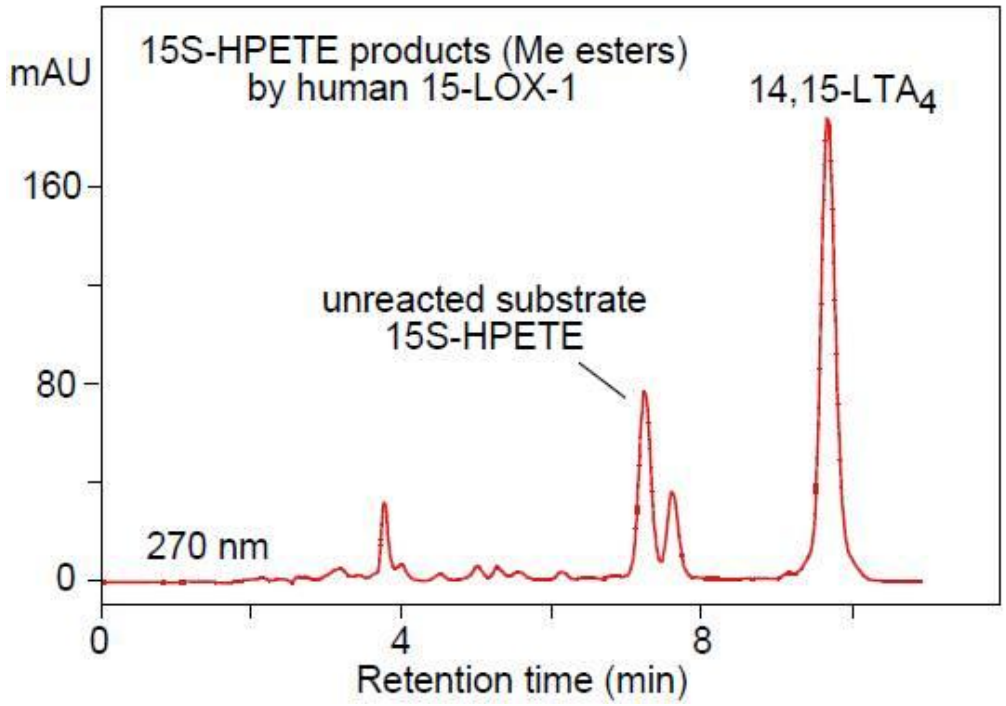

Figure 10: RP-HPLC analysis of the reaction of 15-LOX-1 with 15*S*-HPETE
RP-HPLC analysis used a Waters Symmetry C18 column (0.46 × 25 cm), a flow rate of 1 ml/min, and a solvent system of methanol/20 mM triethylamine pH 8.0 (90/10, by volume) with UV detection at 270 nm.

After preparing the methyl esters of the hexane extract by brief reaction with diazomethane at 0 °C, the remaining 15*S*-HPETE and its products were analyzed on RP-HPLC using conditions suitable for LTA-type epoxides (43,91). **Figure 10** illustrates RP-HPLC analysis with UV detection at 270 nm. The unreacted 15*S*-HPETE (at 7.2 min retention time, the largest peak on the chromatogram but weakly detected at 270 nm) is immediately followed by a minor keto derivative (at 7.6 min retention time, a conjugated dienone, λ_{max} 281 nm), and then by a well-resolved peak of the putative LTA-type epoxide (conjugated triene, λ_{max} 280 nm).

This product 14,15-LTA$_4$ was purified from SP-HPLC runs with a solvent of hexane containing 0.5% triethylamine (**Figure 11**).

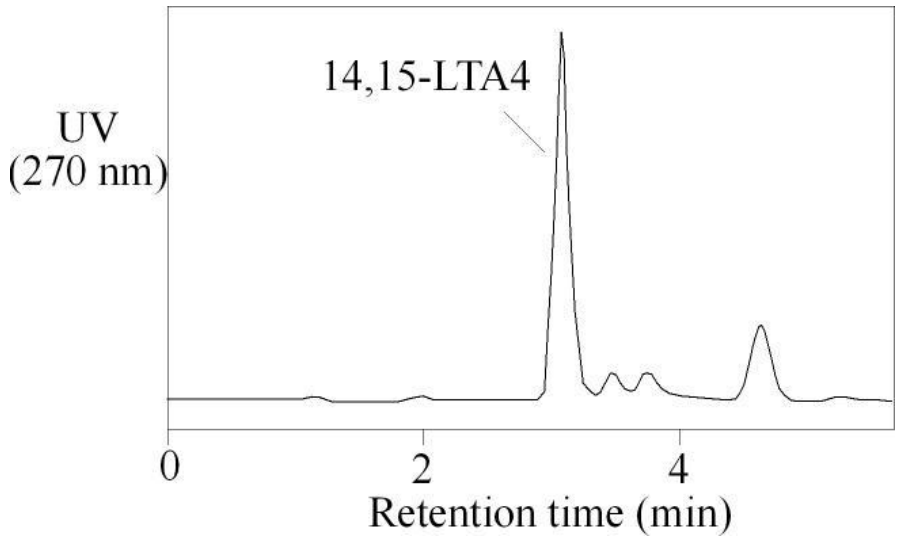

Figure 11: SP-HPLC analysis of the reaction of 15-LOX-1 with 15S-HPETE
SP-HPLC analysis used a silica guard column (0.46 × 4.5 cm), a flow rate of 0.5 ml/min, and a solvent system of Hexane/triethylamine (100/0.5, by volume) with UV detection at 270 nm.

The pooled aliquots of LTA epoxide methyl ester (~ 20 μg) were subsequently analyzed by ^{1}H-NMR in d6-benzene (**Figure 12**). The 2-D COSY spectrum (below) helps confirm the proton assignments. The expanded regions for the olefinic protons (5.0 – 6.5 ppm) and the epoxide protons (2.6 – 3.1 ppm) illustrate the splitting of individual signals and associated coupling constants from which the stereochemistry can be derived. These provide the configuration of the double bonds, in particular identifying the conjugated triene as 8*Z*,10*E*,12*E*, and on the epoxide protons the 2 Hz coupling between H14 and H15 identifies the epoxide configuration as *trans*. Based on these analyses, and with the reasonable assumption that the original 15*S* configuration is retained, the

structure of the epoxide product can be defined as 14*S*,15*S*-*trans*-epoxy-eicosa-5*Z*,8*Z*,10*E*,12*E*-tetraenoate. This confirms the structure originally proposed for this intermediate, now named eoxin A_4, precursor of the pro-inflammatory eoxins of human eosinophils in asthma.

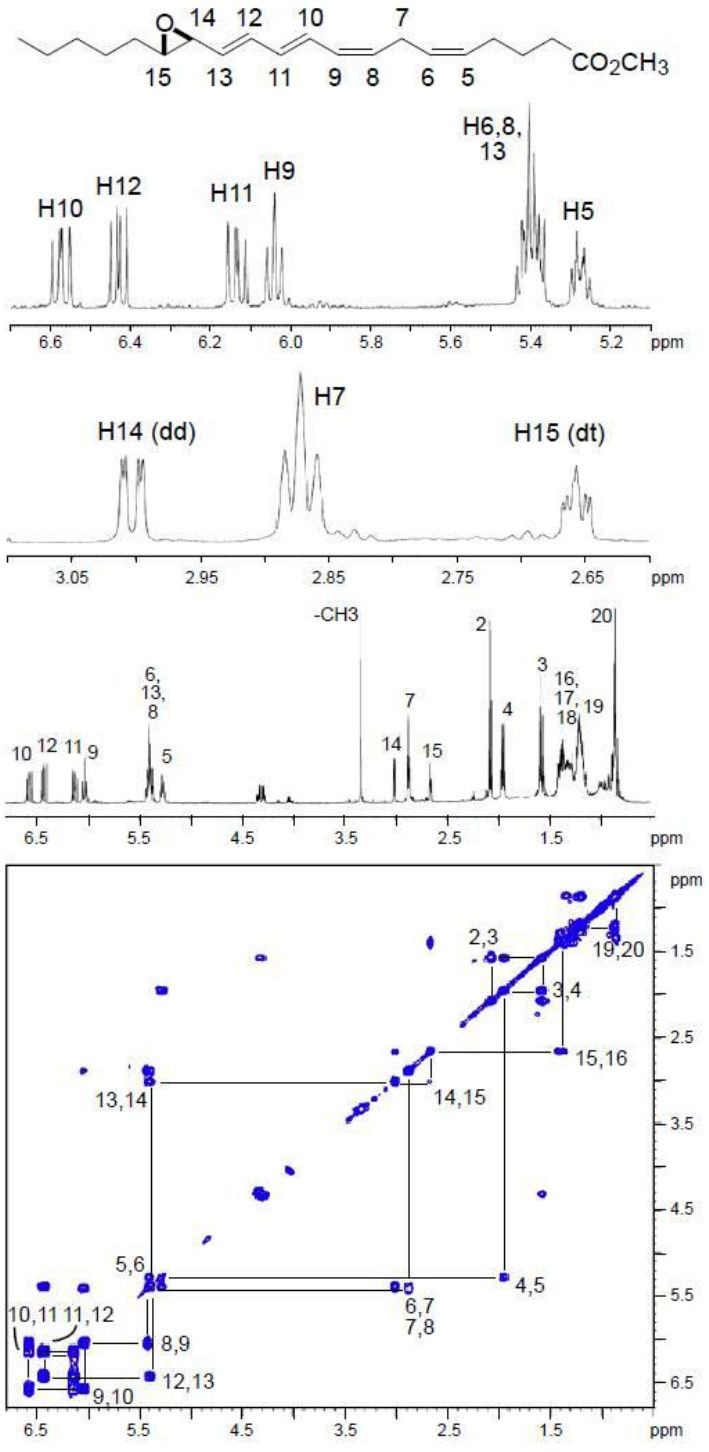

Figure 12: NMR analysis of 14,15-LTA$_4$ methyl ester. Spectra were recorded in d6-benzene at 283 K using a Bruker 600 MHz spectrometer.

RP-HPLC analysis of the aqueous phase of the biphasic reaction

To have a complete view of the biphasic reaction between 15*S*-HPETE and human 15-LOX-1, I analyzed the non-extractable more polar metabolites from the aqueous phase after the biphasic reaction (**Figure 13**).

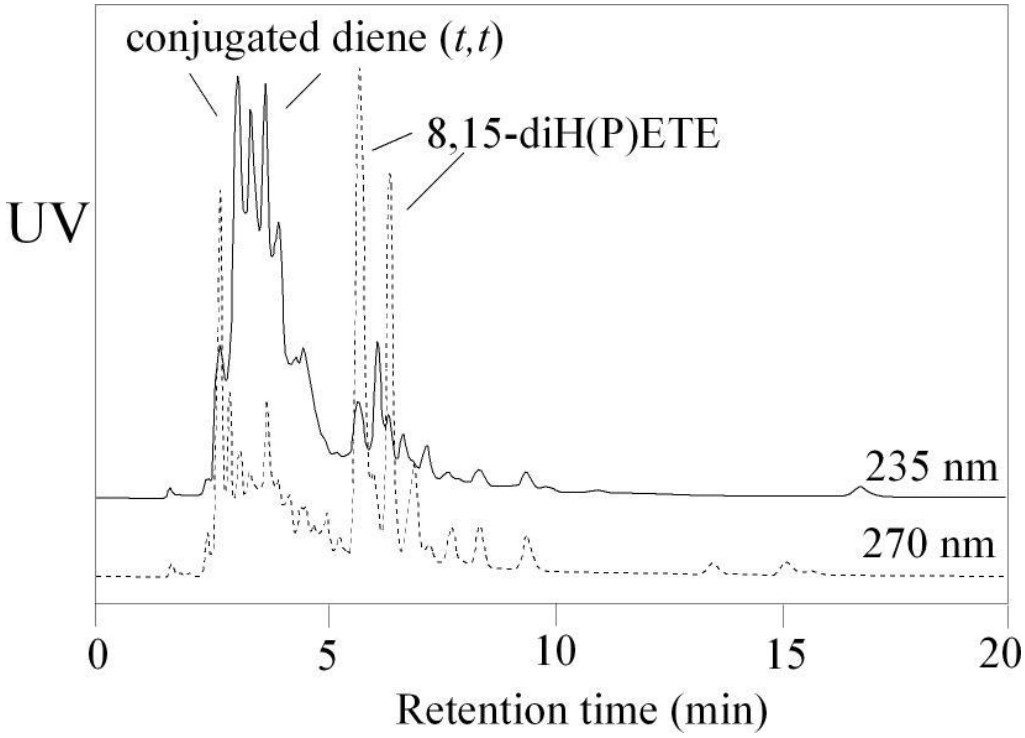

Figure 13: RP-HPLC analysis of the aqueous phase from the biphasic reaction between 15*S*-HPETE and human 15-LOX-1
RP-HPLC analysis used a Waters Symmetry column (25 × 0.46 cm), a solvent of MeOH/H_2O/HAc (80/20/0.01 by volume), at a flow rate of 1 ml/min, with on-line UV detection.

Analysis of the aqueous phase revealed the presence of dihydro(pero)xy derivatives (prominently with all-trans conjugated trienes, λ_{max} 269 nm, typical of LTA epoxide hydrolysis products, but including dihydroperoxides), as well as a mixture of more polar derivatives with trans-trans conjugated dienes (not identified, but possibly epoxyalcohols formed from conjugated triene-containing dihydroperoxides).

Acid-induced hydrolysis of 14,15-LTA_4 methyl ester

In an aqueous system at acidic pH, the LTA epoxide readily reacts with water and gives two pairs of dihydroxy products, each pair epimeric at one carbon position. In optimizing the conditions for the hydrolysis of the LTA epoxides, different conditions were performed with the hydrolysis products analyzed by RP-HPLC. Basically with the purified 14,15-LTA_4 methyl ester in hand, the hydrolysis is carried in a one-phase mixture of the organic solvent and the water in the presence of a strong inorganic acid. Use of methanol as the solvent of LTA methyl ester turns out that the main products are the methoxy derivatives due to the nucleophilc attack on the epoxide ring by methanol. Switch to the solvent CH_3CN helps to get a "clean" hydrolysis product profile with the four hydrolysis products well resolved on RP-HPLC (**Figure 14**). The four hydrolysis products, 8,15-diHETEs (*t,t,t*) and 14,15-diHETEs (*c,t,t*), were identified based on the comparison with the authentic standards about their UV chromophore and retention time on RP-HPLC.

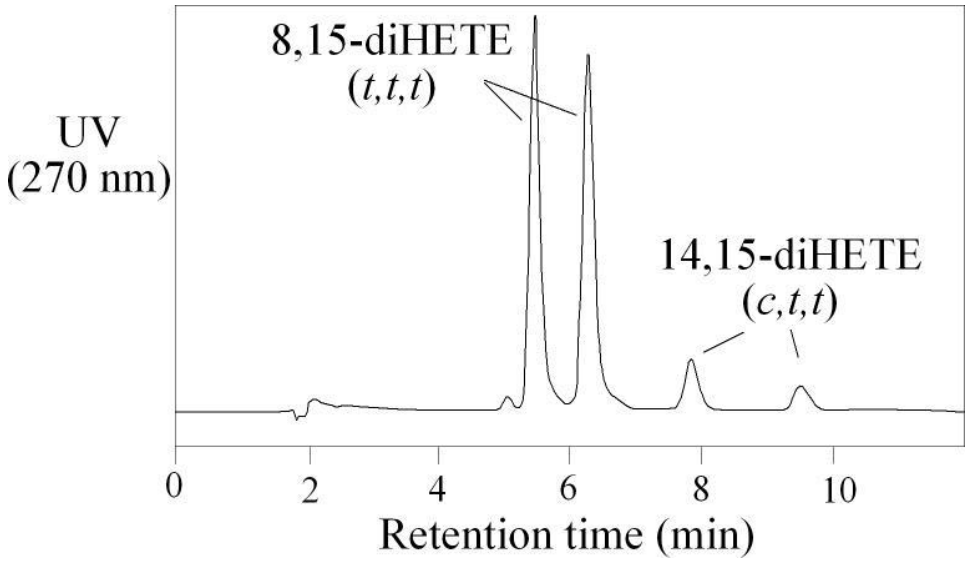

Figure 14: RP-HPLC of the acid-induced hydrolysis of 14,15-LTA_4 methyl ester
14,15-LTA_4 methyl ester is dissolved and put in a mixture of CH_3CN/H_2O/HCl (100/100/0.1, by volume) for 2 h at room temperature. After extraction by DCM, the hydrolysis sample was analyzed by RP-HPLC, using a Waters Symmetry column (25 × 0.46 cm), a solvent of MeOH/H_2O (80/20, by volume), at a flow rate of 1 ml/min, with on-line UV detection at 270 nm.

One potential of studying the hydrolysis of the LTA epoxide is to determine the epoxy configuration of the LTA epoxide based on comparison with standards with respect to the hydrolysis product pattern. However, there are several limits about this application. 1) In addition to the LTA epoxide, a lipoxygenase reaction generates other products. The RP-HPLC chromatogram of a lipoxygenase reaction is usually far more complex than as is shown in **Figure 14** which is directly generated from the purified LTA epoxide. This makes it difficult to calculate the accurate ratio among different hydrolysis products. 2) The hydrolysis conditions (i.e. pH and solvent used) affect the hydrolysis product patterns. 3) **Figure 14** demonstrates the hydrolysis of the LTA methyl ester rather than the free acid. Esterification of the carboxyl group eliminates the effect of the carboxyl ion on the stability of the LTA epoxide and is expected to affect the hydrolysis outcome as well.

Discussion

In this chapter, I developed the biphasic synthesis and simultaneous extraction method to biosynthesize and isolate the unstable LTA-type epoxide from a lipoxygenase reaction. The resulting LTA-type epoxide is purified and structurally characterized by NMR analysis (**Figure 15**).

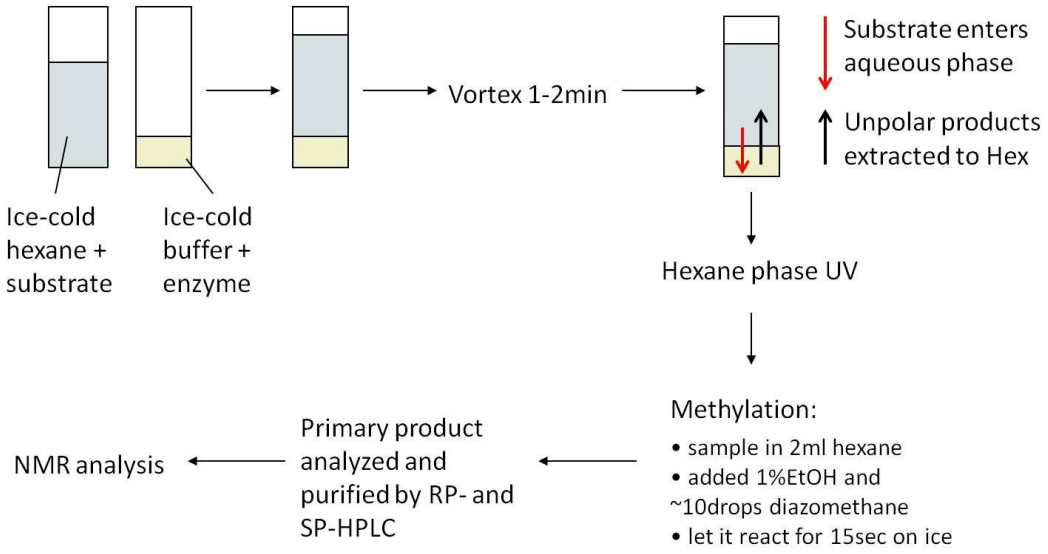

Figure 15: Overview of the biphasic synthesis and simultaneous extraction method.

There are several requirements and special reaction conditions for the successful application of the above method to other lipoxygenase reactions in generating the LTA-type epoxides:

1) The lipoxygenase enzyme needs to be highly active in making the LTA epoxide from the fatty acid hydroperoxide. The high catalytic activity here means not only the efficient consumption of the fatty acid hydroperoxide substrate but also the high yield of the LTA product, which is to ensure the production of the LTA epoxide in the sufficient amount for NMR analysis. On the one hand, mammalian 5-LOX is not a good candidate

as it is not very active towards its substrate 5*S*-HPETE even though the majority of conversion goes to the LTA_4 production. 5-LOX activity is well regulated inside the cells, and the regulation mechanism is not completely understood (92). On the other hand, soybean LOX-1 is not a good candidate either, since it makes mainly double oxygenation products from its substrate 15*S*-HPETE even if the substrate consumption is efficient.

2) The anaerobic environment is made to optimize the yield of LTA product. In Chapter I I reviewed the competition among different secondary metabolic routes of fatty acid hydroperoxides and the important role of molecular oxygen in determining the final reaction outcome. There are several approaches to reduce the oxygen level in the solvents. In the study demonstrating the LTA synthase activity of soybean LOX-1, the anaerobic condition was generated inside an N_2-inflated Aldrich Atmosbag (30). In another study identifying the novel substrates for orphan P450s, they removed air by subjecting a manifold device to several cycles of alternate vacuum and Ar purging (93). In the method developed in this chapter, bubbling the reaction solvent with Ar is utilized to reduce the oxygen concentration.

3) The pH of the aqueous phase of the biphasic system needs to be optimized, which often requires a compromise between the enzymatic activity, the back extraction efficiency and the stability of the resulting LTA product. Lipoxygenase enzymes differ in their pH optima, and for instance the soybean LOX-1 requires an alkaline condition to achieve its best catalytic activity, whereas the human 12*R*-LOX, which plays important roles in generating the skin barrier, is optimal at pH 6 (94). The pH of the aqueous phase has a significant effect on the partition of LTA products. As the measured pKa of linoleic

and arachidonic acids is pH 7 - 8 (95,96), the likely pKa of the epoxide derivatives is probably around pH 6 - 7. Accordingly a change in environmental pH in this range would shift the equilibrium between the ionic and non-ionic forms, thus changing the partition of LTA products between the two phases. Thirdly, the stability of LTA products is another factor that needs to be considered. Although alkaline conditions are generally helpful in stabilizing LTA epoxides, the ionization of the carboxyl group may also be a determinant of stability, especially in the range of pH around the pKa. (LTA_4 methyl ester is considerably more stable than the free acid). Although the half-life of LTA_4 is reported as about 18 s at 4 °C at pH 7.4, lowering the pH will suppress ionization of the carboxyl which may have a protective effect, countering the effects of acid-induced hydrolysis. In my experiments, I found the optimal recoveries of LTA epoxides in reactions conducted at pH 6.5, which may be explained in part by this stabilizing factor.

4) Optimized reaction temperature and reaction time. To prevent the degradation of the unstable LTA products, the reaction temperature needs to be low and the reaction time being short.

CHAPTER III

BIOSYNTHETIC MECHANISMS OF LEUKOTRIENE A EPOXIDE

DUAL ROLE OF LIPOXYGENASE IRON

Introduction

The formation of a *cis*-epoxy leukotriene A in a biological system and from a lipoxygenase reaction in particular was first demonstrated by E.J. Corey and his colleagues in 1989 (58). Their study demonstrated a relationship between the hydrogen abstraction, an inherent property of lipoxygenase catalyst, and the configuration of the resulting LTA epoxide, i.e. with 5*S*-HPETE as substrate, potato "5-LOX" (abstracting 10*R* hydrogen) produced *trans*-epoxy LTA_4 and coral "8*R*-LOX" (abstracting 10*S* hydrogen) produced the *cis*-epoxide isomer of LTA_4 (6-*epi*-LTA_4). This important study has not received much research interest, which is reflected by its moderate citation number. However, we decided to extend their work aiming to investigate 1) whether the formation of the *cis*-LTA epoxide is unique for coral 8*R*-LOX or it could occur with a proper combination of the substrate (fatty acid hydroperoxide) and the enzyme catalyst (lipoxygenase) and 2) whether we can develop a LTA biosynthetic mechanism that can reconcile and explain the LTA formation from reactions of different fatty acid hydroperoxide substrates and different lipoxygenase enzymes. The classical leukotriene biosynthetic pathway regains wide research interest and clinical potential due to the recently discovered anti-inflammatory and pro-resolution pathways which are proposed with the leukotriene pathway as a model. The successful fulfillment of our aim could not

only advance our knowledge on leukotriene formation but also guide the research on those novel potent anti-inflammatory and pro-resolution lipid mediators.

As is discussed in Chapter I, the central hypothesis of our proposed LTA biosynthetic mechanism is that transformation from the fatty acid hydroperoxide to the LTA epoxide depends on participation of the lipoxygenase non-heme iron in catalyzing both the initial hydrogen abstraction and in facilitating cleavage of the hydroperoxide moiety (a dual role of the lipoxygenase iron). This postulate implies that the hydrogen abstracted and the hydroperoxide moiety lie in a suprafacial relationship, which in turn, dictates that the *cis* or *trans* epoxide configuration of the LTA product depends on the pro-*R* or pro-*S* chirality of the H-abstraction (an inherent property of the specific lipoxygenase) and the *R* or *S* chirality of the HPETE substrate.

To test this hypothesis I plan to investigate the LTA epoxide formation from reactions of different enantiomeric fatty acid hydroperoxides (with different hydroperoxide position and chirality) and different lipoxygenase enzymes (holding the fatty acid hydroperoxides in different orientations and abstracting different hydrogens from substrates). Our focus is the epoxy configuration of the resulting LTA product (*cis* or *trans*). One method in determining the epoxy configuration is to compare with the synthetic LTA standards in transformation to their stable hydrolysis products. With the methods developed in Chapter II for biosynthesis, isolation and direct NMR analysis of the LTA epoxide, I will determine the epoxy configuration of LTA product by isolating and directly NMR characterizing the LTA product structure.

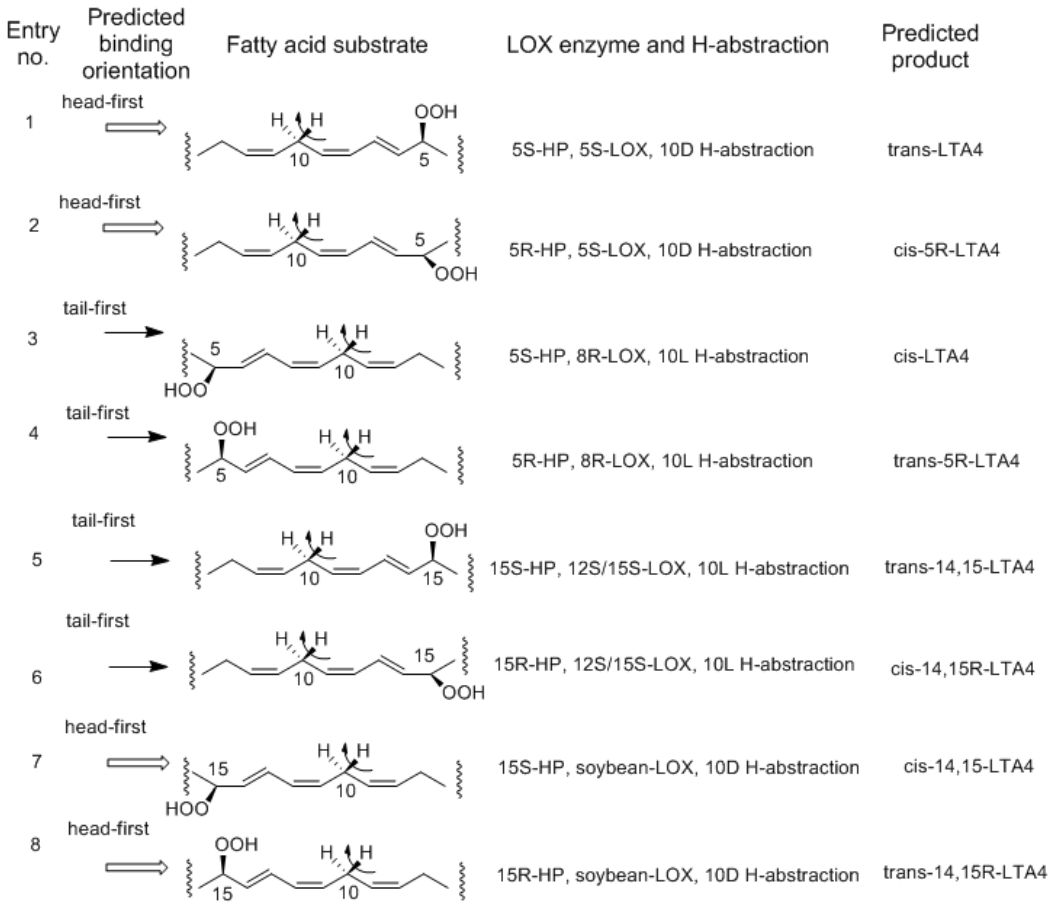

Figure 16: Summary of reactions of the enantiomeric fatty acid hydroperoxides with different lipoxygenases

The reactions to be performed (substrates, enzymes, and expected LTA epoxide products) are listed in **Figure 16**. The top four reactions are on 5-HPETE (*R* or *S*), and the bottom four are on 15-HPETE (*R* or *S*). Four lipoxygenase enzymes in the list are representative in holding the fatty acid hydroperoxides in different orientations (head-first or tail-first) and abstracting the stereospecific hydrogen (10*D* or 10*L*) from arachidonate hydroperoxides.

In entries 1 and 2, 5*S*-LOX is used to react with 5-HPETE (*R* or *S*). Mammalian 5-LOX is the enzyme accounting for the production of the bioactive leukotrienes. Recently the collaborator of Brash lab has obtained the crystal structure of human 5-LOX (97). In human, 5-LOX is expressed primarily in various leukocytes, including polymorphonuclear leukocytes (neutrophils and eosinophils), monocytes/macrophages and etc (98). In resting cells, 5-LOX resides in the cytosol. Upon cell stimulation, 5-LOX is targeted to the nuclear membrane where it acquires its substrate arachidonic acid liberated from the membrane by the action of the cytosolic phospholipase A_2 (98). The process requires the participation of several other factors, including Ca^{2+}, membrane containing phosphatidylcholine and the transmembrane protein FLAP (five-lipoxygenase-activating protein), all of which are also necessary for the enzyme to achieve the optimal catalytic activity *in vitro* (92).

Plant 9-LOX is another option to be utilized as an arachidonate 5-LOX. The abundance of linoleic acid (C18.2ω6) and linolenic acid (C18.3ω6) in higher plants makes them the natural substrates for the multiple plant lipoxygenases. The term plant 9-LOX comes from their catalytic activity in the highly specific hydroperoxidation at C9 of linoleic acid. When arachidonic acid is used as substrate, plant 9-LOX tend to form a mixture of chiral hydroperoxides. Potato 9-LOX gives 5*S*-HPETE as the major hydroperoxide (99). *Arabidopsis thaliana* AtLOX1 and tomato LOXA form 11*S*-HPETE and 5*S*-HPETE (100). The substrate binding orientation and the stereospecificity of the hydrogen abstraction were investigated in 1972, and it was shown that corn 9-LOX binds linoleic acid in a head/carboxyl-first manner and stereospecifically abstracts the $11D_R$ hydrogen (9). The head/carboxyl-first binding orientation is also shown by the work of

this lab on the study of *Arabidopsis thaliana* AtLOX1 and tomato LOXA (100). In addition to the 5*S*-lipoxygenation activity, plant 9-LOX could function as a LTA synthase towards fatty acid hydroperoxide. Potato 5-LOX, one of their homologues, is capable of LTA epoxide synthesis and has been used as a model for the study of 5-LOX-catalyzed leukotriene synthesis in earlier studies (48,99,101).

In entries 3 and 4, 8*R*-LOX is used to react with 5-HPETE (*R* or *S*). In 1986 Bundy and colleagues studied the coral *Pseudoplexaura porosa* and uncovered 8*R*-lipoxygenase activity, the first known existence of an *R*-specific lipoxygenase (59). 8*R*-LOX was subsequently found to be widespread in corals including in *P. homomalla* (102) as well as in many marine invertebrates, and a 12*R*-LOX is highly conserved and functionally essential in mammals (94,103). In the late 1990s this lab achieved the purification of a native 8*R*-LOX (60) and the expression of recombinant 8*R*-LOX from AOS-LOX fusion protein from *P. homomalla* (61). In contrast to the head/carboxyl-first binding within 5-LOX, it is deduced that the substrate enters 8*R*-LOX in a tail/methyl-first manner (104).

In entries 5 to 8, two different 15-LOX are used to react with 15-HPETE (*R* or *S*). The reactions of the two enzymes with 15-HPETE differ mainly in two aspects: 1) The reaction of 12/15-LOX with 15*S*-HPETE leads to both 14,15-LTA_4 and double oxygenation products, 8*S*,15*S*-diHPETE and 5*S*,15*S*-diHPETE (55). Soybean LOX-1 converts 15*S*-HPETE exclusively to 8*S*,15*S*-diHPETE and 5*S*,15*S*-diHPETE (105). The formation of the LTA-type product by soybean LOX-1 can be achieved in the anaerobic conditions (30). 2) The substrate orientation. Because there are no X-ray structures available for a LOX with the bound fatty acid substrate (and the fatty acid hydroperoxide), there has always been debate on the route of substrate access to the LOX

catalytic domain (106,107). The reactions using fatty acids esterified in phosphatidylcholine and the investigations about the stereoselective H-abstraction provide clues to the modeling of the lipoxygenase-substrate interaction. It is well accepted that fatty acid (linoleic acid or arachidonic acid) is bound in the tail/methyl-first orientation in both 12/15-LOX and soybean LOX-1. When it comes to the reactions with the fatty acid hydroperoxide (15*S*-HPETE), the substrate binding orientations differ in the two enzymes. The formation of 8*S*,15*S*-diHPETE and 5*S*,15*S*-diHPETE (rather than 8*R*,15*S*-diHPETE and 5*R*,15*S*-diHPETE) from the further oxygenation of 15*S*-HPETE implies that 15*S*-HPETE binds soybean LOX-1 in the head/carboxyl-first orientation (as is shown in entry 7) (108), the reversed orientation of arachidonic acid binding. This is based on the thinking that the substrates (arachidonic acid and 15*S*-HPETE) need to be exposed to the same open ligand position of the active site iron (1). Alternatively in the transformation of 15*S*-HPETE to 14,15-LTA_4 by 12/15-LOX, the stereoselective hydrogen abstraction from 10L position implies that the 15*S*-HPETE binds in the tail/methyl-first orientation in 12/15-LOX during its transformation to the LTA product (47).

Experimental procedures

Materials

Arachidonic acid and its methyl ester were purchased from NuChek Prep Inc. (Elysian, MN). Soybean LOX-1 (lipoxidase, type V) and α-tocopherol were purchased from Sigma.

Expression and purification of *Arabidopsis thaliana* AtLOX1 and coral 8*R*-lipoxygenase

The cDNA of *Arabidopsis thaliana* AtLOX1 were subcloned into the pET14b vector (with an N-terminal His6 tag). The protein was expressed in *E. coli* BL21 (DE3) cells and purified by nickel affinity chromatography.

The cDNA of the 8*R*-LOX domain of the *P. homomalla* peroxidase/lipoxygenase fusion protein was subcloned into the pET3 vector (with an N-terminal His4 tag), and the protein was expressed in *E. coli* BL21 (DE3) cells and purified by nickel affinity chromatography.

Biphasic reaction conditions for preparation of LTA epoxides

Enzyme reactions were performed at 0 °C, with the HPETE substrate initially in hexane (5 ml, bubbled for 30 min prior to use with argon to reduce the O_2 concentration, and containing ~200 μM HPETE) layered over the recombinant LOX enzyme (1-2 mg, ~20 nmol) in 400 μl of Tris buffer (pH 7.5 for human 15-LOX-1 and pH 6.0 for AtLOX1). The reaction was initiated by vigorous vortex mixing of the two phases. After 1.5 min, the hexane phase was collected and scanned from 200-350 nm in UV light by

using a Perkin-Elmer Lambda-35 spectrophotometer. Then the hexane phase was evaporated to about 2 ml under a stream of nitrogen, treated with ethanol (20 µl) and ethereal diazomethane for 10 s at 0 °C and then rapidly blown to dryness and kept in hexane at -80 °C until further analysis.

HPLC analyses

Aliquots of the methylated hexane phase were analyzed by RP-HPLC using a Waters Symmetry column (25 x 0.46 cm), using a solvent of MeOH/20mM triethylamine pH 8.0 (90/10, by volume), at a flow rate of 1ml/min, with on-line UV detection (Agilent 1100 series diode array detector). Further purification was achieved by SP-HPLC using a silica guard column (0.46 × 4.5 cm), using a solvent of hexane/triethylamine (100/0.5, by volume) run at 0.5 ml/min.

NMR analysis

^{1}H NMR and ^{1}H,^{1}H COSY NMR spectra were recorded on a Bruker AV-III 600 MHz spectrometer at 283 K. The parts/million values are reported relative to residual nondeuterated solvent (δ = 7.16 ppm for C_6H_6). Typically, 1024 scans were acquired for a 1-D spectrum on ~20 µg of LTA epoxide.

GC-MS analysis of 5-oxo-ETE

The methoxime derivative was prepared by treatment with methoxylamine hydrochloride (10 mg/ml in pyridine) at room temperature for 16 h. The trimethylsilyl

(TMS) ester derivative was prepared using bis(trimethylsilyl)-trifluoroacetamide/pyridine (12 µl, 5:1, v/v) for 2 h at room temperature. Analysis of the trimethylsilyl ester methoxime derivative was carried out in the positive ion electron impact mode (70 eV) using a Thermo Finnigan Trace DSQ ion trap GC-MS with the Xcalibur data system. Samples were injected at 150 °C, and after 1 min the temperature was programmed to 300 °C at 20 °C/min. The spectrum was recorded by repetitive scanning over the range of m/z 50-500.

Results

The reactions of 15*S*-HPETE with 15-LOX-1in the presence of 13*S*-HPODE or NDGA

In Chapter 1, it was proposed that the non-heme lipoxygenase iron plays a dual role in leukotriene A epoxide biosynthesis, with the ferric iron in catalyzing the initial hydrogen abstraction and the ferrous iron in catalyzing the subsequent hydroperoxide homolytic cleavage. To show that both states of the lipoxygenase iron are necessary for the LTA formation in the reaction of 15*S*-HPETE with human 15-LOX-1, I performed the reaction in the presence of excess 13*S*-HPODE or NDGA. 13*S*-HPODE is not a substrate for human 15-LOX-1 oxygenation reaction. However, the ferrous lipoxygenase iron cleaves the hydroperoxide bond of 13*S*-HPODE and is converted to the ferric state. In the presence of excess 13*S*-HPODE, the lipoxygenase iron is kept at the ferric state. On the other hand, NDGA, an effective lipoxygenase inhibitor acting by reducing the ferric iron to the ferrous form, keeps the lipoxygenase iron in the ferrous state.

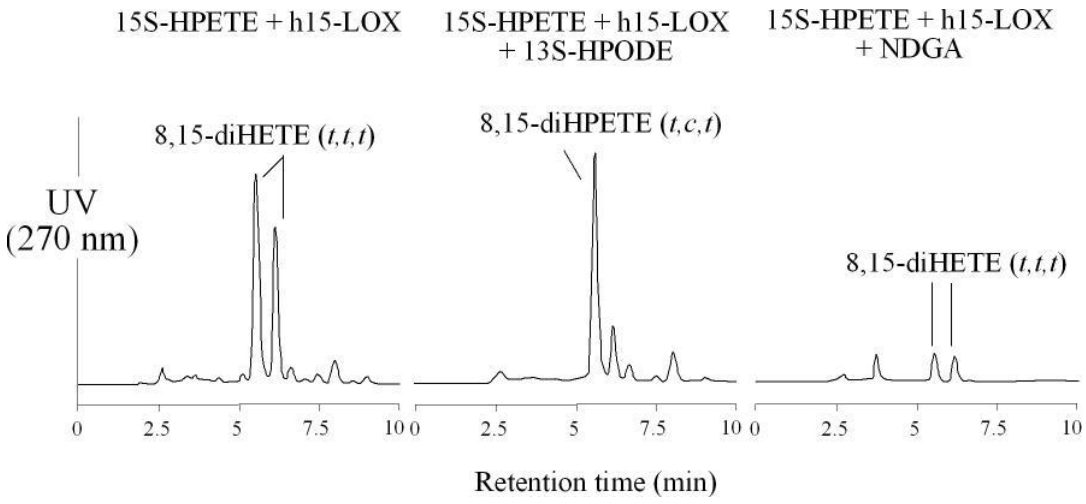

Figure 17: RP-HPLC of reactions of 15*S*-HPETE with human 15-LOX-1
Incubations were performed in a 1 ml reaction buffer (pH 7.5) at room temperature using 15*S*-HPETE (10 μg/ml) and recombinant human 15-LOX-1 (10 μg/ml) (left) in the presence of excess 13*S*-HPODE (50 μg/ml)(middle) or NDGA (10 μM)(right). The same

aliquots of the reaction were analyzed by RP-HPLC using a Waters Symmetry column (25 × 0.46 cm), using a solvent of MeOH/H_2O/HAc (80/20/0.01, by volume), at a flow rate of 1 ml/min, with on-line UV detection at 270 nm.

In the presence of excess 13*S*-HPODE or NDGA, the formation of the LTA epoxide was significantly diminished, which was reflected by the decreased formation of 8,15-diHETE(*t,t,t*), 14,15-LTA_4 non-enzymatic hydrolysis products. This indicates that both states of the lipoxygenase iron are indispensable for the LTA formation. As the ferric iron is the active species in catalyzing the oxygenation reaction, excess 13*S*-HPEDE significantly increased the formation of 8,15-diHPETE*(t,c,t*), the double oxygenation product. The formation of 8,15-diHPETE*(t,c,t*) was almost completely abolished by NDGA (**Figure 17**). The identification of the non-enzymatic hydrolysis products 8,15-diHETE (*t,t,t*) and the double oxygenation product 8,15-diHPETE (*t,c,t*) is based on co-chromatography with authentic standards and their characteristic UV spectra (105).

Synthesis and purification of enantiomeric fatty acid hydroperoxides

5-HPETE (*R* or *S*) and 15-HPETE (*R* or *S*) are the fatty acid hydroperoxides used in the reactions listed in **Figure 16**. For the purpose of producing LTA products in sufficient amounts for NMR analysis, the fatty acid hydroperoxide substrates need to be in the milligram quantities. Preparing the pure enantiomeric fatty acid hydroperoxides is an expertise of this laboratory. The desired hydroperoxide can be produced via the controlled autoxidation or the enzymatic synthesis followed by HPLC purification.

1) Preparation of 5*S*-HPETE, 5*R*-HPETE and 15*R*-HPETE

Racemic hydroperoxides were prepared by vitamin E-controlled autoxidation (109). Arachidonic acid methyl ester (500 mg) was transferred to a 2 L round-bottomed flask, mixed with 10% (w/w) α-tocopherol, evaporated to dryness, and the flask filled with oxygen, capped and placed in an oven at 37 °C. The oxygen was replenished daily. After 3 days, the lipid was dissolved in 10 ml of methylene chloride and stored at -30 °C. The autoxidation sample was first fractionated and partly purified using a 5 g silica Bond-Elut (Varian) with the solvents of hexane/ethyl acetate (three fractions of 10 ml of 95/5, followed by three of 10 ml of 90/10, and then three of 10 ml of 85/5, v/v); the HPETE methyl esters eluted in fractions 6 through 9. Racemic 5-HPETE and 15-HPETE methyl esters were then separated from other positional HPETE isomers by SP-HPLC using a semi-preparative Beckman Ultrasphere 10μ silica column (25 x 1 cm) with a solvent system of hexane/isopropanol (100/1, by volume) run at a flow rate of 4 ml/min. Finally the enantiomeric HPETE methyl esters were resolved using a semi-preparative Chiralpak AD column (Chiral Technologies Inc.), 25 x 1 cm, with a solvent system of hexane/methanol (100/2, by volume) run at a flow rate of 4 ml/min (110).

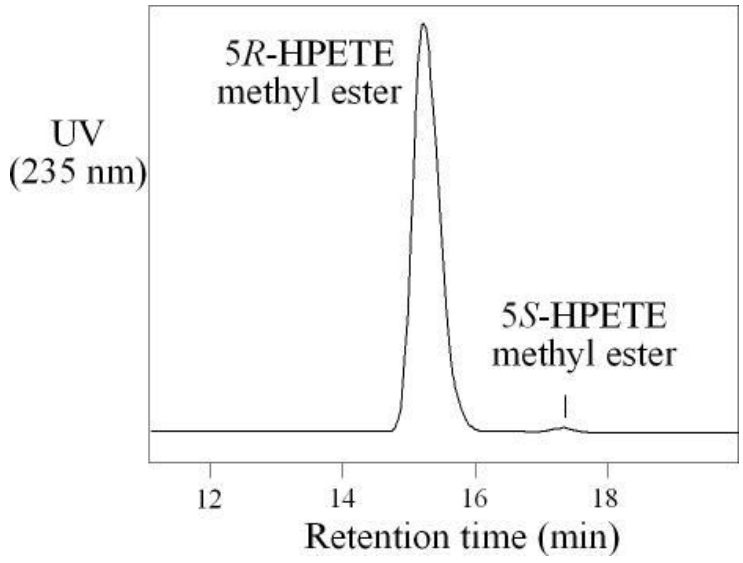

Figure 18: Chiral HPLC of purified 5*R*-HPETE. Chiralpak AD column (Chiral Technologies Inc.), 25 x 0.46 cm, with a solvent system of hexane/methanol (100/2, by volume) run at a flow rate of 4 ml/min.

To prepare the corresponding free acids, the purified HPETE methyl esters (1 mg) in 2 ml methanol/methylene chloride (10/1, by volume) were brought to room temperature, an equal volume of 1M KOH was added, mixed and the sample kept at room temperature under an atmosphere of argon with occasional sonication in a water bath. After 20 min, the sample was acidified to pH 4.5 and extracted with an equal volume of methylene chloride. The organic phase was washed twice with water and then evaporated to dryness under a stream of nitrogen. The dried sample was redissolved in methanol (for 15-HPETE) or acetonitrile (for 5-HPETE, long-time storage of 5-HPETE in the alcohol solvent produces 5-HPETE ethyl ester) and stored at -30 °C. HPETEs were quantified based on the conjugated diene chromophore at 236/237 nm, ε = 25,000 (10 μg/ml = 0.75 AU).

2) Enzymatic preparation of 15*S*-HPETE

15*S*-HPETE is prepared by the reaction of arachidonic acid with the commercially available soybean LOX-1 followed by SP-HPLC purification (hexane/IPA, 100/2, by volume).

Reactions of 5-HPETE (*R* or *S*) with 5-LOX

In reactions 1 and 2 (**Figure 16**), 5-HPETE (*R* or *S*) is reacted with 5-LOX. Considering the requirement that the LOX enzyme used in the biphasic reactions should have a very high catalytic activity (which our available preparations of mammalian 5-LOX do not), I switched to the use of recombinant plant 9-LOX, *Arabidopsis thaliana* AtLOX1 and tomato LOXA, as the arachidonate 5-LOX.

To test the LTA synthase activity of AtLOX1 and tomato LOXA, arachidonic acid was incubated with these two enzymes separately and the reactions were monitored by UV spectrometer. Both enzymes showed a strong activity catalyzing the mono-oxidation of the arachidonic acid substrate, which was reflected by the rapid appearance of a chromophore with the maximal absorbance at ~237 nm. However, while AtLOX1 further converted the mono-hydroperoxides to the secondary metabolites, tomato LOXA showed little secondary transformation (data not shown).

Further investigations were performed on the conversions of enantiomeric 5-HPETEs by AtLOX1 **(Figure 19)**. RP-HPLC of the reaction with 5*S*-HPETE demonstrated that AtLOX1 mainly generated 5,12-diHETE (*t,t,t*), the non-enzymatic hydrolysis products of LTA_4. With 5*R*-HPETE as substrate, AtLOX1 also demonstrated LTA synthase activity. In addition, 5-oxo-eicosatetraenoic acid (5-oxo-ETE) was

generated and was further converted to 5-oxo-12-hydroperoxy-ETE which absorbs UV at 320 nm.

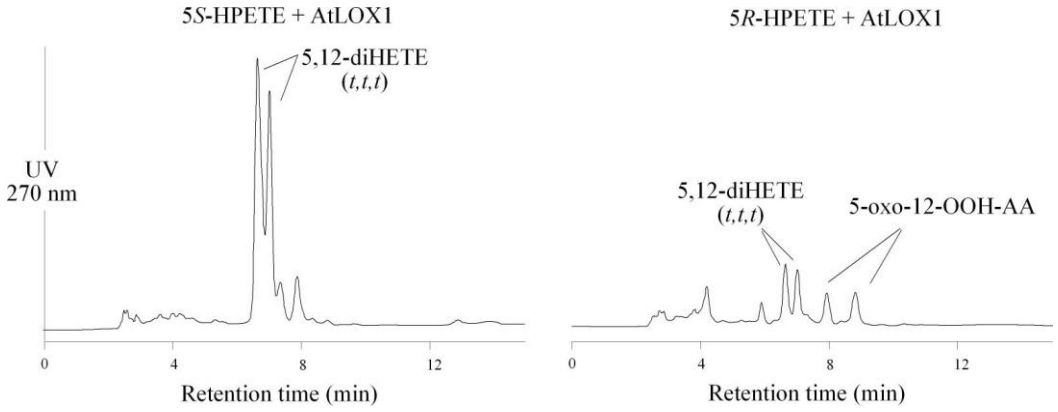

Figure 19: RP-HPLC of *Arabidopsis thaliana* AtLOX1 incubations with 5*S*-HPETE or 5*R*-HPETE. Waters Symmetry column (25 x 0.46 cm), MeOH/H_2O/HAc:80/20/0.01 (by volume), 1 ml/min.

Since AtLOX1 demonstrated LTA synthase activity towards both 5*S*-HPETE and 5*R*-HPETE, I applied the biphasic reaction system developed in Chapter 2 to the reactions of AtLOX1 with the enantiomeric 5-HPETE (**Figure 20**).

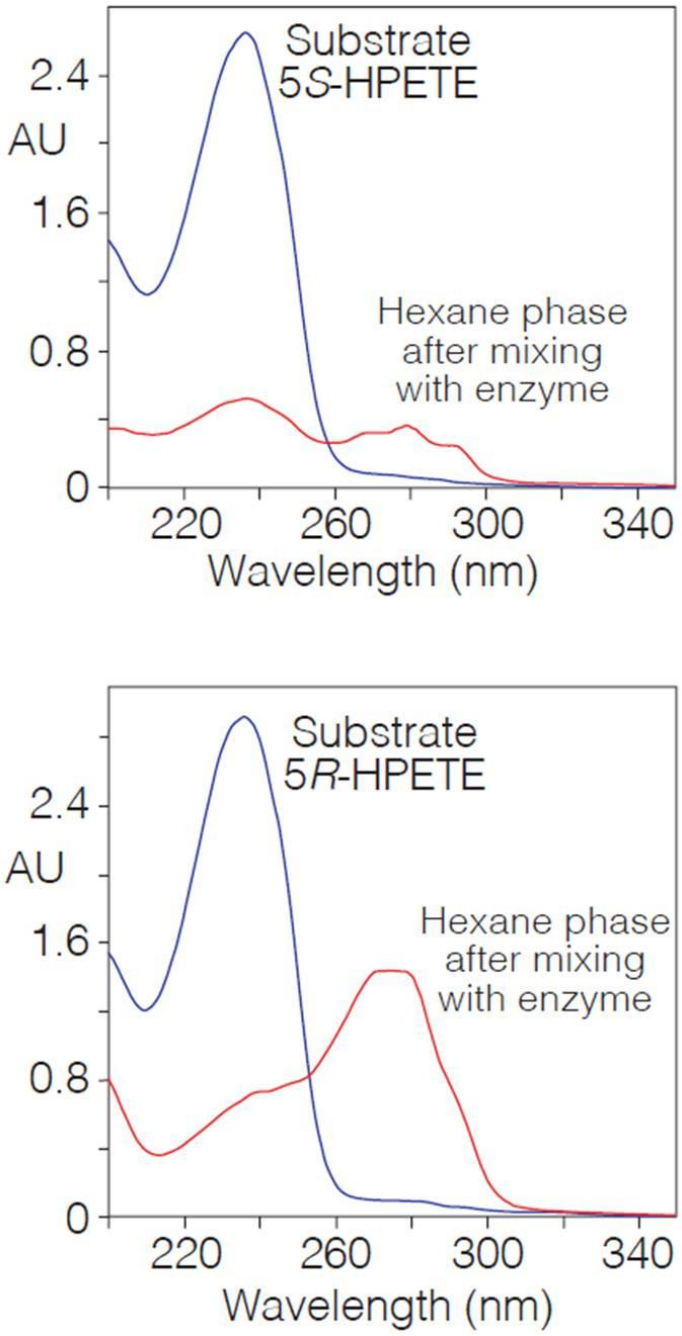

Figure 20: UV spectrum of 5*S*-HPETE (top) and 5*R*-HPETE (bottom) in hexane before and after vortex mixing with 5-LOX enzyme (AtLOX1).

After vortex mixing of AtLOX1 with 5*S*-HPETE at 0 °C, UV spectroscopy of the hexane phase showed a decrease in substrate and appearance of a new chromophore with

λmax at 280 nm, characteristic of LTA_4 epoxide. Incubation of the 5*R* enantiomer of 5-HPETE with 5-LOX was performed under the same conditions. UV spectroscopy of the hexane phase after vortex mixing showed the appearance of a less well-defined spectrum in the 280 nm region, comprised of a mixture (**Figure 20**).

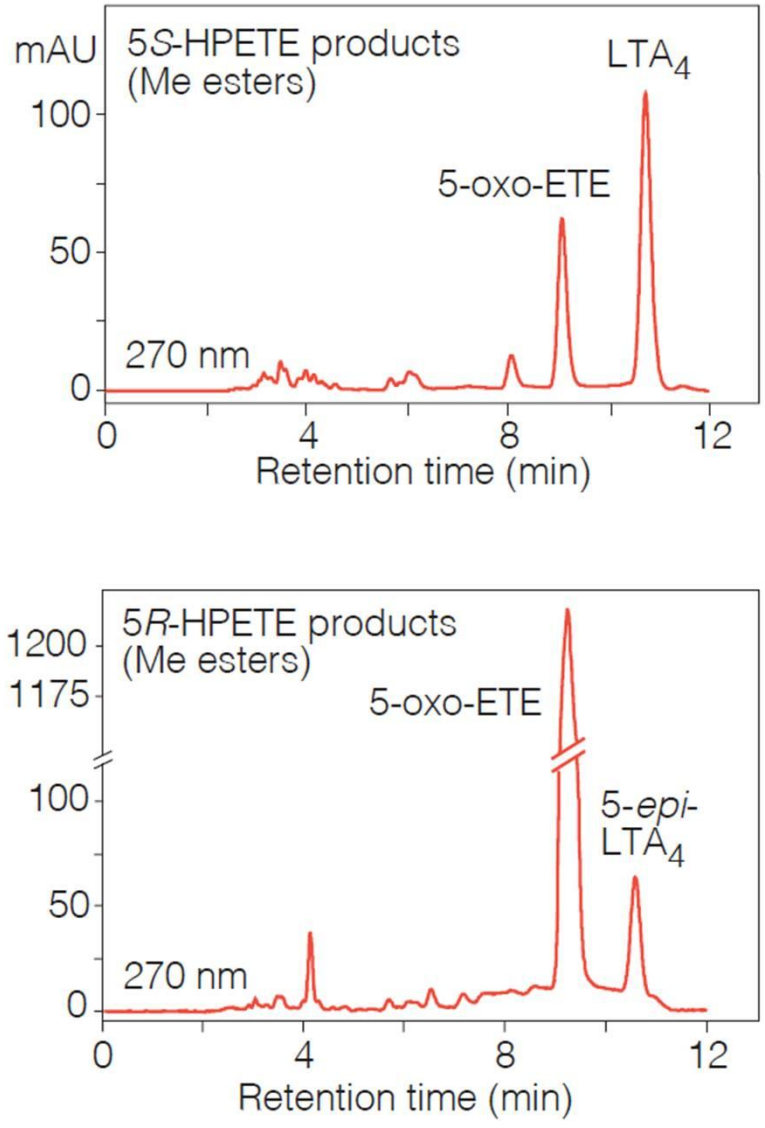

Figure 21: RP-HPLC analyses of the product methyl esters from 5*S*-HPETE (top) and 5*R*-HPETE (bottom). Column: Waters Symmetry C18, 25 x 0.46 cm; solvent, methanol/20mM triethylamine pH 8.0 (90/10, by volume); flow rate, 1 ml/min, UV detection at 270 nm.

After methyl esterification with diazomethane, the products were analyzed by RP-HPLC (**Figure 21**). Incubation of 5*S*-HPETE with AtLOX1 mainly generated LTA_4, whereas two products were derived from 5*R*-HPETE incubation. The major product from 5*R*-HPETE exhibited a dienone chromophore with λmax in MeOH/H2O (90:10) at 281 nm. Its structure was identified as 5-oxo-eicosatetraenoic acid (5-oxo-ETE) by GC-MS analysis of its TMS ester methoxime derivative (**Figure 22**), and by reduction with NaBH4 to 5-hydroxyeicosatetraenoic acid (5-HETE), identified by comparison to an authentic standard.

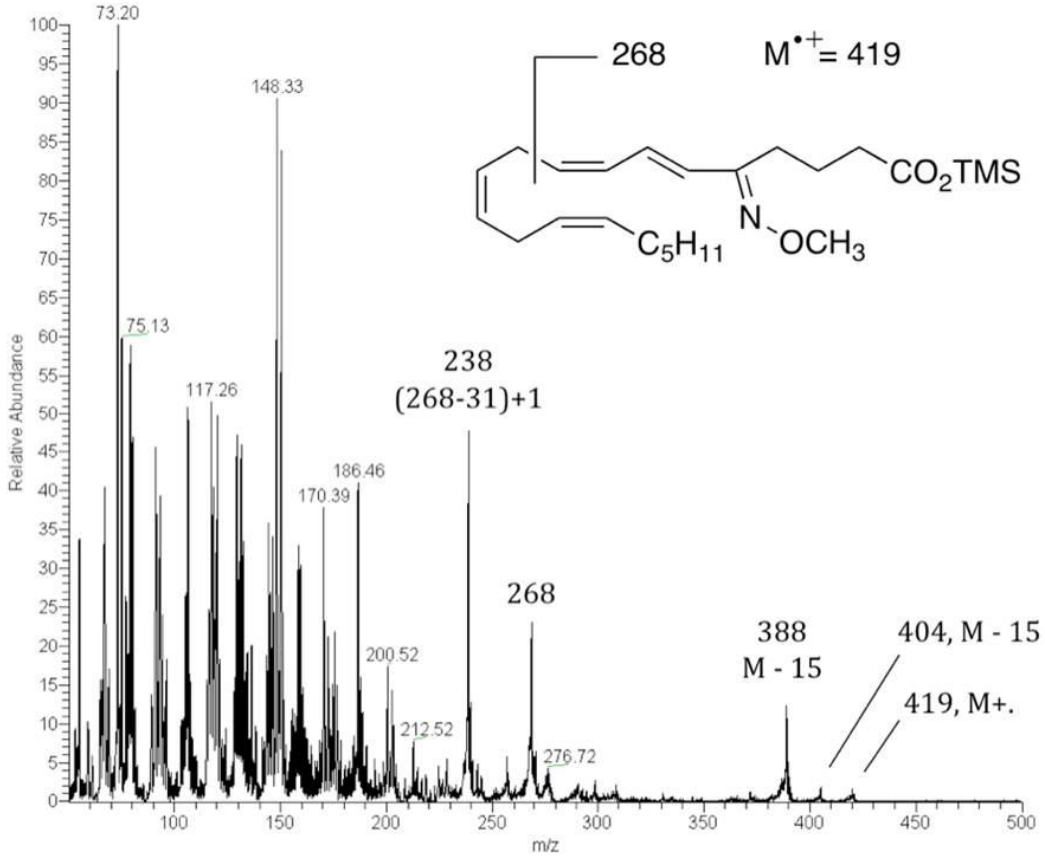

Figure 22: GC/MS analysis of 5-oxo-ETE TMS ester methoxime derivative.

The complete structures of LTA products from 5*S*- and 5*R*-HPETE were then established by 1H-NMR (**Figure 23**).

	Chemical Shift (ppm)			Coupling Constants (Hz)	
Protons	LTA_4 Me	5-*epi*-LTA_4 Me	J	LTA_4 Me	5-*epi*-LTA_4 Me
2	2.05	2.05	$J_{2,3}$	7.4	7.3
3	1.31	1.31	$J_{3,4}$		
4	1.59	1.58	$J_{4,5}$	5.6	6.1
5	2.53	2.75	$J_{5,6}$	1.8	4.3
6	2.91	3.19	$J_{6,7}$	7.9	7.6
7	5.29	5.4-5.5	$J_{7,8}$	15.2	15.2
8	6.33	6.37	$J_{8,9}$	11.0	10.9
9	6.11	6.11	$J_{9,10}$	14.8	14.8
10	6.56	6.54	$J_{10,11}$	11.2	11.2
11	6.05	6.03	$J_{11,12}$	11.2	11.2
12	5.4-5.5	5.4-5.5	$J_{12,13}$	6.1	6.3
13	2.95	2.94	$J_{13,14}$	6.1	6.3
14	5.4-5.5	5.4-5.4	$J_{14,15}$		
15	5.4-5.5	5.4-5.4	$J_{15,16}$		
16	2.03	2.03	$J_{16,17}$		
17	1.2-1.3	1.2-1.3	$J_{17,18}$		
18	1.2-1.3	1.2-1.3	$J_{18,19}$		
19	1.2-1.3	1.2-1.3	$J_{19,20}$		
20	0.88	0.88			

Figure 23: Proton chemical shifts and coupling constants for LTA_4 methyl ester and 5-*epi*-LTA_4 methyl ester in C6D6.

Most importantly, this confirmed the 5,6-*trans* configuration of the epoxide derived from 5*S*-HPETE ($J_{5,6}$ = 2 Hz) and the 5,6-*cis* configuration of the epoxide derived from 5*R*-HPETE ($J_{5,6}$ = 4 Hz), thus identifying the product from 5*S*-HPETE as the 5*S*,6*S trans*

epoxide, LTA_4 and the product from 5R-HPETE as the 5*R*,6*S* *cis* epoxide, 5-*epi*-LTA_4 (**Figure 24**).

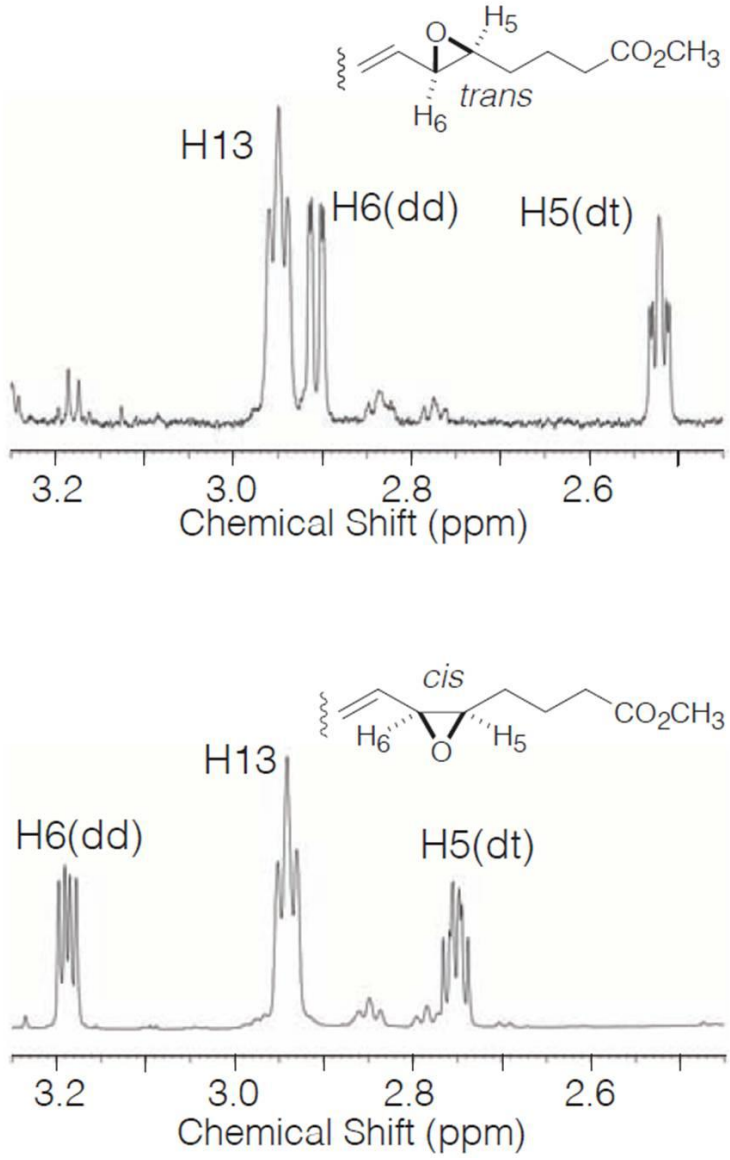

Figure 24: Partial ^{1}H-NMR spectrum (2.45 – 3.25 ppm) of the *trans*-LTA epoxide product from 5*S*-HPETE (top) and the *cis*-LTA epoxide product from 5*R*-HPETE (bottom).

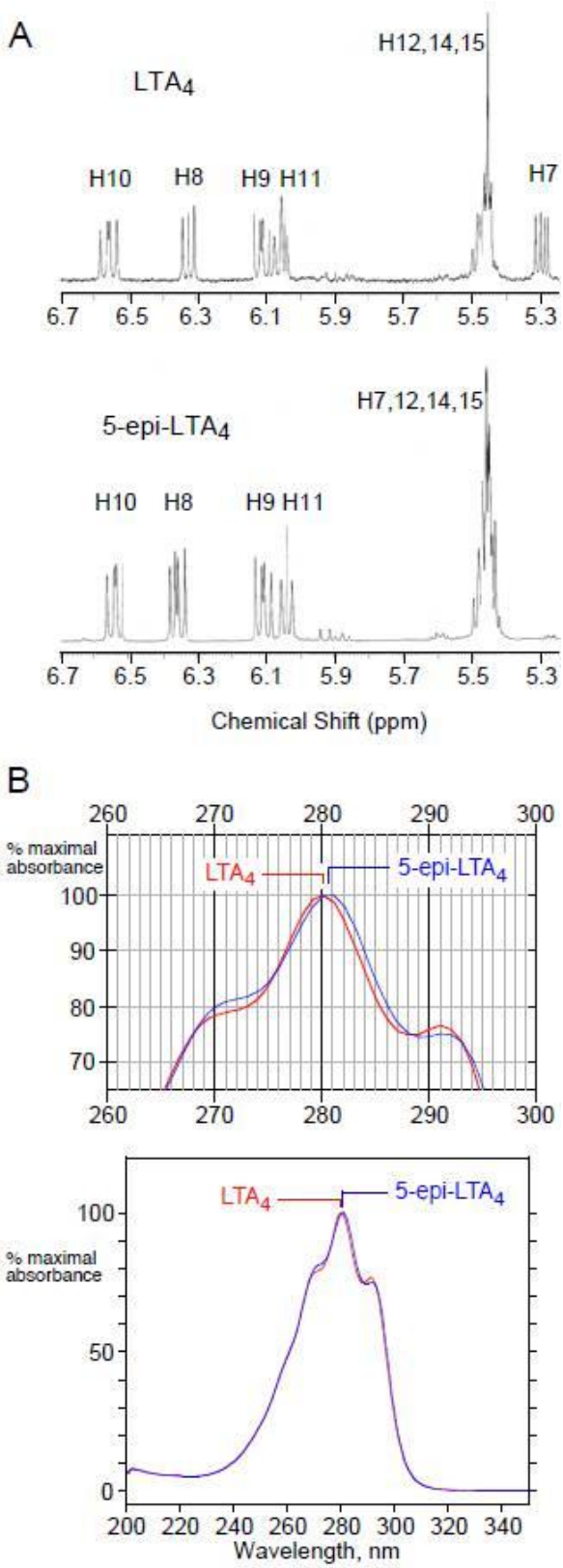

Comparison of the NMR spectra of LTA_4 and its 5-epimer also defined their identical double bond configurations as 7*E*,9*E*,11*Z*,14*Z* (**Figure 25**). Their UV spectra are almost superimposable, with the difference only discernable with the two overlaid.

Figure 25: Spectral comparison of LTA_4 and 5-*epi*-LTA_4
A, NMR spectra of the olefin protons in LTA_4 and 5-*epi*-LTA_4 methyl esters. B, overlay of the UV spectra of LTA_4 and (5*R*,6*S*) 5-*epi*-LTA_4. Top: detailed view. Below: full spectra, 200-350 nm. (LTA_4 has λ_{max} as 280 nm and 5-*epi*-LTA_4 has λ_{max} as 281 nm.)

Reactions of 5-HPETE (*R* or *S*) with 8*R*-LOX

In reactions 3 and 4 (**Figure 16**), 5-HPETE (*R* or *S*) is reacted with 8*R*-LOX. To test the LTA synthase activity of 8*R*-LOX, the incubation was first performed on the racemic 5-HPETE by the recombinant 8*R*-LOX from AOS-LOX fusion protein from *P. homomalla*. RP-HPLC analysis of the incubation demonstrated that the major products are double oxygenation products 5,12-diHPETEs and 5,8-diHPETEs, with the second hydroperoxidation on either C8 or C12 position (**Figure 26**). 5,8-diHPETEs are the bis-allylic hydroperoxides with a relatively high λ_{max} at 242 nm. It is notable that detection of this type of bis-allylic fatty acid hydroperoxides is uncommon especially from a room-temperature incubation. This implies that there is a highly efficient hydrogen donor within the 8*R*-LOX active site.

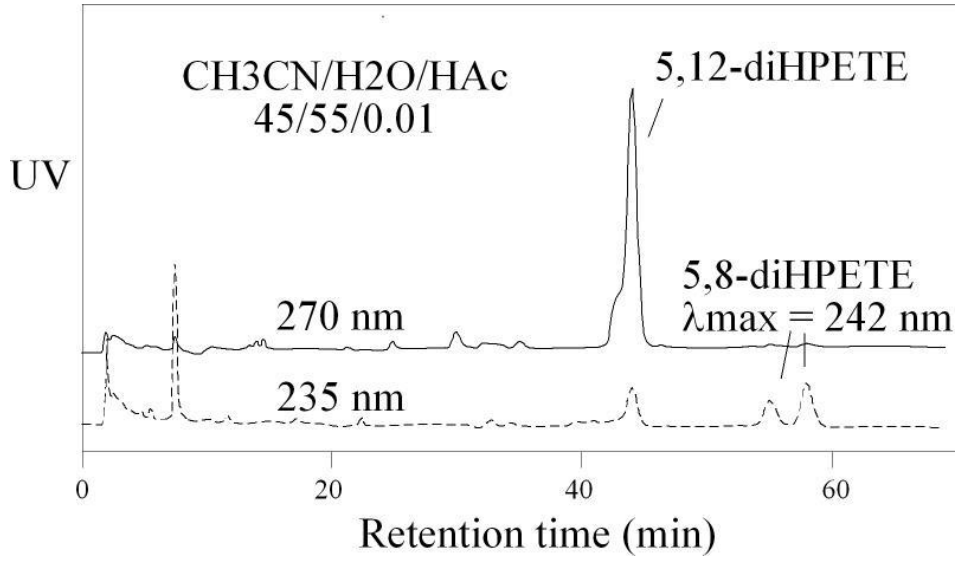

Figure 26: RP-HPLC of incubation of the racemic 5-HPETE with 8*R*-LOX. Column: Waters Symmetry C18, 25 x 0.46 cm; solvent, CH_3CN/H_2O/HAc (45/55/0.01, by volume); flow rate, 1 ml/min.

As the indicator of the LTA epoxide formation, the non-enzymatic hydrolysis products 5,12-diHETEs (*t,t,t*) were not significantly detected from the RP-HPLC analysis (**Figure 26**). The similar product profile was obtained when the native 8*R*-LOX purified from *P. homomalla* was used in the incubation.

Reactions of 15-HPETE (*R* or *S*) with 12/15-LOX

In reactions 5 and 6 (**Figure 16**), 15-HPETE (*R* or *S*) is reacted with 12/15-LOX. In Chapter 2, reaction 5 (incubation of 15*S*-HPETE with 12/15-LOX) is the model reaction based on which the biphasic synthesis and instantaneous extraction method was developed to produce the LTA epoxide in the amount sufficient for NMR analysis. To investigate the significance of substrate chirality to the LTA epoxide formation, I examined the reaction of human 15-LOX-1 with the mirror image substrate, 15*R*-HPETE (**Figure 27**).

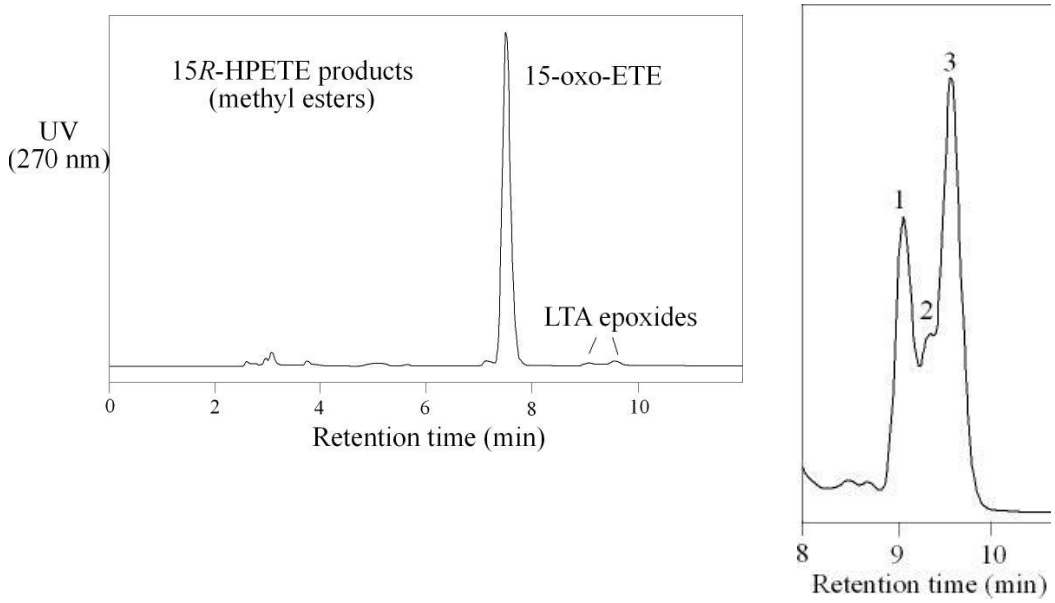

Figure 27: RP-HPLC analysis of the product methyl esters from the biphasic reaction of 15*R*-HPETE with human 15-LOX-1. Column: Waters Symmetry C18, 25 x 0.46 cm; solvent: methanol/20mM triethylamine pH 8.0 (90/10, by volume); flow rate: 1 ml/min,

UV detection at 270 nm. Right: RP-HPLC chromatogram over the range of LTA epoxide products.

Similar to the reaction of 5*R*-HPETE with AtLOX1, RP-HPLC analysis of the reaction between 15*R*-HPETE and human 15-LOX-1 showed that the predominant product was 15-oxo-ETE. The yield of the LTA epoxides is low and NMR analysis of their stereochemistry becomes difficult. In addition, there are three LTA products resolved on RP-HPLC. By comparison to the standard, peak 3 is the 14,15-LTA_4. According to that 5-*epi*-LTA_4 (*cis*-epoxide) elutes earlier than LTA_4 (*trans*-epoxide) on this RP-HPLC system, peak 1 or peak 2 is likely to be the 15-*epi*-14,15-LTA_4.

Reactions of 15-HPETE (*R* or *S*) with soybean LOX

In reactions 7 and 8 (**Figure 16**), 15-HPETE (*R* or *S*) is reacted with soybean LOX-1. Soybean LOX-1 is generally considered as the prototypical LOX enzyme. Unlike mammalian 5-LOX which transforms its primary product 5*S*-HPETE almost exclusively to LTA_4, soybean LOX-1 normally produces no detectable leukotrienes. Instead soybean LOX-1 further oxygenates its primary product 15*S*-HPETE to 5,15-diHPETE and 8,15-diHPETE. It is reasoned that the high availability of molecular oxygen within the LOX active sites results in this reaction outcome.

In this lab, it has been demonstrated that under anaerobic conditions soybean LOX-1 converted 15*S*-HPETE partly to a pair of 8,15-diHETEs with all-*trans*-conjugated trienes, the non-enzymatic hydrolysis products of the 14,15-LTA_4 epoxide. However, by applying the biphasic reaction system to the reaction of 15*S*-HPETE with soybean LOX-1, no significant LTA epoxide formation was detected.

In the original paper showing the LTA synthase activity of soybean LOX-1, the incubation time required to produce 8,15-diHETEs (*t,t,t*) was relatively long (2 hours) and the anaerobic conditions were achieved by using an N_2-inflated Aldrich Atmosbag. The short reaction time (a compromise between the substrate consumption and the product stability) and the incomplete oxygen exclusion from the reaction environment (molecular oxygen is excluded by bubbling the reaction solvent with argon for 20 min) may constitute two factors that prevent the biphasic reaction system being applied to the soybean LOX-1 reactions.

Discussion

The two purposes of this project were to enable the direct structural analysis of the unstable LTA-type epoxides from lipoxygenase reactions and to further the understanding of factors that control their precise stereochemistry. In Chapter II, methods were developed to isolate and directly NMR characterize 14,15-LTA_4 from the reaction of 15*S*-HPETE with human 15-LOX-1. In this chapter, the methods were applied to a list of reactions of different enantiomeric fatty acid hydroperoxides and lipoxygenase enzymes. The reactions listed in **Figure 16** reflect the combinations of different factors that might contribute to the stereochemistry control of the resulting LTA products. The factors include 1) the chirality of the substrate hydroperoxide group, 2) the stereo-specific hydrogen abstraction by the lipoxygenase enzyme and 3) the substrate binding orientation within the enzyme active site.

Isolation and direct NMR analysis of LTA products were achieved in three reactions listed in **Figure 16**. They are the reactions of 5*S*-HPETE with AtLOX1, 5*R*-HPETE with AtLOX1 and 15*S*-HPETE with human 15-LOX-1. The application of the biphasic system to the other five reactions led to the minimal production of LTA products. In these "failed" reactions other products dominate. Soybean LOX-1 and coral 8*R*-LOX turn out to be poor LTA synthases, the most significant secondary products being the double oxygenation products. In the reaction of 15*R*-HPETE with human 15-LOX-1, the major product is the keto derivative, 15-oxo-eicosatetraenoic acid (15-oxo-ETE). In the reaction of 5*R*-HPETE with AtLOX1, the major product is 5-oxo-ETE which is much more prominent than 5-*epi*-LTA_4. The biosynthesis of keto derivatives from the fatty acid hydroperoxides is both biologically and mechanistically interesting.

Instead of being involved in the metabolic inactivation, the keto derivative could function as a highly potent chemoattractant or act an electrophile which is to adduct with the nucleophilic amino acid residues in the biologically important proteins (26). Mechanistically, it has been well established that 5-HETE (reduced form of 5-HPETE) is oxidized to 5-oxo-ETE by 5-hydroxyeicosanoid dehydrogenase. My results here show that the keto derivative could be directly produced from the fatty acid hydroperoxide by a specific lipoxygenase. The lipoxygenase transformation from the fatty acid hydroperoxide to the corresponding keto derivative is supposed to be initiated by the homolytic cleavage of the hydroperoxide group which is catalyzed by the ferrous non-heme iron (**Figure 28**).

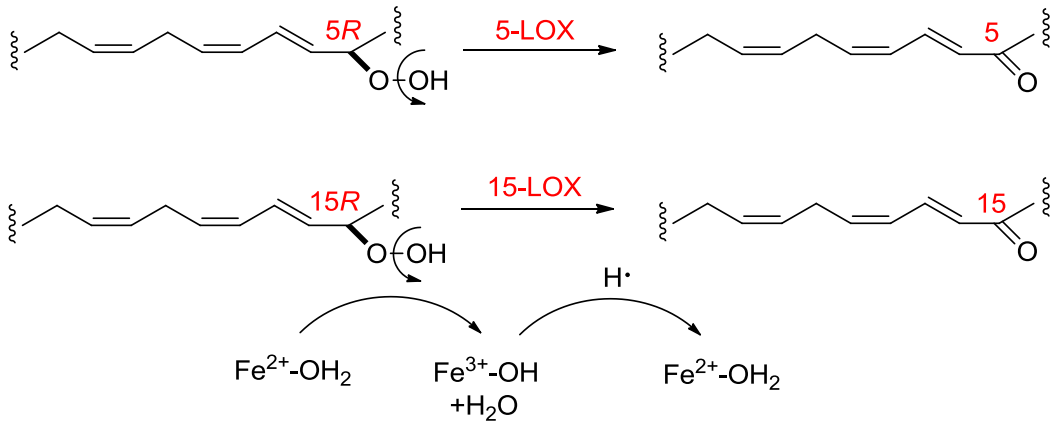

Figure 28: Dehydration of fatty acid hydroperoxides to keto derivatives by lipoxygenase

In order to understand the relationship between the control factors and the resulting product stereochemistry, I focused on the reactions of the enantiomeric 5-HPETE with AtLOX1 in which the biphasic system was successfully applied and the structures of the resulting LTA products were unequivocally established by NMR analysis. The structure

of the classic 5-lipoxygenase product, LTA_4, was confirmed directly from the reaction of 5*S*-HPETE with the recombinant 5-LOX, AtLOX1. More importantly, incubation of 5*R*-HPETE with AtLOX1 produced 5*R*,6*S* *cis* epoxide, 5-*epi*-LTA_4.

To explain the observations that enantiomeric 5-HPETEs produced *trans*- or *cis*-LTA epoxide by the same lipoxygenase enzyme, we developed a conceptual model underlying the mechanistic basis of the LOX-catalyzed transformation of HPETE precursor to LTA-type epoxide (**Figure 29**). The non-heme iron in the LOX active site must be involved in the initial hydrogen abstraction from the HPETE substrate, and cleavage of the hydroperoxide moiety. Key to our thinking, therefore, is that the hydrogen and hydroperoxide should exhibit a suprafacial relationship. As the conversion of [10*R*-^{3}H]5-HPETE to LTA_4 is associated with a primary isotope effect resulting in an enrichment in the specific activity of the unreacted substrate (49,65,66), this provides critical evidence identifying the 10pro-*R* hydrogen abstraction as the first irreversible step in leukotriene A_4 biosynthesis. In turn, this implicates the ferric iron (hydroxide) in 5-LOX as the active species catalyzing the first step of the transformation from 5-HPETE. The observation that reducing inhibitors of the lipoxygenase that leave the active site iron in the ferrous state block both the dioxygenase reaction and LTA synthesis provides further support for involvement of the ferric iron in catalyzing the initial hydrogen abstraction:

$$Fe^{3+}—OH + HR-OOH \rightarrow Fe^{2+}—OH_2 + \cdot ROOH$$

Further reaction will entail homolytic cleavage of the hydroperoxide, thus cycling the lipoxygenase ferrous iron back to ferric, as radical recombination produces the epoxide product:

$$Fe^{2+}—OH_2 + \cdot ROOH \rightarrow Fe^{3+}—OH_2 + H_2O + R(O)$$

It follows from this that the iron must have access to the initial hydrogen abstracted, as well as the hydroperoxide, i.e. the two are on the same face of the substrate. In achieving this, 5*S*-HPETE (the natural enantiomer) must assume the *transoid* conformation at the 5-carbon, thus dictating the natural trans-epoxy configuration of LTA4 (**Figure 29A**). The enantiomeric substrate, 5*R*-HPETE, on the other hand has to assume the *cisoid* conformation, which results in its transformation to 5-*epi*-LTA4, now established experimentally (**Figure 29B**).

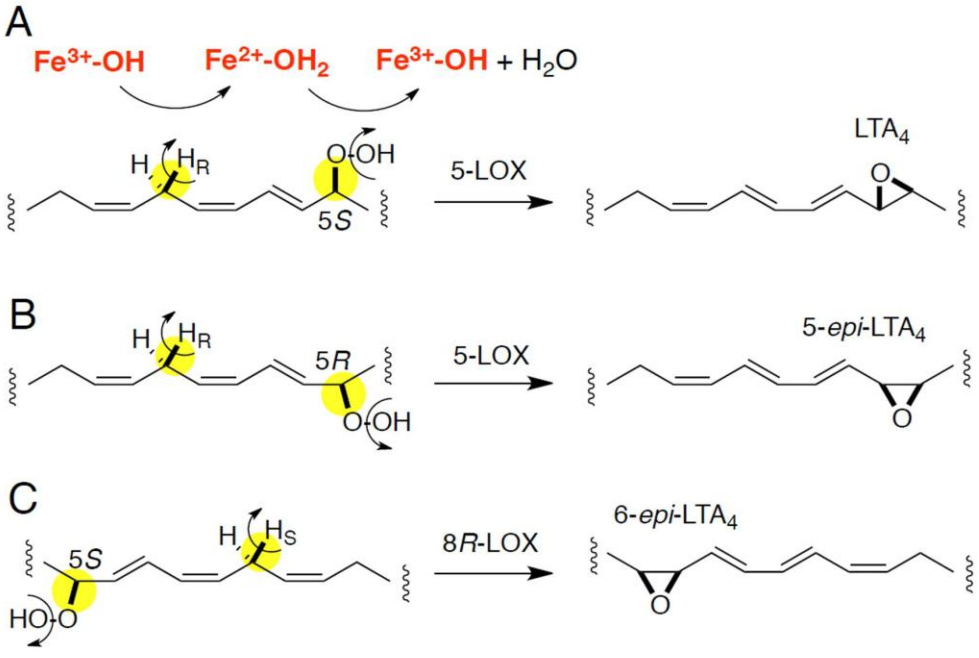

Figure 29: Lipoxygenase-catalyzed transformations to LTA epoxides involve a dual role of the lipoxygenase non-heme iron.

To complete the picture with related transformations, **Figure 29C** illustrates the result reported by E. J. Corey and coworkers, in which an 8*R*-LOX activity, which catalyzes pro-*S* hydrogen abstraction from C-10, converted 5*S*-HPETE to the *cis* epoxide, 6-*epi*-LTA_4; by contrast, 5*S*-LOX, which abstracts the 10pro-*R* hydrogen produced trans-epoxy LTA_4 from 5*S*-HPETE, as expected. The epoxides were identified indirectly based on a difference in pattern of the hydrolysis products in comparison to hydrolysis of the synthetic standards. As it is now known that *R* and *S* lipoxygenases are closely related enzymes and that substrate is exposed to the same open ligand position of the active site iron, we deduce that the 5*S*-HPETE substrate binds in an opposite head-to-tail orientation in 5*S*-LOX and 8*R*-LOX in order to present the appropriate C-10 hydrogen for abstraction by the non-heme iron. Accordingly the substrate is shown in the reversed orientation in the 8R-LOX reaction illustrated in **Figure 29C**.

The concepts developed here on the determinants of *cis* or *trans* LTA_4 epoxide configuration establish a rational mechanism underlying the structures of these key biosynthetic intermediates. The concepts can be applied to the enzymatic formation of novel LTA-type epoxides postulated as intermediates in biosynthesis of the resolvin, protectin and maresin lipid mediators from eicosapentaenoic (20:5ω3) and docosahexaenoic (22:6ω3) fatty acids. In fact, because *S*-lipoxygenases predominate in higher animal biology, and are implicated in the synthesis of the resolvin/protectin/maresin mediators, it is very likely that novel transformations involving the LTA-type epoxides in higher animals follow the same relationships as in the 5*S*-LOX pathway to the leukotrienes. Isolation and identification of these intermediates are presented in **Chapter IV**.

CHAPTER IV

SYNTHESIS AND STRUCTURAL ANALYSIS OF NOVEL EPOXIDES IN LIPOXYGENASE PATHWAYS OF DHA AND EPA METABOLISM

Introduction

ω-3 fatty acid-derived bioactive lipid mediators

The beneficial effects of omega-3 polyunsaturated fatty acids (PUFAs) on human health have been debated for years. One example is that treatment with marine derived omega-3 fatty acids for the prevention of major cardiovascular adverse outcomes has been supported by a number of randomized clinical trials (RCTs) and refuted by others (111,112). One of the best approaches to address this issue is to directly investigate the functional basis of omega-3 PUFA on human health and disease. In most experimental systems, where the actions of omega-3 fatty acids were assessed, the concentrations required to evoke beneficial effects are usually in the high range (from high microgram to high milligram). One reasonable conclusion is that administration with the high dose of omega-3 PUFA diverts the *in vivo* fatty acid metabolism away from transformation of omega-6 fatty acid arachidonic acid, thus decreasing the production of pro-inflammatory prostaglandins and leukotrienes, the "bad guys" in promoting inflammation. On the other hand, multiple studies emerged during the last decade supporting the important roles

played by the potent local bioactive mediators derived from omega-3 PUFA. The term "specialized pro-resolving mediators" (SPM) was chosen for this class of mediators due to their dual anti-inflammation and pro-resolution role.

Almost all the original studies on these novel bioactive lipid mediators are from the laboratory of Dr. C. N. Serhan at Harvard University (**Figure 30** and **Figure 31**). The SPMs produced from EPA were first isolated from resolving exudates of mice which were pre-injected with TNF-α and treated with EPA and aspirin. The exudates proved to contain 18*R*-hydroxy-eicosapentaenoic acid (18*R*-HEPE) (113). The first bioactive product isolated from exudates, coined Resolvin E1 (RvE1, "E" for EPA), reduced inflammation and blocked human PMN trans-endothelial migration. Its complete structure was established as 5*S*,12*R*,18*R*-trihydroxy-6*Z*,8*E*,10*E*,14*Z*,16*E*-eicosapentaenoic acid, an analogue of arachidonic acid-derived lipoxins (75). The most likely human pathway was reconstructed *in vitro*, demonstrating that the sequential actions of firstly vascular endothelial cells and then PMNs are involved in RvE1 formation (113). A second bioactive member of the E series Resolvins that is produced during RvE1 biosynthesis was identified as 5*S*,18*R*-dihydroxy-EPA (114). Recently the same lab presented evidence for new 18*S* series resolvins (115). Aspirin increased formation of 18*S*-HEPE compared with 18*R*-HEPE, and 18*S*-HEPE was further converted to 18*S*-resolvin E1 by human recombinant 5-lipoxygenase and recombinant LTA_4 hydrolase.

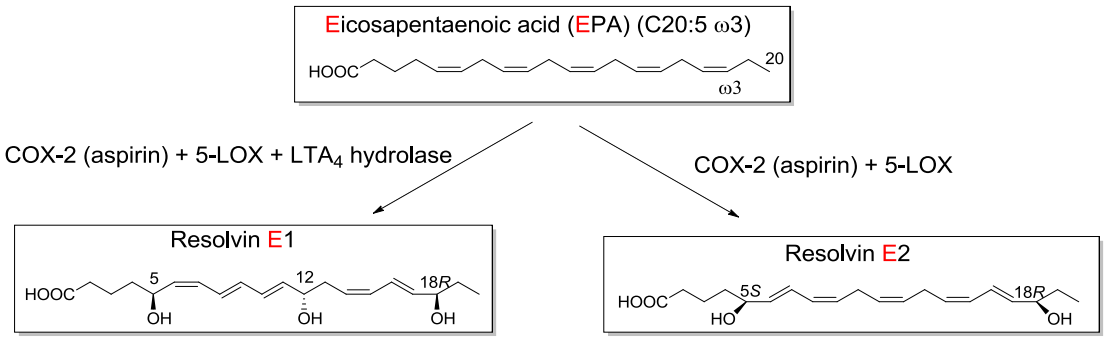

Figure 30: Biosynthesis of novel SPMs from EPA

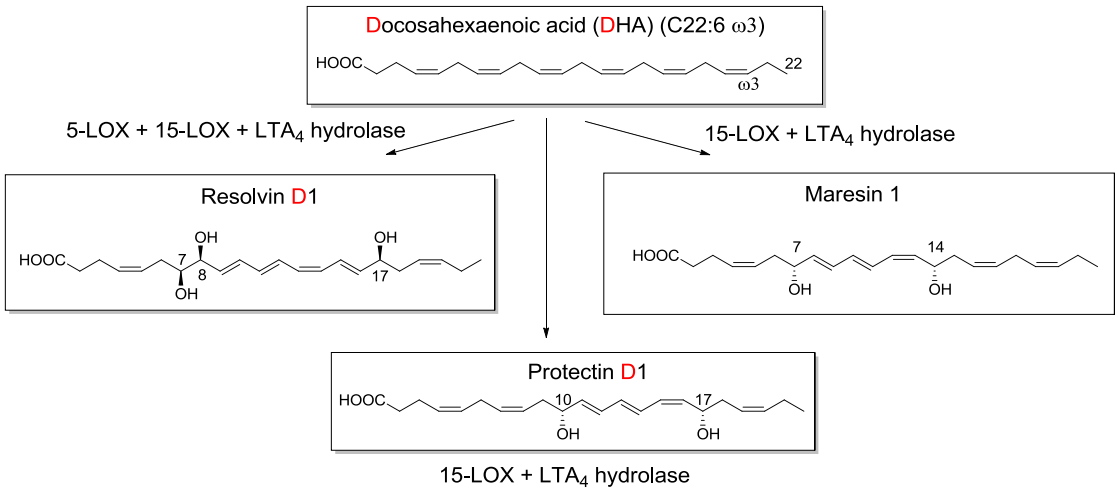

Figure 31: Biosynthesis of novel SPMs from DHA

Figure 31 lists the novel bioactive mediators synthesized from DHA. The *in vivo* oxygenation biomarkers of DHA include 17*S*-hydroperoxide-DHA (17*S*-HP-DHA) (116) and 14*S*-hydroperoxide-DHA (14*S*-HP-DHA) (79) which are biosynthesized via the LOX-catalyzed mechanisms. 17*S*-HP-DHA is further converted to bioactive D series of Resolvins by a different lipoxygenase or protectin D1 (PD1) by the same lipoxygenase.

In addition, in the presence of aspirin, DHA is converted to a 17*R*-alcohol-containing series of Rvs (AT-Rvs) (77). In another pathway, 14*S*-HP-DHA is converted to bioactive Maresin 1 via a 13,14-LTA epoxide intermediate (79).

Of these many fine studies on biosynthesis of the novel lipid mediators nearly all utilize cells, which establish the physiological relevance to some extent. However, in terms of defining the mechanism of the transformations and the enzymes involved, there is no substitute for the defining data that come from enzymological studies with purified enzymes. With the leukotriene and lipoxin pathway as the models, it is not difficult to propose the biosynthetic routes for leukotriene and lipoxin analogues, resolvin (Rv), protectin (PD) and maresin. Relevant to this thesis is that one can reproduce the pathways by *in vitro* enzymatic assays and therefore provide experimental support for these pathways which are only proposed "on paper".

The followings summarize the proposed biosynthetic pathways to the novel SPMs derived from ω-3 fatty acids:

RvE1 – (5,12,18-triOH-EPA)

Typical 5-LOX to LTA to LTB except using 18*R*-HEPE as substrate

RvD1 – (7,8,17-triOH-DHA)

Typical LXA synthesis except on 17*S*-H(P)DHA, or 15-LOX on 7,8-LTA epoxide

RvD2 – (7,16,17-triOH-DHA)

Typical LXB synthesis, except on 7*S*-H(P)DHA

RvD3 – (4,11,17-triOH-DHA)

C-4 oxygenation of 17S-H(P)DHA, to LTA epoxide, and non-enzymic hydrolysis

RvD4 – (4,5,17-triOH-DHA) -

The 4,5 diol formed along with RvD3

AT-RvD1

AT = aspirin-triggered, similar to RvD1 except the substrate is 17*R*-HDHA

PD1 – (10,17-diOH-DHA)

Equivalent to the 14,15-LTA pathway, except on 17*S*-HPDHA and giving LTB-like 10*R*,17*S*-diol

Maresin 1 - (7,14-diOH-DHA)

Analogous reactions to PD1, except starting with 14*S*-HPDHA and giving a LTB-like 7*R*,14*S*-diol

Some enzymological studies are reported, notably with the use of recombinant human 5-LOX to study resolvin E synthesis (114), and soybean LOX-1 to characterize double dioxygenation reactions on DHA (117). To expand on this, I will use our expressed LOX enzymes to establish their catalytic activities with DHA and EPA and their hydroperoxides, and subsequently compare with the "in cell" metabolism.

Roles of 12/15-lipoxygenase in inflammation

It is becoming increasingly clear that mammalian 12/15-LOX and its products play important roles in inflammation. However, despite much work in this area, the biochemical mechanisms by which 12/15-LOX regulates the inflammation process are not fully understood. This is partly due to its complex expression pattern which is species-specific, tissue-specific and highly regulated (118). In humans the 12/15-LOX

(15-LOX-1) is constitutively expressed at high levels in immature red blood cells during anemia, in eosinophils and in airway epithelial cells (119,120). Lower expression levels have been reported for polymorphonuclear leukocytes (PMN), alveolar macrophages, vascular cells etc (121). In addition, the expression of 12/15-LOX is inducible. Peripheral blood monocytes do not express 12/15-LOX in the circulation. Instead, its induction can be achieved *in vitro* in human monocytes (122) and in elicited murine macrophages (123). In human neutrophils, induction of 15-LOX-1 can be achieved by PGE_2 via cAMP elevation (124). It is proposed that 12/15-LOX induction in neutrophils may initiate the lipid mediator class switching during acute inflammation and therefore contribute to the resolution of inflammation.

12/15-LOX is implicated in the biosynthesis of several lipid mediators, either pro-inflammatory or anti-inflammatory. 12/15-LOX alone is proposed to be responsible for the production of precursors to the pro-inflammatory eoxin and anti-inflammatory protectin and maresin. When combined with 5-LOX, 12/15-LOX is capable of producing precursors to lipoxins and resolvins. The missing here is the *in vitro* enzymatic evidence which can substantiate the proposed pathways. In this chapter I will use the highly catalytically active recombinant human 15-LOX-1 and the methods developed in Chapter II to fill this blank.

Cellular metabolism of ω-3 fatty acids

Cellular incubations with fatty acids and fatty acid hydroperoxides led to the discovery of bioactive lipid mediators. In this chapter the study is conducted in a different order. The capabilities of human 15-LOX-1 in producing bioactive lipid mediator

precursors, 16,17-LTA_6 and 14,15-LTA_5, are first established by utilizing the purified recombinant enzyme. The comparison between the enzyme incubations and *ex vivo* cellular metabolism on product profiles and reaction rates is then conducted, which helps substantiate the physiological relevance of the enzymatic study.

It has been shown that ω-3 fatty acids (DHA and EPA), like arachidonic acid, can be incorporated into cell membrane phospholipids (125) and upon stimulation be released and utilized by lipoxygenases to yield bioactive lipids. In the presence of exogenous EPA, 5-lipoxygenase activity of mouse mastocytoma cells produced LTB_5 and LTC_5, the analogues of LTB_4 and LTC_4 (126). 5- and 15-lipoxygenase activities of porcine leukocytes converted 15-HP-EPA to di- and tri-hydroxyeicosapentaenoic acid derivatives (127), suggesting the formation of LTA intermediates. Concerning the transformation of DHA, the conversion from 17*S*-HP-DHA to the bioactive protectin D1 has been demonstrated in incubations using murine brain and human leukocytes (116).

In this chapter mouse resident peritoneal macrophages are to be used for the incubations with omega-3 fatty acid hydroperoxides. Mouse macrophages are a valid experimental system to test the transformation of fatty acids. Incubations of mouse macrophages with 14*S*-HP-DHA led to the discovery of bioactive maresin, and this conversion is proposed to be catalyzed by the prominent 12/15-LOX activity of the cells (79). Mouse 12/15-LOX is the functional equivalent of human reticulocyte 15-LOX-1. Thus mouse macrophage incubations are good reflections of fatty acid metabolism by 15-LOX activity in cells.

Specific Aims in Chapter IV

Specific aim 1: Analyze the metabolism of omega-3 fatty acid (DHA and EPA) hydroperoxides by the purified recombinant lipoxygenases. This could help to establish the mechanisms underlying the transformation, identify the enzymes involved in the biosynthesis, and guide the discovery of new metabolites that have potential bioactivities.

Specific aim 2: Isolation and characterization of the LTA-type epoxides from EPA and DHA. These intermediates could be the direct analogues of the arachidonic acid epoxides studied in Chapter 2 and Chapter 3. More specifically, in this part the isolation and characterization of the LTA epoxide intermediates in formation of the 10,17-diol protectins and 8,15-diol EPA-derived mediator will be performed. The achievement of this aim could help the studies in detecting the specific hydrolases that metabolize these LTA epoxides to the bioactive lipid mediators.

Specific aim 3: Analyze metabolism of omega-3 fatty acid (DHA and EPA) hydroperoxides by mouse macrophages and conduct comparison with the enzymatic metabolism in **Specific aim 1**.

Experimental procedures

Materials

Docosahexaenoic acid (DHA) and eicosapentaenoic acid (EPA) were purchased from NuChek Prep Inc. (Elysian, MN). Soybean LOX-1 (lipoxidase, type V) was purchased from Sigma. C57BL/6NCrl mice (6-8 weeks) were purchased from Charles River Laboratories. Zymosan A was purchased from Sigma.

Synthesis and purification of enantiomeric fatty acid hydroperoxides

15*S*-hydroperoxide-EPA (15*S*-HP-EPA) and 17*S*-hydroperoxide-DHA (17*S*-HP-DHA) were prepared by the reaction of EPA or DHA with the commercially available soybean LOX-1. 14*S*-hydroperoxide –DHA (14*S*-HP-DHA) was prepared by the reaction of DHA with mouse platelet-type 12*S*-LOX. The purification of fatty acid hydroperoxides was achieved by SP-HPLC (hexane/IPA, 100/2, by volume).

Biphasic reaction conditions for preparation of LTA epoxides

Enzyme reactions were performed at 0 °C, with the fatty acid hydroperoxide substrate initially in hexane (5 ml, bubbled for 30 min prior to use with argon to decrease the O_2 concentration, and containing ~200 μM substrate) layered over the recombinant LOX enzyme (1-2 mg, ~20 nmol) in 400 μl of Tris buffer (pH 7.5 for human 15-LOX-1). The reaction was initiated by vigorous vortex mixing of the two phases. After 1.5 min, the hexane phase was collected and scanned from 200-350 nm in UV light by using a Perkin-Elmer Lambda-35 spectrophotometer. Then the hexane phase was evaporated to about 2 ml under a stream of nitrogen, treated with ethanol (20 μl) and ethereal

diazomethane for 10 s at 0 °C and then rapidly blown to dryness and kept in hexane at -80 °C until further analysis.

HPLC analyses

Aliquots of the methylated hexane phase from the biphasic reaction were analyzed by RP-HPLC using a Waters Symmetry column (25 x 0.46 cm), using a solvent of MeOH/20mM triethylamine pH 8.0 (90/10 by volume), at a flow rate of 1ml/min, with on-line UV detection (Agilent 1100 series diode array detector). Further purification was achieved by SP-HPLC using a silica guard column (0.46 × 4.5 cm), using a solvent of hexane/triethylamine (100/0.5) run at 0.5 ml/min. Aliquots of the room temperature incubation of human 15-LOX-1 with omega-3 fatty acid hydroperoxides were analyzed by RP-HPLC using a Waters Symmetry column (25 x 0.46 cm), using a solvent of CH_3CN/H_2O/HAc (45/55/0.01 by volume), at a flow rate of 1ml/min. Aliquots of mouse macrophage incubations were analyzed by RP-HPLC using a Waters Symmetry column (15 x 0.21 cm), using a solvent of CH_3CN/H_2O/HAc (50/50/0.01 by volume), at a flow rate of 0.2 ml/min.

NMR analysis

^1H NMR and $^1H,^1H$ COSY NMR spectra were recorded on a Bruker AV-III 600 MHz spectrometer at 283 K. The parts/million values are reported relative to residual nondeuterated solvent (δ = 7.16 ppm for C_6H_6). Typically, 1024 scans were acquired for a 1-D spectrum on ~20 μg of LTA epoxide.

Mouse peritoneal resident macrophage incubations

Mouse peritoneal resident macrophages were collected by lavage from naive mice (6-8 week old C57BL/6NCrl mice; Charles River Laboratories). All animal studies were approved and performed in accordance with guidelines provided by the Vanderbilt Medical Standing Committee on Animals.

After centrifugation at 400 g and addition of (DMEM+10%FBS), macrophages (5 x 10^6 cells/ml) were incubated with zymosan A (200 μg/ml) and fatty acids or fatty acid hydroperoxides (20 μg/ml) at 37 °C for 30 min. Incubations were stopped with 2 vol of cold methanol. After cells were removed by centrifugation at 10,000 rpm, the supernatant was added 3 vol of water and the apparent pH was adjusted to approximately pH 3. The products were extracted by C18 cartridge and analyzed by RP-HPLC.

Isomerization of 10*S*,17*S*-diOH-DHA (*t,c,t*) to 10*S*,17*S*-diOH-DHA (*t,t,t*)

A solution of 10*S*,17*S*-diOH-DHA (*t,c,t*) in argon-bubbled isopropanol (1 mg/ml) was placed in a quartz cuvette. Then, 2-mercaptoethanol (1 mg/ml) was added, and the solution was irradiated by low-pressure mercury lamp for 10 min. The isomerization was checked by injecting aliquots of the irradiated sample on RP-HPLC.

Results

Reaction of 17*S*-HP-DHA with human 15-LOX-1

One of the oxygenation biomarkers of DHA *in vivo* is 17*S*-hydro(pero)xy-DHA, which is further converted to protectin D1 via a 15-LOX-catalyzed LTA intermediate. The incubation of 17*S*-HP-DHA with human 15-LOX-1 was performed to check the possible metabolites (**Figure 32**).

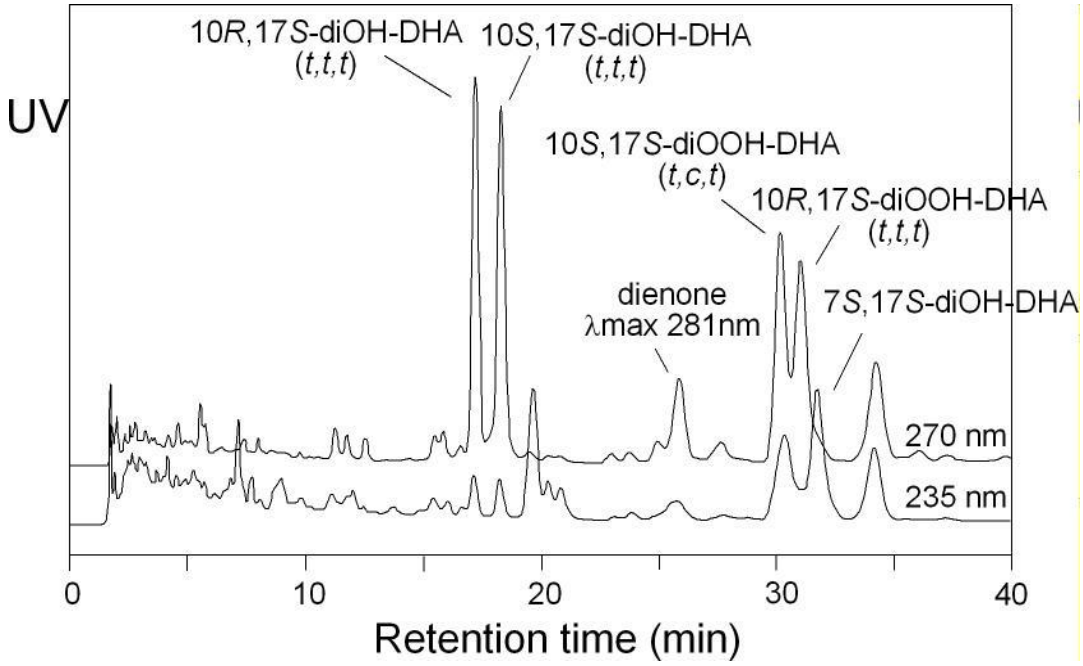

Figure 32: RP-HPLC analysis of the reaction of 17*S*-HP-DHA with human 15-LOX-1. Column: Waters Symmetry C18, 25 x 0.46 cm; solvent, CH_3CN/H_2O/HAc (45/55/0.01, by volume); flow rate, 1 ml/min, UV detection at 270 nm and 235 nm.

At retention times of 16-19 min, the significant formation of 10,17*S*-diOH-DHAs (*t,t,t*) was detected, implicating a potential 16,17-LTA_6 intermediate in the pathway. To further specify the identities of the two peaks, the 10*S*,17*S*-diOH-DHA (*t,t,t*) standard was prepared from 10*S*,17*S*-diOH-DHA (*t,c,t*) using the method in which UV irradiation and thiyl radical exposure are used to isomerize the conjugated double bond

configuration in fatty acids (128). By comparing the chromatographic mobility with the standard on HPLC, the first eluting peak was established as 10*R*,17*S*-diOH-DHA (*t,t,t*) and the second as 10*S*,17*S*-diOH-DHA (*t,t,t*). This elution order is consistent with the fact that 8*R*,15*S*-diOH-AA (*t,t,t*) elutes earlier than 8*S*,15*S*-diOH-AA (*t,t,t*) on RP-HPLC (54).

The double oxygenation products eluted after 30 min, and include 10*S*,17*S*-diOOH-DHA(*t,c,t*), 7*S*,17*S*-diOOH-DHA, and 10*R*,17*S*-diOOH-DHA(*t,t,t*). The first two products are direct analogues of 8*S*,15*S*-diHPETE(*t,c,t*) and 5*S*,15*S*-diHPETE formed in the reaction of 15*S*-HPETE with soybean LOX-1. The formation of 10*R*,17*S*-diOOH-DHA(*t,t,t*) is consistent with a bis-allylic C14-peroxyl radical formed as an intermediate (See the following scheme).

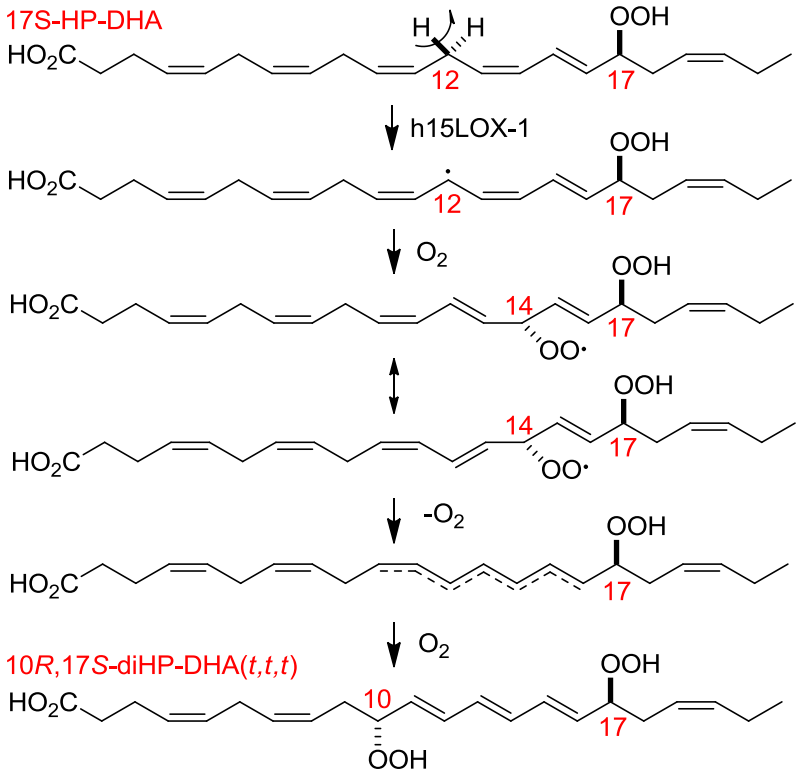

Scheme: Proposed mechanism of formation of 10*R*,17*S*-diHP-DHA(*t,t,t*)

Reaction of 15*S*-HP-EPA with human 15-LOX-1

Human 15-LOX-1, at low concentrations, oxygenates EPA to 15*S*-HP-EPA and 12*S*-HP-EPA, which upon further enzyme exposure are converted to secondary metabolites. It has been demonstrated that 15-lipoxygenase activity in eosinophils metablizes arachidonic acid to eoxin A_4, precursor to the pro-inflammatory eoxins. Here I analyzed the incubation of 15*S*-HP-EPA with human 15-LOX-1 by RP-HPLC and checked the production of secondary metabolites (**Figure 33**).

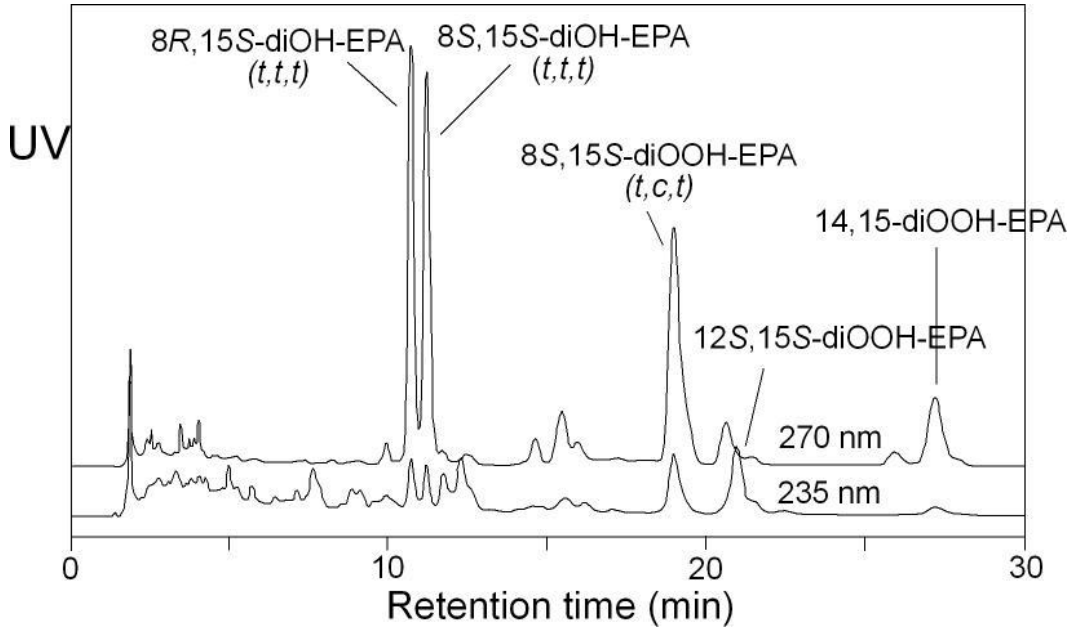

Figure 33: RP-HPLC analysis of the reaction of 15*S*-HP-EPA with human 15-LOX-1. Column: Waters Symmetry C18, 25 x 0.46 cm; solvent, CH_3CN/H_2O/HAc (45/55/0.01, by volume); flow rate, 1 ml/min, UV detection at 270 nm and 235 nm.

Similar to the reaction of 17*S*-HP-DHA with human 15-LOX-1, 8,15-diOH-EPAs (*t,t,t*) are the prominent products of the reaction of 15*S*-HP-EPA with human 15-LOX-1, suggesting the formation of 14,15-LTA_5.

In addition to the formation of 8,15-diHP-EPA and 5,15-diHP-EPA, a bis-allylic dihydroperoxide 12,15-diHP-EPA was detected. 12,15-diHP-EPA showed a unique UV chromophore with a smooth profile (as opposed to the angular shoulders on a typical conjugated diene) and a relatively high λ_{max} at 243 nm. The arachidonate analogue 12,15-diHPETE was detected as the product of reaction of 15*S*-HPETE with human 15-LOX-1 or mouse platelet-type 12*S*-LOX, and 8,11-diHPETE was formed from the reaction of 8*R*-HPETE with the recombinant 8*R*-LOX. Importantly, these bis-allylic dihydroperoxides, under the catalysis of the lipoxygenase enzymes, are cleaved and then converted to 4-hydro(pero)xy-alkenal products (see **Chapter VI**).

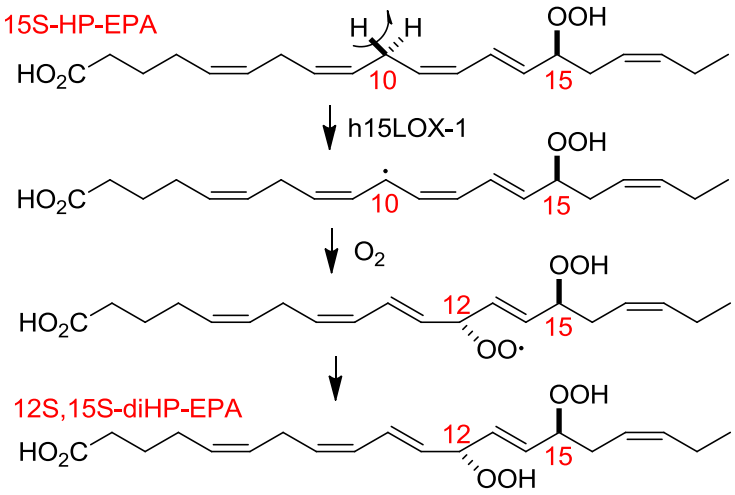

Scheme: Proposed mechanism of formation of 12*S*,15*S*-diHP-EPA

Biosynthesis, isolation, and characterization of 16,17-LTA$_6$

The next step is to apply the biphasic reaction system developed in **Chapter II** to the reactions of ω3 fatty acid hydroperoxides with human 15-LOX-1. After vortex mixing of human 15-LOX-1 with 17*S*-HP-DHA at 0 °C, UV spectroscopy of the hexane phase showed a decrease in substrate and appearance of a new chromophore with λ_{max} at 280 nm, characteristic of a LTA-type epoxide (**Figure 34**).

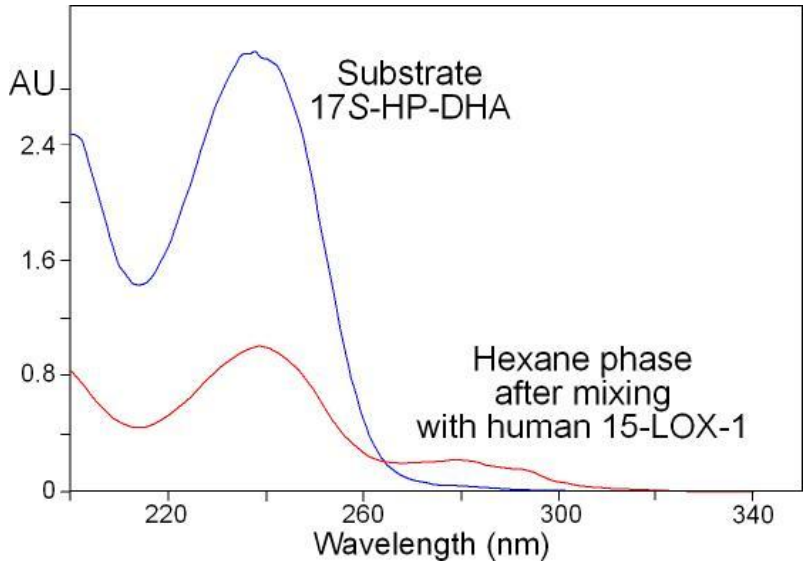

Figure 34: UV analysis of LTA epoxide formation from 17*S*-HP-DHA with human 15-LOX-1 under biphasic reaction conditions.

After preparing the methyl esters of the hexane extract by brief reaction with diazomethane at 0 °C, the remaining 17*S*-HP-DHA and its products were analyzed on RP-HPLC using conditions suitable for the LTA-type epoxide. **Figure 35** illustrates RP-HPLC analysis with UV detection at 270 nm. The product profile is similar with that from the reaction of 15*S*-HPETE. The unreacted 17*S*-HP-DHA is immediately followed by a minor keto derivative (a conjugated dienone, λ_{max} 281 nm), and then by a well-resolved peak of the putative LTA-type epoxide (conjugated triene, λ_{max} 280 nm).

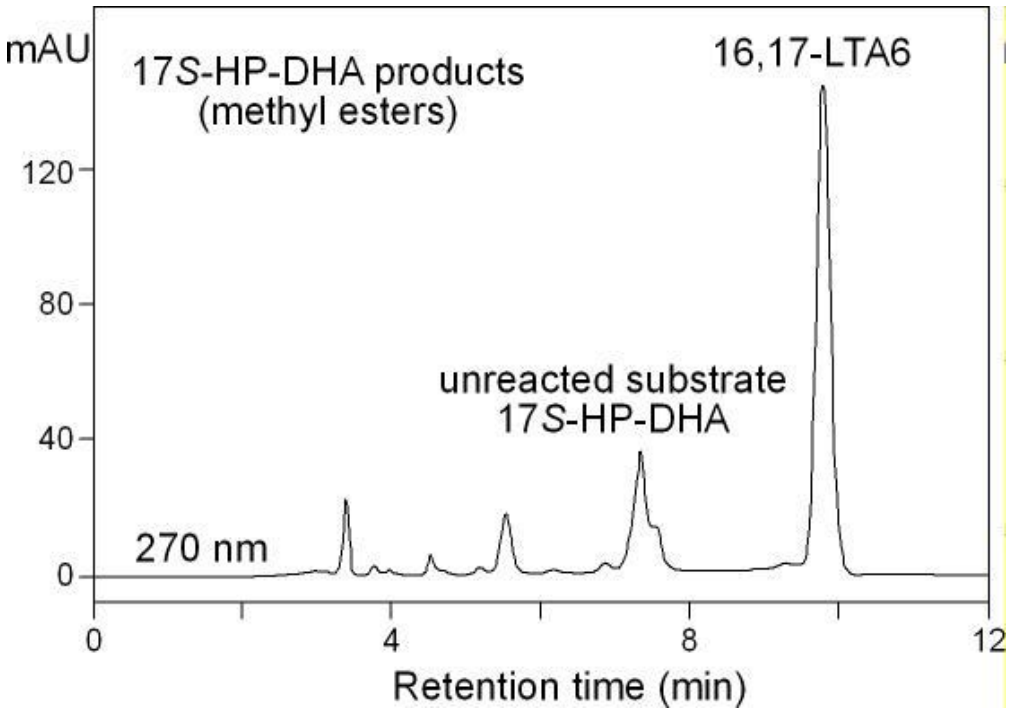

Figure 35: RP-HPLC analysis of the reaction of 15-LOX-1 with 17*S*-HP-DHA. RP-HPLC analysis used a Waters Symmetry C18 column (0.46 × 25 cm), a flow rate of 1 ml/min, and a solvent system of methanol/20 mM triethylamine pH 8.0 (90/10, by volume) with UV detection at 270 nm.

The pooled aliquots of LTA epoxide methyl ester were subsequently analyzed by ^{1}H-NMR and COSY in d6-benzene (**Figure 36**). The expanded regions for the olefinic protons (5.0 – 6.7 ppm, top spectrum) and the epoxide protons (2.65 – 3.10 ppm, middle spectrum) illustrate the splitting of individual signals and associated coupling constants from which the stereochemistry can be derived. The top spectrum of the olefinic region, which is more complicated than that of 14,15-LTA$_4$ methyl ester due to two additional double bonds, provides the configuration of the double bonds, in particular identifying the conjugated triene as 10*Z*,12*E*,14*E*. On the epoxide protons, which is illustrated in the middle spectrum, the 1.8 Hz coupling between H16 and H17 identifies the epoxide configuration as *trans*. Between H16 and H17 are two methylene protons, H6 and H9,

which display triplet splitting patterns. Based on these analyses, and with the reasonable assumption that the original 17*S* configuration is retained, the structure of the epoxide product can be defined as 16*S*,17*S*-*trans*-epoxy-docosa-4*Z*,7*Z*,10*Z*,12*E*,14*E*,19*Z*-hexaenoate. This confirms the structure originally proposed for this intermediate, precursor of the pro-inflammatory protectin D1.

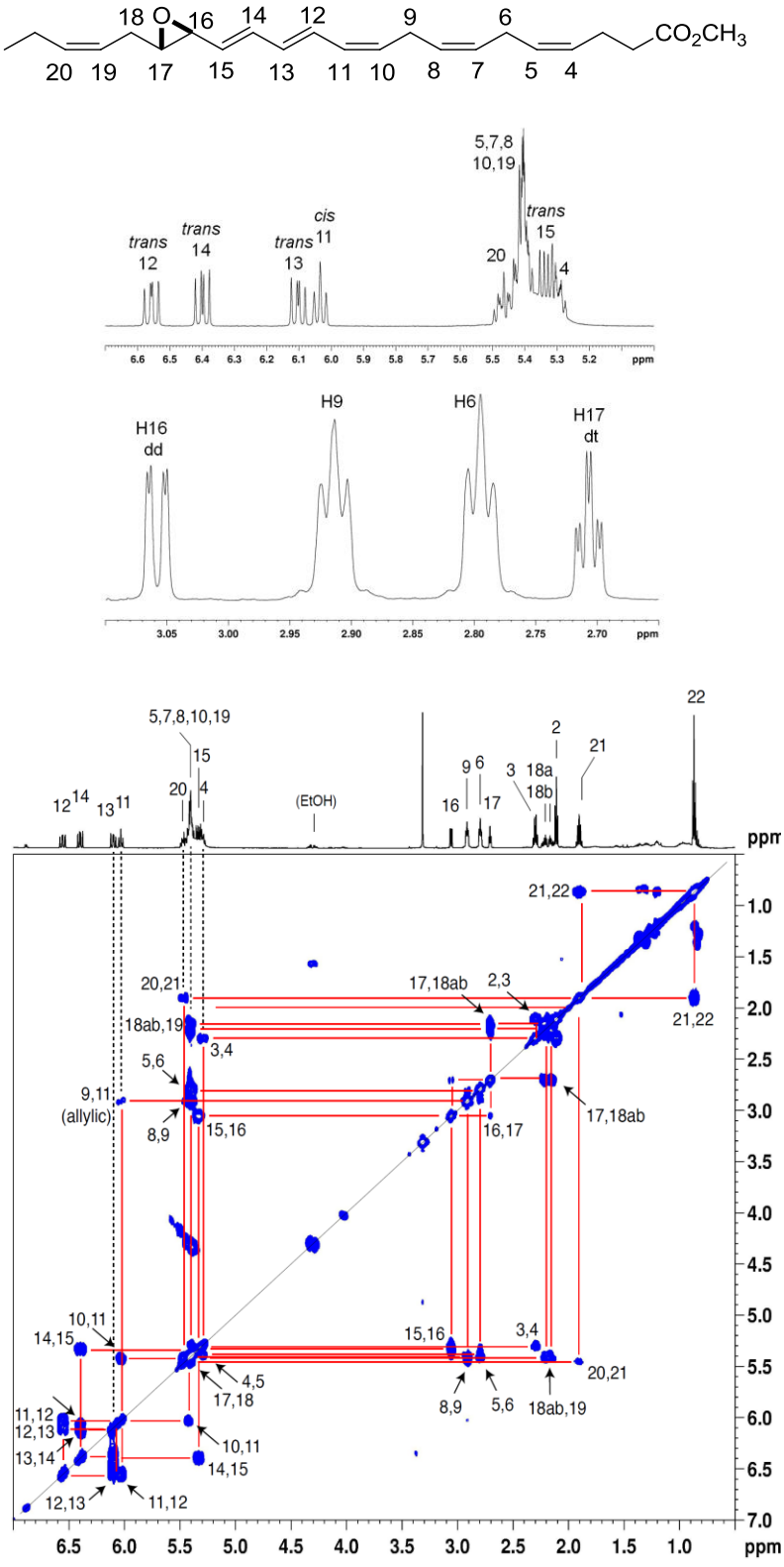

Figure 36: NMR analysis of 16,17-LTA$_6$.

Biosynthesis, isolation, and characterization of 14,15-LTA_5

The same methods used in synthesis, purification and NMR characterization of 16,17-LTA_6 were utilized in the study of 14,15-LTA_5 from the reaction of 15*S*-HP-EPA with human 15-LOX-1.

Biphasic incubation of 15*S*-HP-EPA with human 15-LOX-1:

Enzyme reactions were performed at 0 °C, with the 15*S*-HP-EPA substrate initially in hexane layered over the recombinant human 15-LOX-1 in Tris buffer (pH 7.5 for human 15-LOX-1). After vortex mixing of human 15-LOX-1 with 15*S*-HP-EPA at 0 °C, UV spectroscopy of the hexane phase showed a decrease in substrate and appearance of a new chromophore with λ_{max} at 280 nm, characteristic of a LTA-type epoxide (**Figure 37**).

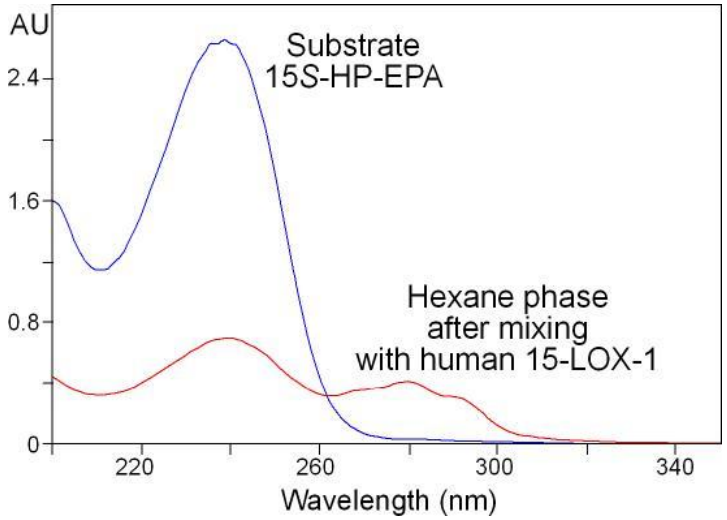

Figure 37: UV analysis of LTA epoxide formation from 15*S*-HP-EPA with human 15-LOX-1 under biphasic reaction conditions.

SP-HPLC purification of 14,15-LTA$_5$ methyl ester:

RP-HPLC analysis of the organic phase after the vortex mixing demonstrated that in addition to the unreacted 15*S*-HP-EPA substrate, a new peak with the UV absorbance at ~280 nm was detected (data not shown). The new peak was further purified by SP-HPLC (**Figure 38**).

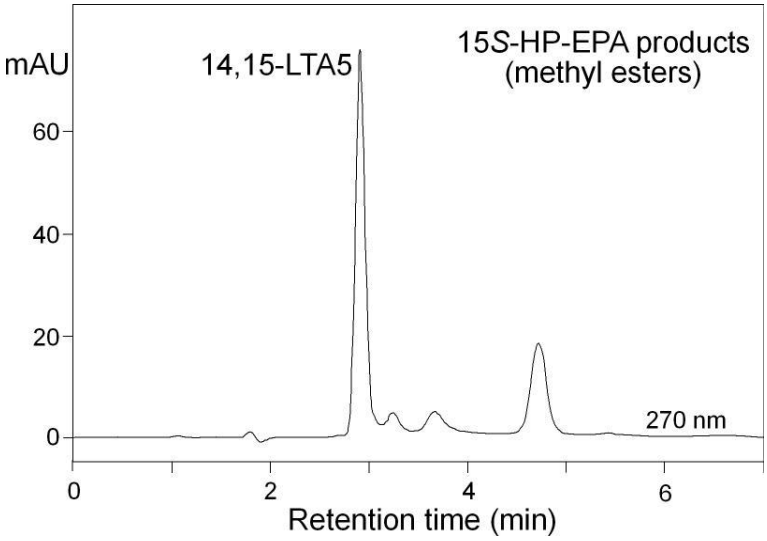

Figure 38: SP-HPLC analysis of the reaction of 15-LOX-1 with 15*S*-HPETE. SP-HPLC analysis used a silica guard column (0.46 × 4.5 cm), a flow rate of 0.5 ml/min, and a solvent system of Hexane/triethylamine (100/0.5, by volume) with UV detection at 270 nm.

NMR analysis of 14,15-LTA$_5$ methyl ester:

The pooled aliquots of the LTA epoxide methyl ester were subsequently analyzed by ^{1}H-NMR and COSY in d6-benzene (**Figure 39**). The expanded regions for the olefinic protons (5.1 – 6.6 ppm, top spectrum), the epoxide protons (2.65 – 3.10 ppm, middle spectrum) and the full COSY spectrum (bottom) are shown. The top spectrum of the olefinic region provides the configuration of the double bonds, in particular identifying the conjugated triene as 8*Z*,10*E*,12*E*. On the epoxide protons, illustrated in the middle spectrum, the 1.8 Hz coupling between H14 and H15 identifies the epoxide configuration

as *trans*. Based on these analyses, and with the reasonable assumption that the original 15*S* configuration is retained, the structure of the epoxide product can be defined as 14*S*,15*S*-*trans*-epoxy-eicosa-5*Z*,8*Z*,10*E*,12*E*,17*Z*-pentaenoate. This structure has never been reported before and could potentially lead to the production of a family of novel lipid mediators.

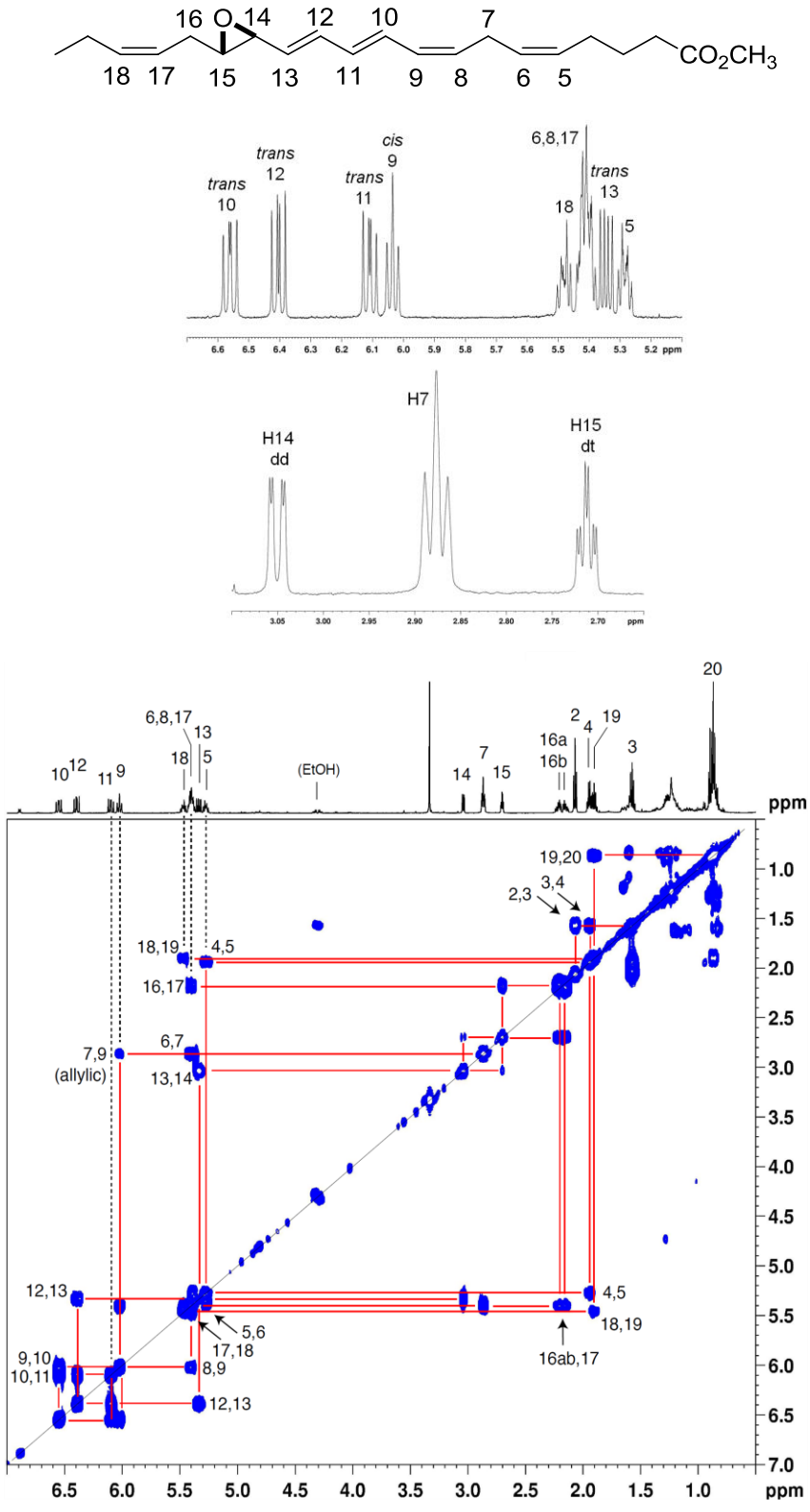

Figure 39: NMR analysis of 14,15-LTA$_5$.

Mouse peritoneal macrophage incubations with omega-3 fatty acid hydroperoxides

Mouse resident peritoneal macrophages were isolated using the method adapted from a published protocol (129). The macrophage incubations were conducted with DHA, 17*S*-HP-DHA and 15*S*-HP-EPA as substrate. Cellular inflammation is induced by Zymosan A, or Ca-ionophore A23187 is used to enhance LOX activity.

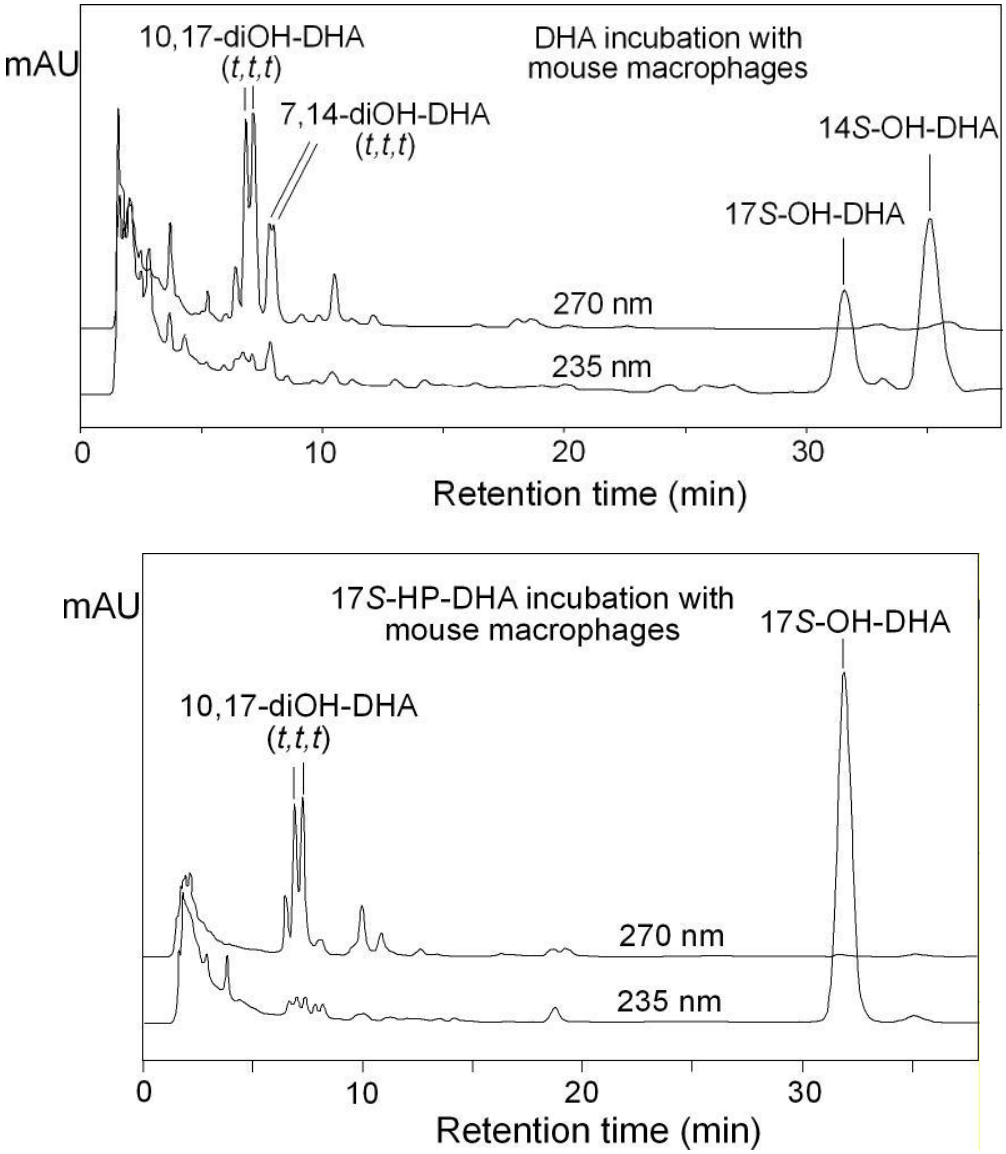

Figure 40: RP-HPLC analysis of the incubation of DHA (top) and 17*S*-HP-DHA (below) with mouse resident peritoneal macrophages. Column: Waters Symmetry C18, 15 x 0.21 cm; solvent, CH_3CN/H_2O/HAc (50/50/0.01, by volume); flow rate, 0.2 ml/min, UV detection at 270 nm and 235 nm. The assignment of each peak identity was based on the

comparison of the UV chromophore and the retention time on HPLC with the authentic standards as well as the assumption that the stereochemistry and the position of the hydroperoxide group of the substrate are retained.

Incubation of DHA with mouse macrophages led to the formation of mono-oxygenation products 14*S*-HP-DHA and 17*S*-HP-DHA which appeared as their reduced form 14*S*-OH-DHA and 17*S*-OH-DHA due to the presence of cellular peroxidases. Different from the enzymatic incubations in which double oxygenation products are detected prominently, the macrophage incubations further converted 17*S*-HP-DHA and 14*S*-HP-DHA to LTA-type epoxides which were manifested by the production of LTA non-enzymatic hydrolysis products, 10,17-diOH-DHAs(*t,t,t*) and 7,14-diOH-DHAs(*t,t,t*). Incubations with 17*S*-HP-DHA confirmed the secondary transformations in the pathway. It is noted that mouse macrophages transformed DHA to 14*S*-HP-DHA and 17*S*-HP-DHA in a ratio of ~2:1, whereas the secondary transformations to LTA epoxides are more efficient for 17*S*-HP-DHA than for 14*S*-HP-DHA. This is consistent with the hydrogen abstraction occurring at C12 of DHA by mouse 12-LOX.

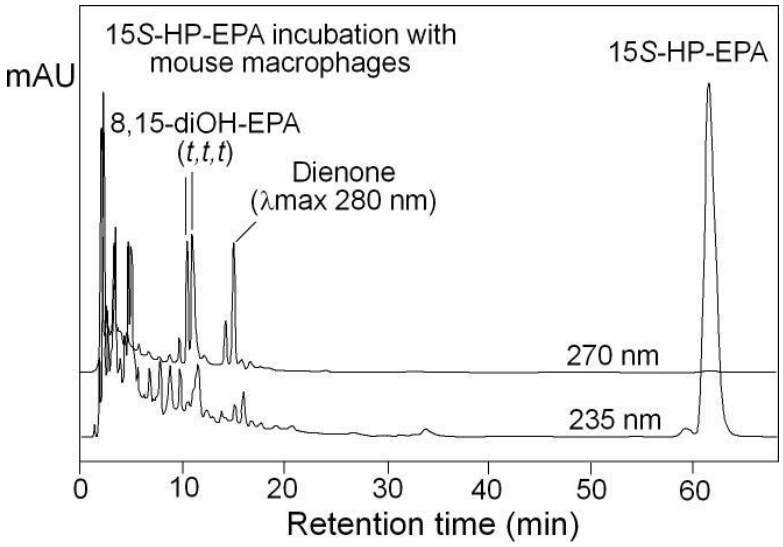

Figure 41: RP-HPLC analysis of the incubation of 15*S*-HP-EPA with mouse resident peritoneal macrophages. Column: Waters Symmetry C18, 25 x 0.46 cm; solvent,

CH_3CN/H_2O/HAc (50/50/0.01, by volume); flow rate, 1 ml/min, UV detection at 270 nm and 235 nm.

Figure 41 demonstrates the products derived from the incubation of 15*S*-HP-EPA with mouse macrophages. In addition to some dienone products which probably result from the carbon chain cleavage of the substrate, the non-enzymatic hydrolysis products, 8,15-diOH-EPAs (*t,t,t*) were detected, which suggests the production of 14,15-LTA_5.

The bioactive end-products, protectin D1 derived from 16,17-LTA_6 and maresin 1 from 13,14-LTA_6 with their unique *cis,trans,trans*-conjugated triene configuration, were not detected in the macrophage incubation. One explanation for the failure in detecting protectin D1 is that mouse macrophages do not express the specific LTA hydrolase. On the other hand, maresin 1 was detected from the mouse macrophages in the work leading to its discovery, implying that the incubation conditions utilized here were not optimal for the corresponding LTA hydrolase activity. The original work utilized a preparation of purified peritoneal macrophages, which may have enriched this enzymatic activity.

Discussion

In this chapter the biosynthetic pathways of LTA-type epoxides from omega-3 fatty acids EPA and DHA are investigated by using the recombinant human 15-LOX-1 and mouse resident macrophages. 14,15-LTA_5 and 16,17-LTA_6 were unequivocally established as the 15-LOX products of EPA and DHA by direct biosynthesis, isolation and NMR analysis. The non-enzymatic hydrolysis products of both epoxides were detected from the mouse macrophage incubations with the corresponding omega-3 fatty acids, providing strong evidence for their existence in a physiological environment.

The conversions from the LTA-type epoxides to the "specialized pro-resolving mediators" (SPM) were not studied in this chapter due to the unavailability of the corresponding LTA-type epoxide hydrolase enzymes. Efforts were made to detect the SPMs, which have the characteristic conjugated-triene configuration, from the mouse macrophage incubations with omega-3 fatty acids. However, only the non-enzymatic hydrolysis products were detected. This is probably because mouse macrophages do not express the required hydrolase enzyme or the incubation conditions are not optimal for the hydrolase activity. Another possible explanation is that the work leading to the discovery of SPMs utilized a preparation of purified peritoneal macrophages, which may have enriched this enzymatic activity, while in my experiments the macrophages were prepared without further enrichment.

In a recent study, 13,14-LTA_6, the intermediate to maresin, was demonstrated to inhibit the LTA hydrolase activity and shift the macrophage phenotype (130). The paper suggests that other than serving as the intermediate to the bioactive end products, the LTA-type epoxides may provide direct regulatory effects to various physiological events.

The study in this chapter has successfully isolated 14,15-LTA_5 methyl ester and 16,17-LTA_6 methyl ester in the amount sufficient for NMR analysis. The corresponding LTA free acids, which can be obtained by alkaline-induced hydrolysis of the methyl esters, can be further used to test their bioactivity.

Another significance of this study is that the proposed pathways of omega-3 fatty acid metabolism have been substantiated by a series of *in vitro* enzymatic assays conducted in this chapter. Compared with the many fine studies utilizing cell incubations, the enzymological studies with the purified enzymes provide a clear view about each step of the pathways. This could be especially necessary when it comes to the discovery of inhibitors or inducers of the pathway.

CHAPTER V

8*R*-LIPOXYGENASE-CATALYZED SYNTHESIS OF A PROMINENT *CIS*-EPOXYALCOHOL

Introduction

In the late 1960's and early 1970's, high concentrations of prostaglandin esters were identified in the Caribbean sea whip coral *Plexaura homomalla* (131). Attempts were made to investigate the putative non-cyclooxygenase pathway of prostaglandin biosynthesis and it turned out that cyclooxygenase accounts for the biosynthesis (132). Research into polyunsaturated fatty acid metabolism in coral extracts still uncovered other interesting biochemistry. Bundy and colleagues studied the related coral *Pseudoplexaura porosa* and uncovered 8*R*-lipoxygenase activity, the first known existence of an *R*-specific lipoxygenase (59). 8*R*-LOX was subsequently found to be widespread in corals including in *P. homomalla*, as well as in many marine invertebrates (133), and a 12*R*-LOX is highly conserved and functionally essential in mammals (94). A second novel activity detected in coral extracts was allene oxide synthase (134), which transforms the 8*R*-LOX product, 8*R*-HPETE, to an allene epoxide, a proposed intermediate in biosynthesis of cyclopentenones, and that hydrolyzes *in vitro* to an α-ketol derivative.

The work described in this chapter concerns an unexpected difference we observed in the metabolism of arachidonic acid (20:4ω6) and dihomo-γ-linolenic acid (20:3ω6) in extracts of *P. homomalla*; a prominent, relatively polar, product is formed specifically

from 20:3ω6. This difference had been noted before in work from the E. J. Corey laboratory, but the detailed assignments of the polar product was not completed. Although the naturally-occurring prostaglandin products in *P. homomalla* are all 2-series derived from arachidonic acid, we included a study of the metabolic fate of 20:3ω6 because it was originally reported as a substrate for the enzymatic activity in the coral (135). The work was initiated in the early 1990's, prior to the cloning of *P. homomalla* cyclooxygenases and lipoxygenases. With the availability of cloned recombinant enzymes from *P. homomalla*, we recently returned to the issue of the origin of this extra product from 20:3ω6. The novel product we characterize herein is formed specifically by 8*R*-lipoxygenase metabolism, and its unusual stereochemistry may represent a feature of the secondary reactions of *R*- as opposed to *S*-lipoxygenases.

Experimental procedures

Materials

Arachidonic (C20:4ω6) and dihomo-γ-linolenic acids (C20:3ω6) were purchased from NuChek Prep Inc. (Elysian, MN). [1-^{14}C]20:4ω6, and [1-^{14}C]20:3ω6 were purchased from Perkin Elmer Life Sciences. *Plexaura homomalla* was collected in the Florida Keys and placed on dry ice until long-term storage in the laboratory at -70°C.

Incubation with coral extracts

Frozen *P. homomalla* was cut into small pieces with scissors then placed in 10 volumes of 50 mM Tris, pH 8, containing 1M NaCl on ice and homogenized using a Polytron blender (Brinkmann) in ten second bursts. The homogenate was allowed to settle under gravity for up to 30 min; aliquots of the supernatant were diluted ten-fold into fresh buffer for incubations with fatty acid substrates (100 μM), typically for 5 min at room temperature. Products were extracted by addition of 1M KH_2PO_4 plus sufficient 1N HCl to give pH 4 followed by extraction with 2 volumes of ethyl acetate. The organic phase was collected, washed with water to remove traces of acid and taken to dryness under nitrogen. The extracts were redissolved in a small volume of MeOH prior to HPLC analysis.

HPLC analyses

Typically, aliquots of the extracts were analyzed initially by RP-HPLC using a Beckman ODS Ultrasphere 5μ column (25 x 0.46 cm) or Waters Symmetry column (25 x 0.46 cm), using a solvent of MeOH/H_2O/HAc (80/20/0.01, or 75/25/0.01 by volume), at a

flow rate of 1ml/min, with on-line UV detection (Agilent 1100 series diode array detector) and radioactive monitoring (Radiomatic Flo-One). Larger amounts (0.5-1 mg of total fatty acids) were injected for collection of products, or a semi-preparative column (Beckmann Ultrasphere ODS, 25 x 1 cm) was used for larger quantities. Further analysis and purification was achieved by SP-HPLC using an Alltech 5μ silica or Beckmann Ultrasphere 5 μ silica column using a solvent of hexane/isopropanol/glacial acetic acid (100/2/0.1 for H(P)ETE free acids and 100/1 for methyl esters; 100/5/0.1 and 100:3 for more polar derivatives and their methyl esters) run at 1 or 2 ml/min.

Expression and purification of 8R-lipoxygenase

cDNA of the 8*R*-LOX domain of the *P. homomalla* peroxidase-lipoxygenase fusion protein was subcloned into the pET3a vector (with an N-terminal His4 tag), and the protein was expressed in *E. coli* BL21 (DE3) cells and purified by nickel affinity chromatography according to a previously published protocol (61).

The second *P. homomalla* 8*R*-lipoxygenase tested here was the soluble enzyme purified in 1996 (60); aliquots from the original purification were stored at -70°C and these retained sufficient activity for use 15 years later. This enzyme is referred to here as the soluble 8*R*-LOX.

Incubation with enzymes

Side-by-side incubations were performed at room temperature in 1 ml of 50 mM Tris pH 8.0 containing 500 mM NaCl, 2 mM $CaCl_2$ and 0.01% Emulphogene detergent using [^{14}C]20:3ω6 or [^{14}C]20:4ω6 fatty acids (each 25μg/ml and 300,000 CPM) and

recombinant 8*R*-LOX (10 μg in 1 ml) or soluble 8*R*-LOX. Under these conditions the recombinant enzyme completely metabolized 50 μM 20:4ω6 or 20:3ω6 substrate within 1 min, while 50 μl (~ 50 μg) of the soluble 8*R*-LOX converted 50 μM 20:4ω6 or 20:3ω6 to the corresponding 8R-hydroperoxide in 5 min; an additional 20 μl enzyme was added to promote further metabolism of the 8*R*-hydroperoxide. Incubations were conducted in a 1 ml quartz cuvette and the rate of reaction monitored by repetitive scanning from 350-200 nm using a Lambda-35 spectrophotometer (Perkin-Elmer). Reactions were stopped by addition of 500 μl MeOH and the solution placed on ice. After addition of 3 ml of water, 100 μl 1M KH_2PO_4, and 40 μl 1N HCl to give pH ~4.5, the samples were extracted using C18 Oasis cartridge and eluted with MeOH and analyzed by HPLC as described above.

LC-MS analysis of ^{18}O incorporation in product from 8R-LOX

[$^{18}O_2$]8*R*-HPETrE was prepared using recombinant 8*R*-LOX (from the *P. homomalla* fusion protein) reacted with C20.3ω6 (20 μg/ml) in pH 8.0 Tris buffer (5 ml) under an atmosphere of $^{18}O_2$; (the 100 ml bulb of oxygen gas contained about ~35% of normal air ($^{16}O_2$), because it had been used three times previously for ^{18}O syntheses). The [$^{18}O_2$]8*R*-HPETrE labeled in the hydroperoxy group was purified by SP-HPLC and reacted with recombinant 8*R*-LOX under a normal atmosphere to produce the corresponding epoxyalcohol. The ^{18}O content of the 8*R*-HPETrE and its corresponding epoxyalcohol product (which share the same molecular weight, 338 for the unlabeled species) were measured by negative ion electrospray LC-MS using a ThermoFinnigan TSQ Quantum instrument by rapid repetitive scanning over the mass range encompassing

the M-H anions (m/z 330-350, 5 scans/sec). 20-30 scans over the HPLC peaks were averaged to obtain the partial mass spectra of labeled and unlabeled epoxyalcohol and 8*R*-HPETrE.

NMR analysis

^{1}H NMR and $^{1}H,^{1}H$ COSY NMR spectra were recorded on a Bruker 400 MHz or Bruker DRX 500 MHz spectrometer at 298 K. The parts/million values are reported relative to residual non-deuterated solvent (δ = 7.16 ppm for C_6H_6, 7.26 ppm for $CDCl_3$).

Results

Metabolism in extracts of *P. homomalla*

When arachidonic acid (20:4ω6) is incubated with extracts of *P. homomalla*, the fatty acid is rapidly metabolized by 8*R*-LOX and the resulting 8*R*-HPETE is further transformed by allene oxide synthase, leading to the appearance of α-ketol and cyclopentenone end products (**Figure 42**, lower panel). Metabolism of dihomo-γ-linolenic acid (20:3ω6) is similar, except for the appearance of a prominent more polar product that is absent (or present in insignificant amounts) in the arachidonic acid incubations (**Figure 42**).

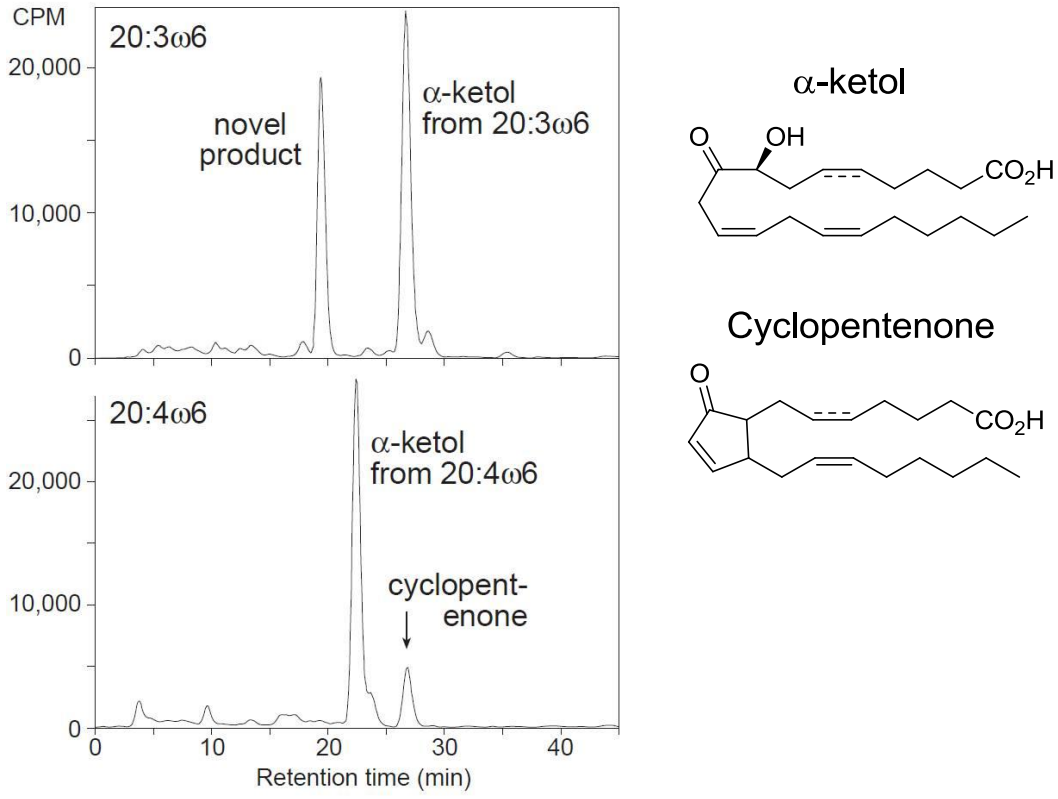

Figure 42: RP-HPLC analysis of products formed from 20:3ω6 and 20:4ω6 in homogenates of *P. homomalla*. Right: structures of α-ketol and cyclopentenone.

Identification of the novel 20:3ω6 product

The structure was established based on GC-MS (**Figure 43**) and NMR data (next page).

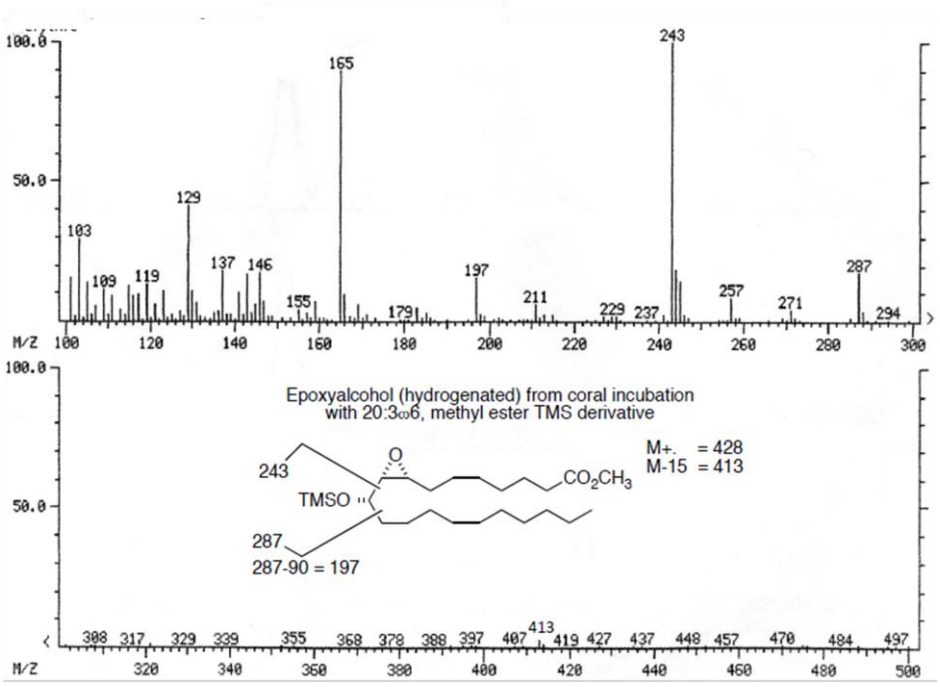

Figure 43: GC-MS of the epoxyalcohol 8,9-epoxy-10-hydroxy-eicosadienoic acid (Obtained by Dr. Brash).

The purified polar product displayed only end absorbance in the UV, indicating no conjugated double bonds. A quantity of ~100 μg was prepared and the proton NMR and COSY spectra were recorded in $CDCl_3$. These results indicated the presence of an 8,9-*cis* epoxide, (H8, dd, 3.03 ppm; H9, dt, 2.92 ppm; $J_{8,9}$ = 4 Hz; cf. *cis* epoxides 4-5 Hz, *trans* epoxides ~ 2 Hz), with α-hydroxyl at C-10, and two *cis* double bonds at 11,12 and 14,15 (NMR data see next page). So far this established the covalent structure as 8,9-*cis*-epoxy-10-hydroxy-eicosa-11*Z*,14*Z*-dienoic acid, an epoxyalcohol of the hepoxilin B-type, yet distinctive in being a *cis*-epoxide.

Chemical shift (ppm)	Multiplicity	Proton(s) [carbon no.]	Coupling constants (Hz)
0.9	t	H20	$J_{19,20} = 7$
1.26-1.44	m	H4,5,6,17,18,19	
1.6-1.8	m	H3,7	
2.06	dt	H16	$J_{15,16} = 7.3$, $J_{16,17} = 7.3$
2.32	t	H2	$J_{2,3} = 7.5$
2.89	m	H13	J_{13a}, J_{13b}
2.96	dd	H9	$J_{8,9} = 4$, $J_{9,10} = 7$
3.03	dt	H8	$J_{7,8} = 5.5$, $J_{8,9} = 4$
3.68	s	-OCH3	
4.47	dt	H10	$J_{10,11} = 2$, $J_{9,10} = 8$
5.34	dt	H14	$J_{13,14} = 7.3$, $J_{14,15} = 11$
5.44	dt	H15	$J_{14,15} = 11$, $J_{15,16} = 7.3$
5.56	dd (unresolved)	H11	$J_{10,11} \leq 2$, $J_{11,12} = \sim 10$
5.65	dt	H12	$J_{11,12} = 11$, $J_{12,13} = 7.7$

Determination of the C-10 hydroxyl configuration

To establish the relative stereochemistry of the epoxide to the C-10 hydroxyl, two saturated analogs of the natural product were prepared by Dr. Jin K. Cha of Wayne State University by total chemical synthesis as outlined in the published paper (136). These synthetic standards, 8*R*,9*S*-*cis*-epoxy-10-hydroxy-eicosanoates with the 9,10 *erythro* and *threo* relative configurations, were compared with the hydrogenated natural product in the respect of GC-MS (EI mode) retention time, pattern of GC-MS ion fragments and NMR spectra (**Figure 44**). The *erythro* standard had an indistinguishable mass spectrum, retention time and NMR spectrum to the hydrogenated epoxyalcohol product of *P. homomalla*. These data confirmed the *erythro* relative configuration at 9,10 in the natural product. As *P. homomalla* exhibits only 8*R*-LOX activity, the *cis* epoxide moiety can be assigned as the 8*R*,9*S* enantiomer. Thus, the complete structure of the novel product from 20:3ω6 is established as 8*R*,9*S*-*cis*-epoxy-10*S*-hydroxy-eicosa-11*Z*,14*Z*-dienoic acid.

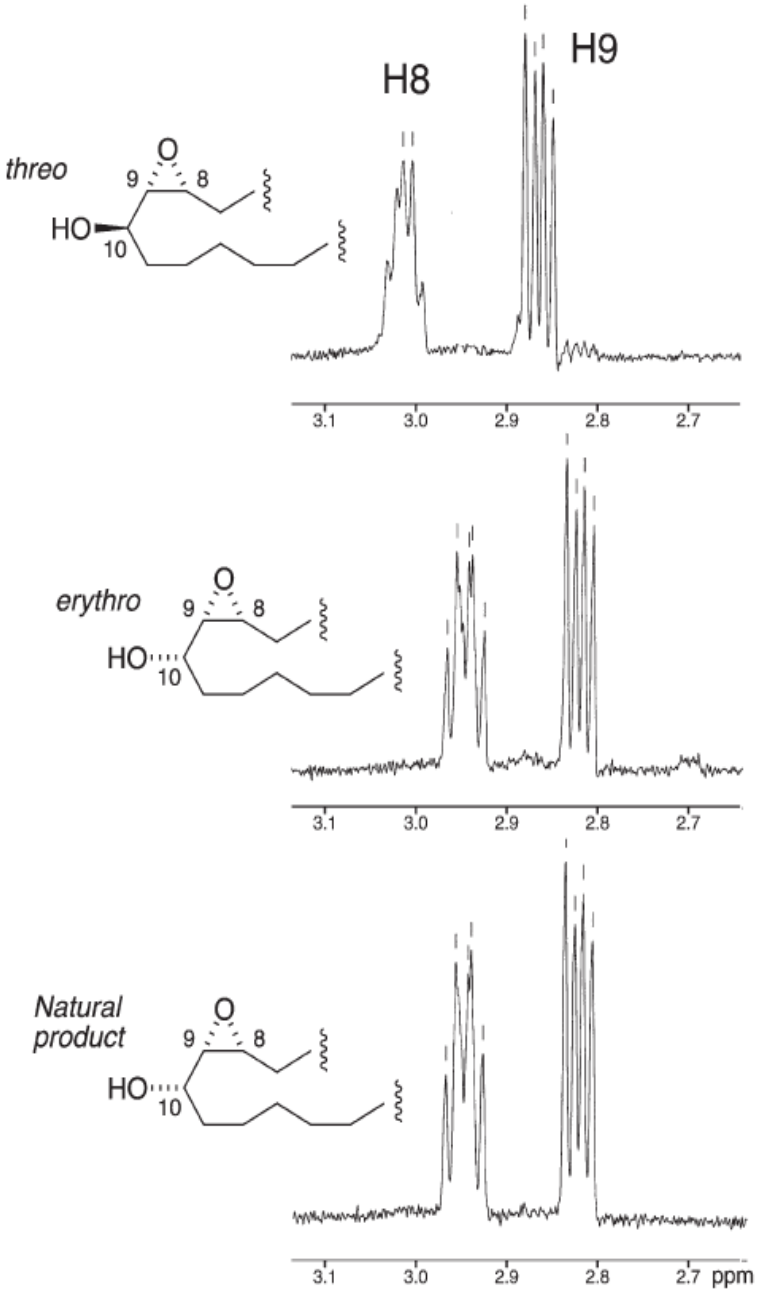

Figure 44: Partial ^{1}H-NMR spectra of the hydrogenated *P. homomalla* product from C20:3ω6 with *erythro* and *threo* fatty acid standards.

Metabolism in the coral extracts is summarized in **Figure 45**.

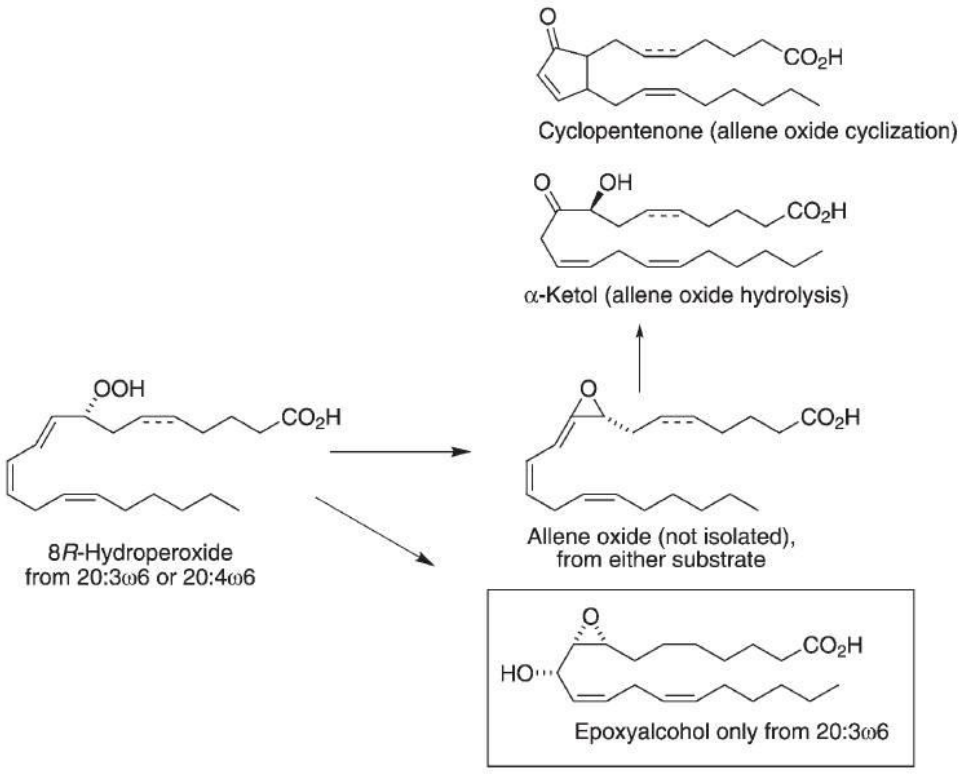

Figure 45: Biosynthesis from 20:4ω6 and 20:3ω6 in *P. homomalla*

Lack of product using allene oxide synthase

There are several precedents for the transformation of fatty acid hydroperoxides to epoxyalcohols catalyzed by allene oxide synthase (AOS) and related enzymes (83,137,138), and it seemed possible that this might account for formation of the 20:3ω6-derived epoxyalcohol. However experiments with the expressed AOS domain of the *P. homomalla* AOS-LOX fusion protein produced only allene oxide as product (detected as the major α-ketol hydrolysis product and cyclopentenone) from either 8*R*-HPETE or 8*R*-HPETrE.

Formation of epoxyalcohol by 8*R*-LOX enzymes

To investigate the mechanistic origin of the 20:3ω6-derived epoxyalcohol, the recombinant LOX domain of the AOS-LOX fusion protein and the purified soluble 76 kD 8*R*-LOX from *P. homomalla* were used for the reaction with 20:3ω6 or 20:4ω6. When sufficient enzyme is used to quickly transform (< 1 min) all the fatty acid to the corresponding 8*R*-hydroperoxide, further reaction proceeded to generate secondary products. When observed by repetitive scanning in the UV, the rapid appearance of the conjugated diene at 237 nm is followed by the gradual decrease in intensity at this wavelength, with the appearance of a new chromophore characteristic of a conjugated triene(s) centered on ~ 270 nm, and a weaker broad absorbance in the area of 300-350 nm. (See below – the main product of the 20:3ω6 reaction absorbs relatively weakly, at 205 nm, and is not detected by UV scanning). In side-by-side incubations monitored in the UV it was apparent that the 20:3ω6-derived 8*R*-HPETrE disappeared more quickly than the corresponding arachidonic acid-derived 8*R*-HPETE. These side-by-side reactions were also conducted using ^{14}C-labeled fatty acid substrate, and after extraction of these samples using C18 cartridges, RP-HPLC analysis showed distinctly different profiles of products (**Figure 46A**). The results confirmed the more extensive metabolism of the 20:3ω6-derived 8R-HPETrE (less remaining compared to 8*R*-HPETE), and more significantly, the prominent appearance of a polar product unique to 20:3ω6 metabolism. This distinctive peak at ~10 min is the most abundant secondary product from 20:3ω6, detected at 205 nm in the UV. In larger scale incubations, this polar product from 20:3ω6 was prepared in sufficient amounts for structural analysis by ^{1}H-NMR. On the basis of

these data, the 8*R*-LOX product was shown to be identical to the coral epoxyalcohol, 8*R*,9*S*-*cis*-epoxy-10*S*-hydroxy-eicosa-11*Z*,14*Z*-dienoic acid.

I also tested the soluble 76 kD 8*R*-LOX from *P. homomalla*. It reacted very similarly to the recombinant 8*R*-LOX from the AOS-LOX fusion protein. 20:4ω6 and 20:3ω6 were comparable substrates for oxygenation to the corresponding 8*R*-hydroperoxide; however, 8*R*-HPETrE was converted to further products at over twice the rate of 8*R*-HPETE. When reactions with identical amounts of enzyme were analyzed and stopped at the same time (with half of the 20:3ω6 hydroperoxide consumed), subsequent RP-HPLC analysis confirmed the more extensive metabolism of 8*R*-HPETrE and the appearance of a single prominent more polar peak detected at 205 nm, with no comparable prominent product from 8*R*-HPETE (**Figure 46B**). This polar product from 20:3ω6 was identified as the same epoxyalcohol identified earlier by its identical UV profile and co-chromatography on both RP-HPLC and SP-HPLC with the epoxyalcohol formed by the recombinant 8*R*-LOX.

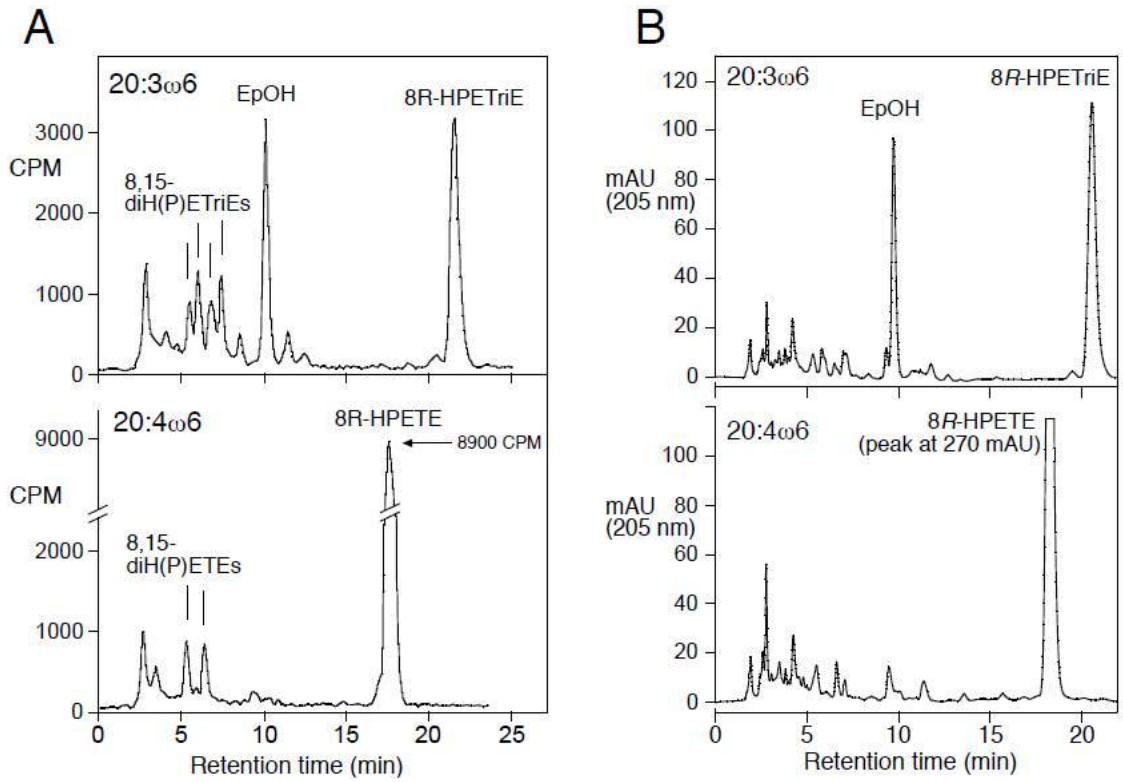

Figure 46: RP-HPLC analysis of products formed from 20:3ω6 and 20:4ω6 by two purified 8*R*-lipoxygenases. (A) Reactions with the recombinant LOX domain of the AOS-LOX fusion protein. (B) Reactions with soluble 76 kD 8*R*-LOX from *P. homomalla*.

Retention of hydroperoxy oxygens in the epoxyalcohol

When 8*R*-HPETrE containing a ~1:2 mixture of $2^{16}O$ and $2^{18}O$ in the hydroperoxide group was reacted with the recombinant 8*R*-LOX, the ^{18}O contents of the substrate and epoxyalcohol product were almost indistinguishable (**Figure 47**). Close inspection indicated 98% retention of both hydroperoxy oxygens in the epoxyalcohol, pointing to a mechanism involving close control of the transformation by the 8*R*-LOX enzyme.

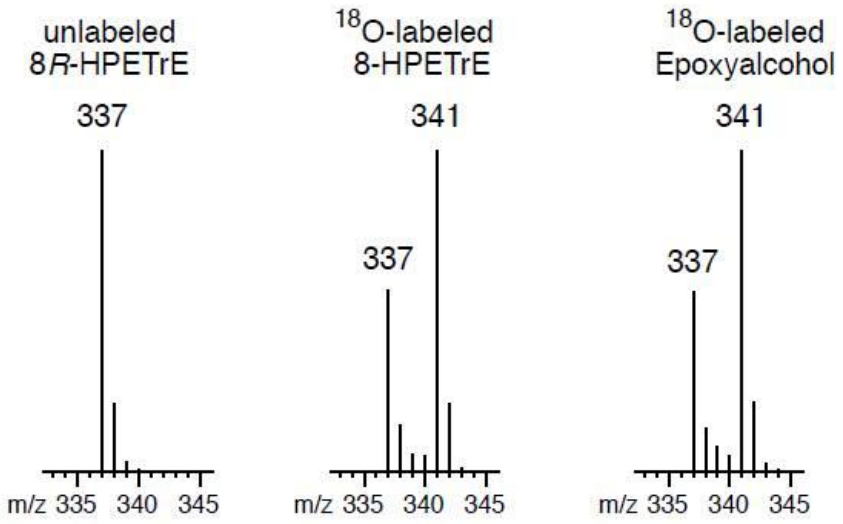

Figure 47: Mass spectrometric analysis of 8*R*-LOX-catalyzed transformation of [^{18}O]8*R*-HPETrE to epoxyalcohol. Epoxyalcohol formed by recombinant 8*R*-LOX from ^{18}O-labeled 8*R*-HPETrE (comprised of a ~1:2 ratio of 2^{16}O to 2^{18}O). The ion abundances were measured by LC-MS (details in Methods) for the unlabeled species (on the left), the hydroperoxy substrate (middle), and epoxyalcohol product (right side).

Discussion

Hydroperoxide isomerase activity

The typical dioxygenation reaction catalyzed by the lipoxygenase enzymes is initiated by the ferric form of the non-heme iron abstracting the hydrogen from polyunsaturated fatty acid substrates. In the present study, the hydroperoxide isomerase activity of 8*R*-LOX which catalyzes the epoxyalcohol biosynthesis is initiated by the ferrous iron catalyzing the homolytic cleavage of the hydroperoxide O-O bond. Several lines of evidence suggest that a lack of access of molecular oxygen within the active site will promote hydroperoxide isomerase activity (13). If present, molecular oxygen will react readily with radical intermediates, thus intercepting and blocking hydroperoxide isomerase cycling, and furthermore, molecular oxygen promotes enzyme activation to the ferric form, also inhibiting isomerase activity (27). Therefore, one can deduce that the 8*R*-HPETrE is an acceptable substrate for interaction with the ferrous iron, and that O_2 is excluded from intercepting the radical intermediates. With the arachidonic acid-derived 8*R*-hydroperoxide, the overall rate of reaction is comparatively sluggish, and very little epoxyalcohol product is formed. The main products are dihydroperoxides or leukotriene A-related diols, both of which are products of the ferric enzyme. This suggests that the selective reaction with the 20:3 8*R*-hydroperoxide is facilitated by exclusion of O_2 within a critical part of the active site, and that this does not occur with binding of the arachidonate analog.

Proposed catalytic cycle

Reaction is catalyzed and controlled by the active site iron, which must first cleave the hydroperoxide and subsequently catalyze an oxygen rebound and hydroxylate the intermediate epoxyallylic radical, while both hydroperoxy oxygens are retained in the epoxyalcohol product (**Figure 48**). This is easy to conceptualize for the reactions of *S*-configuration fatty acid hydroperoxides, because all steps occur on the same face of the reacting molecule, allowing formation of a *trans* epoxide and *threo* alcohol (**Figure 48**, box). Our results with the *R*-configuration hydroperoxide indicate, not only formation of a *cis*-epoxide, which itself presents no conceptual problem, but also the *erythro* configuration of the alcohol. Assuming the iron is in control, this necessitates either a 9,10 bond rotation prior to hydroxylation, or flipping over of the reacting epoxyallylic radical intermediate (**Figure 48**, right and left options). Perhaps the 8*R*-hydroperoxide sits partly turned away from square, so that the epoxyallylic intermediate, when formed, further rotates to expose the opposite face of the intermediate for hydroxylation. We note too that the formation of *cis*-epoxides may be a characteristic of 8*R*-LOX, because the activity in *P. homomalla* extracts was shown to convert 5*S*-HPETE, not to the well-known *trans*-epoxy leukotriene A_4, but to *cis*-epoxy LTA_4 instead (58). Although the mechanisms of epoxyalcohol and LTA_4 synthesis differ, the reactions being initiated by the ferrous and ferric enzymes, respectively, the substrate conformation that predisposes to *cis*-epoxide formation will be dictated by binding in the active site and thus could be dictated in similar fashion by an enzyme that favors *R* versus *S* oxygenation.

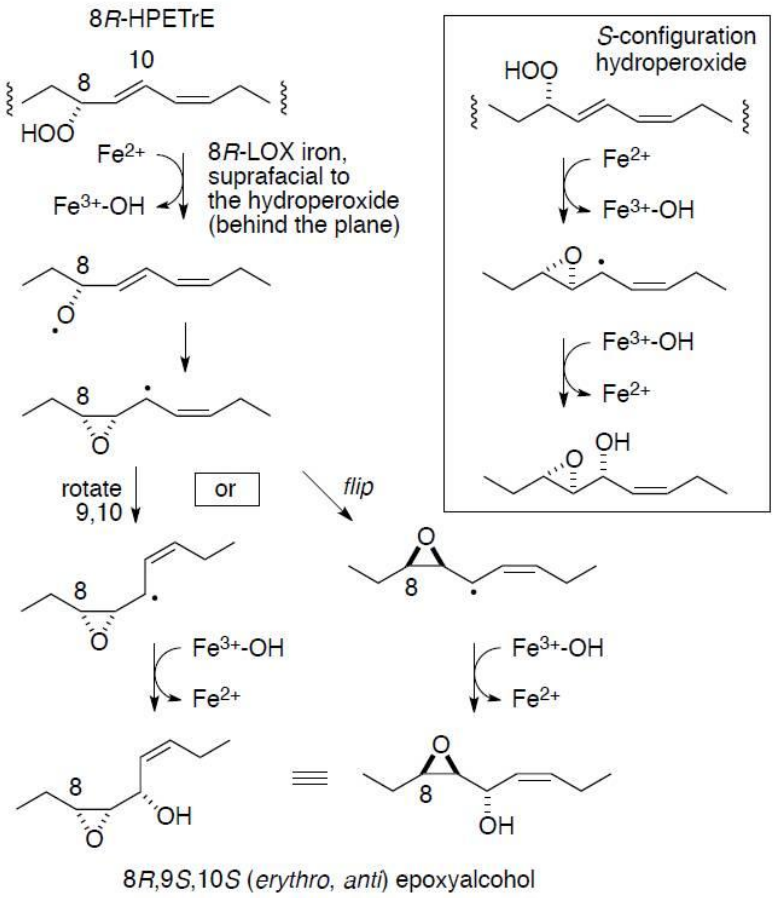

Figure 48: Mechanism of 8*R*-LOX-catalyzed epoxyalcohol synthesis from 8*R*-HPETrE

CHAPTER VI

A POTENTIAL ROUTE TO HNE-LIKE ALDEHYDES VIA LIPOXYGENASE-CATALYZED SYNTHESIS OF A BIS-ALLYLIC DIHYDROPEROXIDE INTERMEDIATE

Introduction

4-Hydroxy-alkenals are a class of cytotoxic aldehydes that play significant roles in various injurious and disease states involving cellular oxidative stress (139). Their toxicity resides on the α,β-unsaturated carbonyl moiety which is highly electrophilic and adducts with biological nucleophiles to exert toxic potential (26,140,141). The prototypical 4-hydroxy-alkenal is 4-hydroxy-nonenal (HNE), representing the tail-end nine carbons of the common polyunsaturated lipids, linoleic and arachidonic acids. In the cellular environment this results in the release of a diffusible cytotoxin. As most fatty acids exist in esterified form in cellular membranes, 4-hydroxy-alkenals generated via lipid peroxidation may also remain attached in complex membrane lipids. This has negative consequences through protein or DNA adduction and a resulting cellular toxicity (142,143).

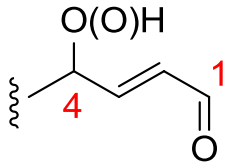

4-hydro(pero)xy-alkenal

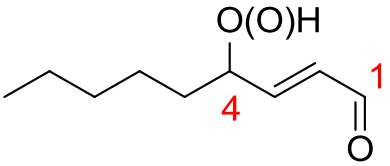

4-hydro(pero)xy-nonenal

One of the intriguing issues in the lipid peroxidation field is the mechanistic origin of HNE and the related 4-hydroxy-alkenals. Multiple mechanistic proposals have appeared over the years, their most common feature being the involvement of a polyunsaturated lipid hydroperoxide. Beyond this step, there are several highly plausible potential pathways, and based on the current evidence there seems little doubt that there are diverse synthetic routes to HNE-related aldehydes. Over two decades ago, hypothetical pathways to HNE were suggested by Pryor and Porter (144), and these remain valid proposals. Indeed, experimental evidence appeared recently supporting one of their schemes involving a pseudo-symmetrical diepoxy carbon radical intermediate (145). Among other potential routes, this lab advanced alternate pathways via the intermediacy of fatty acid radical dimmers (see experimental studies in **Chapter VII**) (146), and provided experimental support for the concept (147). Convergence of the activities of 5-lipoxygenase (5-LOX) and cyclooxygenase provides yet another route to these short-chain aldehydes (148).

Among the many possibilities for the synthesis of HNE-related aldehydes during lipid peroxidation, of direct relevance to the present study is the postulated intermediacy of a bis-allylic fatty acid dihydroperoxide (**Figure 49**).

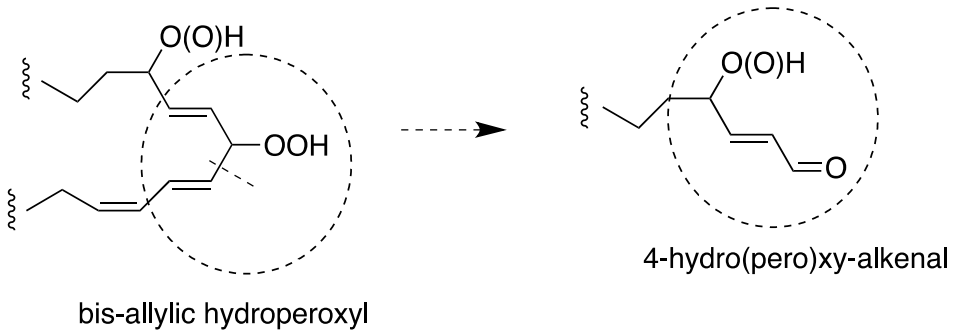

Figure 49: Bis-allylic fatty acid hydroperoxide and its cleavage to a 4-hydro(pero)xy-alkenal

This pathway was invoked by this lab to account for retention of the hydro(pero)xyl chirality in the transformation of 13*S*-H(P)ODE to 4*S*-H(P)NE (149,150). It was subsequently proposed also as a potential intermediate in diverse biochemical transformations (151,152). In following up on these observations this lab had prepared model linoleate dihydroperoxides (diHPODEs) by singlet oxygen treatment of linoleic acid and examined their stability. Disconcertingly, it was found that the purified diHPODEs, in the absence of any catalyst, show little propensity to degrade to HNE-related aldehydes when allowed to stand in air at 37°C (153). By comparison, the mono-hydroperoxides of linoleate do form H(P)NE upon standing in air with no added catalyst. Conversion of the diHPODEs to H(P)NE was induced by treatment with acid, in line with the much-invoked Hock cleavage, an acid-catalyzed reaction. This, however, does not mimic the neutral environment under which HNE was formed using our autoxidation conditions. If diHPODEs or the corresponding dihydroperoxides of arachidonate (diHPETEs) are involved in formation of HNE, then some other catalyst has to be active. In earlier experiments using the *P. homomalla* 8*R*-LOX (**Chapter V**) we noticed the formation of polar products from arachidonic acid, prompting our investigation of their structures and mechanism of formation. This led to the present report in which we identified a bis-allylic dihydroperoxide pathway to an HPNE-related aldehyde with a lipoxygenase (LOX) enzyme promoting the transformations.

Experimental procedures

Materials

Arachidonic acid was purchased from NuChek Prep Inc. (Elysian, MN). [1-^{14}C] C20.4ω6 was purchased from Perkin Elmer Life Sciences. 9*E*,11*Z*,14*Z*-20:3ω6 was synthesized by Dr. Jin K. Cha, Wayne State University, as described previously (27). Nordihydroguaiaretic acid (NDGA) was purchased from Cayman Chemical Co. (Ann Arbor, MI). Triphenylphosphine (TPP) was purchased from Sigma.

Expression and purification of 8R-lipoxygenase

cDNA of the 8*R*-LOX domain of the *P. homomalla* peroxidase-lipoxygenase fusion protein was subcloned into the pET3a vector (with an N-terminal His_4 tag), and the protein was expressed in *E. coli* BL21 (DE3) cells and purified by nickel affinity chromatography according to a previously published protocol (61). For clarity, this 8*R*-lipoxygenase is referred to here as the recombinant 8*R*-LOX.

Enzymatic incubation

Incubations were performed at room temperature in 1 ml of 50 mM Tris, pH 8.0, 500 mM NaCl, 2 mM $CaCl_2$ and 0.01% Emulphogene detergent using recombinant 8*R*-LOX (10 μg/ml) and fatty acid substrates, arachidonic acid (25 μg/ml) or purified 8*R*,11*R*-diHPETE (5 μg/ml). Incubations were conducted in a 1 ml quartz cuvette, monitored by repetitive scanning from 350-200 nm using a Lambda-35 spectrophotometer (Perkin-Elmer) and stopped by acidification to pH ~4.5. After extraction using C18 Oasis cartridges the samples were further analyzed by HPLC.

HPLC analyses

Aliquots of the extracts were analyzed by RP-HPLC using a Waters Symmetry 5μ column (25 x 0.46 cm) at a flow rate of 1 ml/min with CH_3CN/H_2O/HAc (45/55/0.01, by volume). Peaks were monitored using on-line UV detection (Agilent 1100 series diode array detector). Further purification was achieved by normal-phase HPLC using a Beckmann Ultrasphere 5μ silica column using a solvent of hexane/isopropanol/glacial acetic acid (100/2/0.1, by volume) at 1 ml/min. For chiral analysis, the enantiomers were resolved using a Chiralpak AD column (25 x 0.46 cm) with a solvent system of hexane/methanol (100/2, by volume) run at 1 ml/min.

Preparation of 8*R*,11*R*-diHPETE

Arachidonic acid (100 μg/ml) in Tris enzyme buffer (pH 8.0, 500 mM NaCl, 2 mM $CaCl_2$ and containing 0.01% Emulphogene detergent) was reacted with 8*R*-LOX (10 μg/ml) for 30 min on ice, with the reaction monitored by scanning UV spectroscopy. The reaction was stopped by acidification using 1M KH_2PO_4 and 1N HCl to give pH 4 and the sample applied to an Oasis C18 cartridge, which was washed with water and the products eluted with methanol. The 8*R*,11*R*-diHPETE was subsequently purified by RP-HPLC followed by methylene chloride extraction from the HPLC solvent. The organic phase was washed with water and then blown to dryness under a nitrogen stream. The purified 8*R*,11*R*-diHPETE in ethanol was quantified by UV spectroscopy assuming an extinction coefficient of 25,000 at 242 nm, and stored at -30 ℃ prior to use.

Compound Derivatization

Catalytic hydrogenations were performed in 100 μL of ethanol using about 1 mg of palladium and bubbling with hydrogen for 2 min at room temperature. The hydrogenated products were recovered by the addition of water and extraction with ethyl acetate. Methyl esters were prepared using ethereal diazomethane in methanol. Methoxime derivatives were prepared by treatment with 5 μl of methoxylamine hydrochloride in pyridine (10 mg/ml) overnight at room temperature. Trimethylsilyl (TMS) ether derivatives were prepared using bis(trimethylsilyl)-trifluoracetamide (10 μL) at room temperature for 2 hour. PFB esters were prepared using 10% diisopropyl ethanolamine in acetonitrile (20 μl) and 10% pentafluorobenzylbromide (40 μl) at 37 ℃ for 15 min.

GC-MS analyses

Analyses of product derivatives were performed in the positive ion electron impact mode (70 eV) using a Thermo Finnigan Trace DSQ ion trap GC-MS. The RTX-1701 fused silica capillary column, 17 m x 0.25 mm internal diameter, was programmed from 150 ℃ to 300 ℃ at 20 ℃ /min. The samples were subjected to rapid repetitive scanning over the mass range of 50-500 a.m.u. covering the major fragment ions.

NMR analyses

^{1}H NMR and COSY spectra were recorded on a Bruker 600 MHz spectrometer at 298 K. Chemical shifts are reported relative to tetramethylsilane (0.0 ppm), using the residual non-deuterated NMR solvent as the lock signal (δ = 7.16 ppm for C_6D_6, 7.26 ppm for $CDCl_3$).

Results

Metabolism of arachidonic acid by recombinant 8*R*-LOX

Recombinant 8*R*-LOX from the *P. homomalla* AOS-LOX fusion protein oxygenates arachidonic acid specifically to 8*R*-HPETE, and then on further exposure to the enzyme the 8*R*-HPETE is slowly transformed to secondary products via multiple oxidative pathways. After extraction using a C18 cartridge, RP-HPLC analysis with diode-array detection at multiple wavelengths shows a complex mixture of products (**Figure 50**).

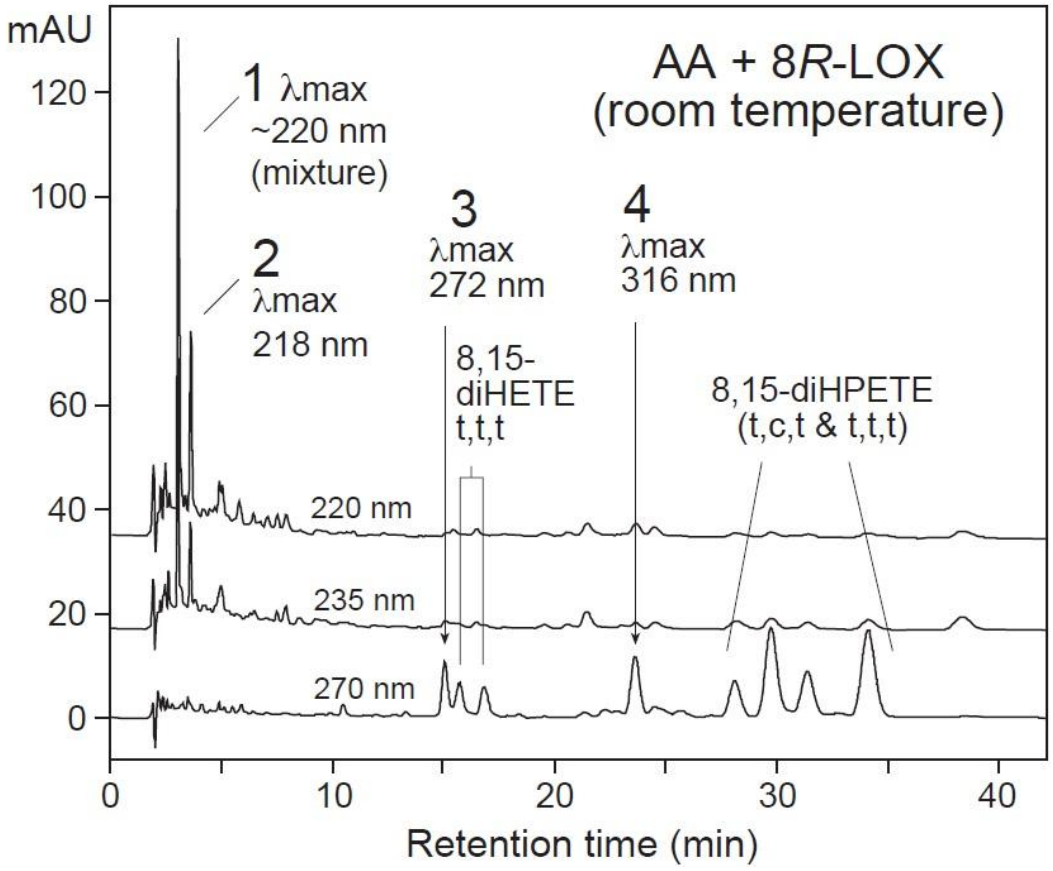

Figure 50: RP-HPLC analysis of reaction of arachidonic acid with 8*R*-LOX. Waters Symmetry column (25 x 0.46 cm), a solvent of CH_3CN/H_2O/HAc (45/55/0.01, by volume), at a flow rate of 1 ml/min, with diode array detection.

The peaks labeled **1-4** each exhibit a smooth UV chromophore typical of a conjugated enone, while the later-eluting groups of products (mainly 8,15-diH(P)ETEs) exhibit the characteristic UV chromophore of a conjugated triene. After further chromatography, the main components of peak **1** were separated and identified by NMR as a mixture of a C_7 keto acid, 5-oxo-hept-6-enoic acid (**Figure 51**), and C_7 aldehyde acid, 7-oxo-hept-5*E*-enoic acid (**Figure 52**).

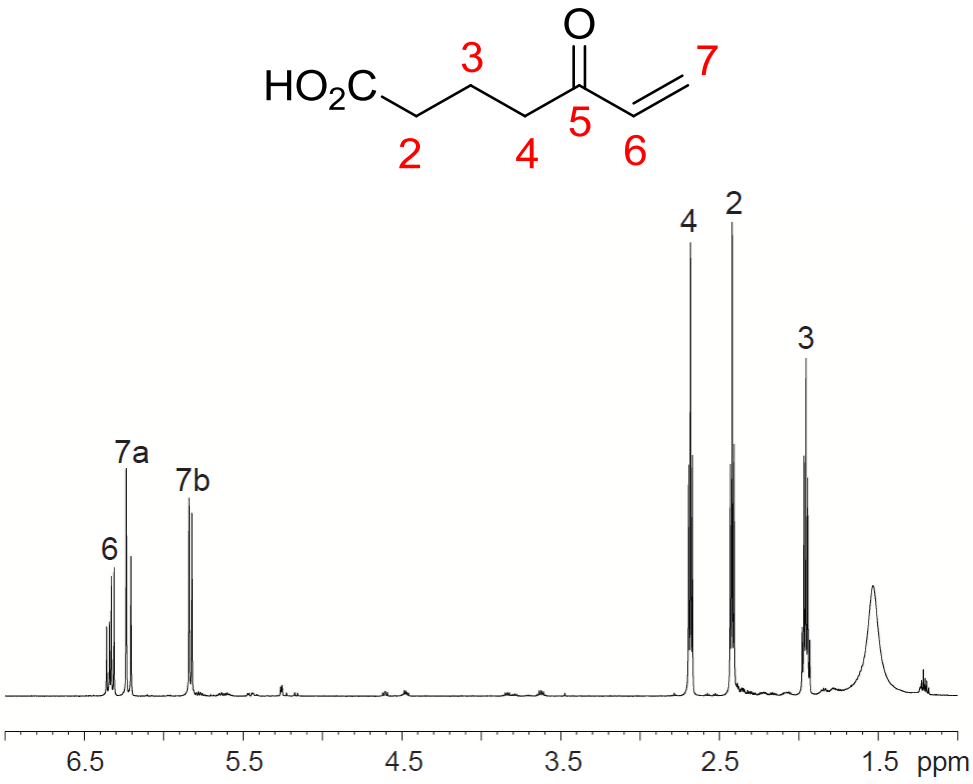

Figure 51: ^{1}H-NMR spectrum of 5-oxo-hept-6-enoic acid (one of the two main components of peak 1 in **Figure 50**). The spectrum was recorded in d6-benzene at 298K using a Bruker 600 MHz spectrometer.

The molecular weight of the peak "5-oxo-hept-6-enoic acid" was confirmed as 142 by LC-MS (Q-TOF, negative-ESI, $[M-H]^-$ ion, predicted 141.0552, found 141.0557, $C_7H_9O_3$.

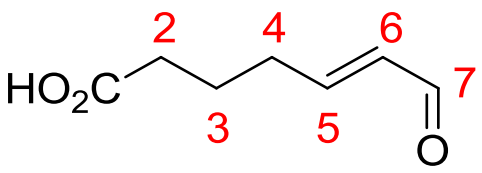

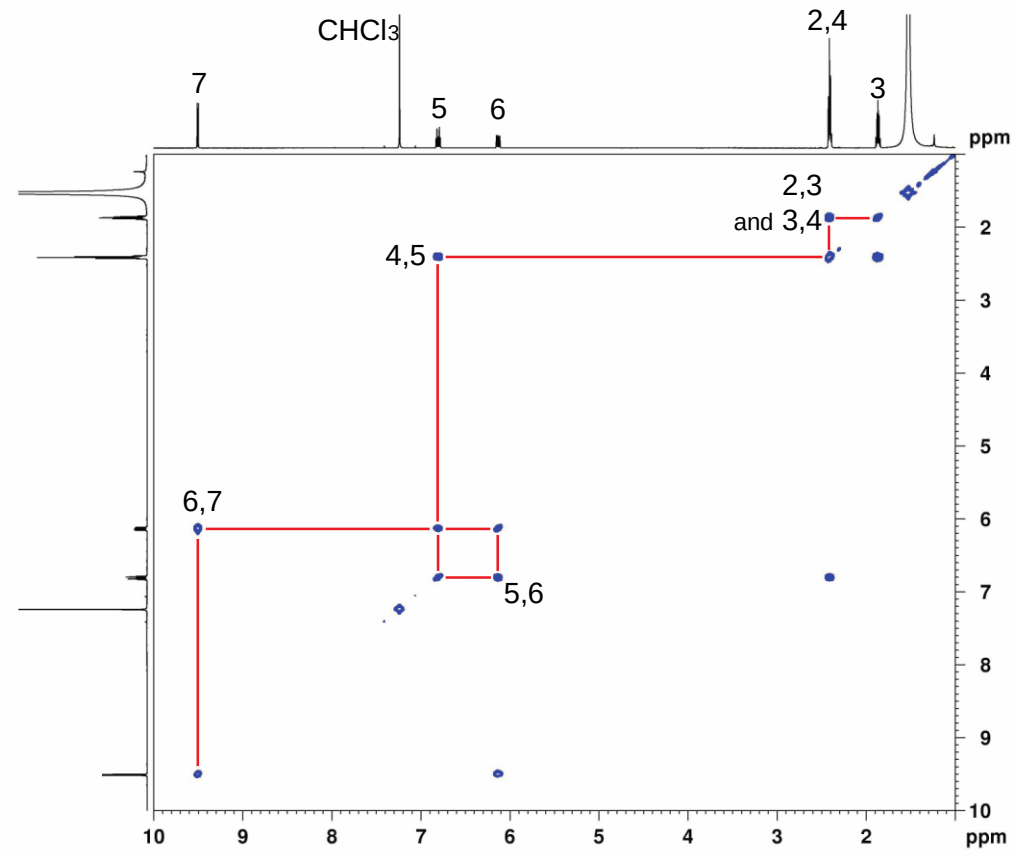

Figure 52: COSY NMR spectrum of 7-oxo-hept-5*E*-enoic acid (the second main component of peak 1 in **Figure 50**). The spectrum was recorded in d6-benzene at 298K using a Bruker 600 MHz spectrometer.

7-oxo-hept-5*E*-enoic acid. ^{1}H-NMR, 600 MHz, $CDCl_3$, 283K, δ9.50, d, 1H, H7, $J_{6,7}$ = 7.8 Hz; 6.81, dt, 1H, H5, $J_{4,5}$ = 6.7 Hz, $J_{5,6}$ = 15.7 Hz; 6.13, dd, 1H, H6, $J_{5,6}$ = 15.7 Hz, $J_{6,7}$ = 7.8 Hz; 2.38-2.44, m, 4H, H2, H4; 1.86, p, 2H, H3, $J_{2,3}$ = 7.4 Hz, $J_{3,4}$ = 7.4 Hz.

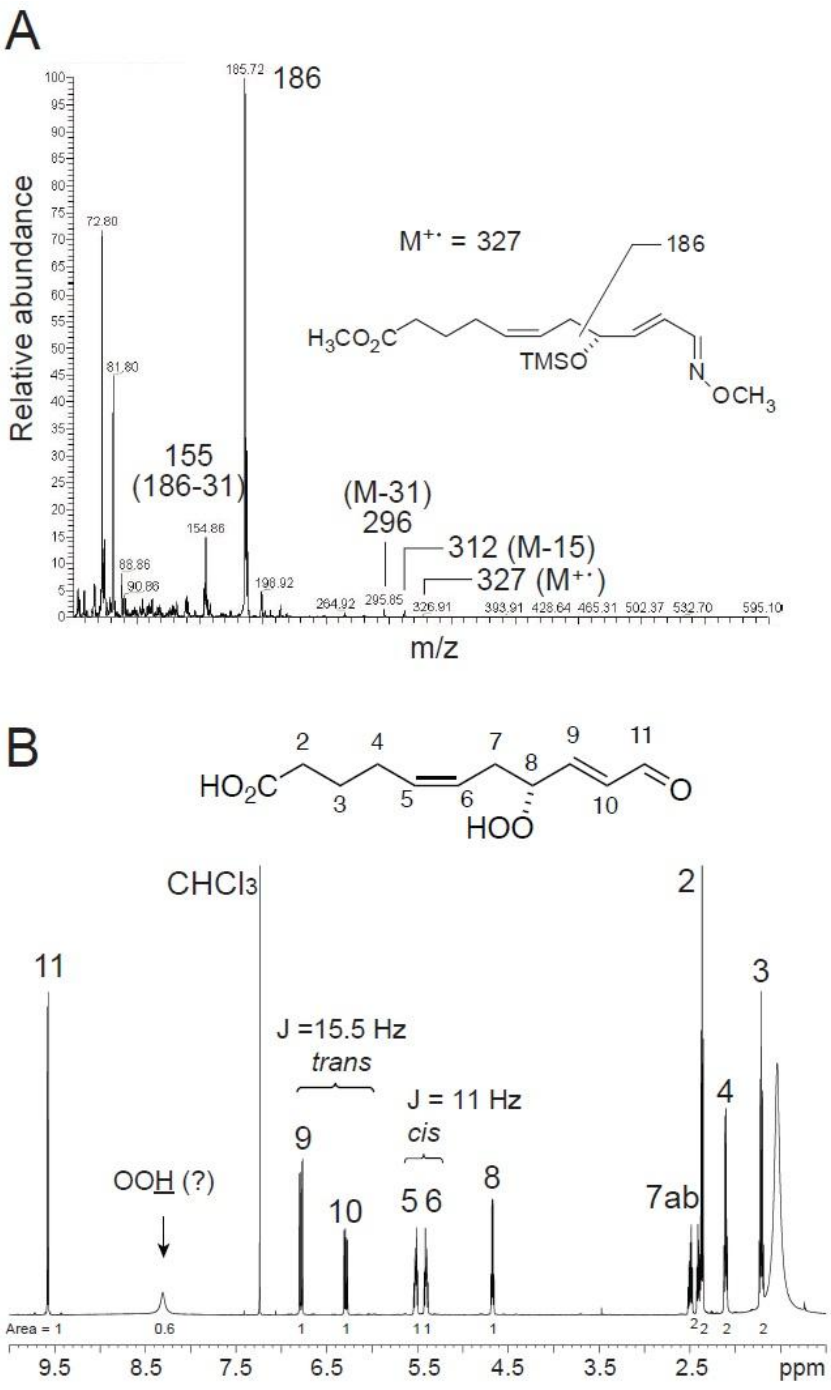

Figure 53: GC-MS and NMR analyses of 8*R*-hydroperoxy-11-oxo-undeca-5*Z*,9*E*-dienoic acid.
A. Mass spectrum of the methyl ester TMS ether methoxime derivative of TPP-reduced **2**. **B.** ^{1}H-NMR spectrum of **2**.

It turns out that the peak **2** in **Figure 50** is directly relevant to the *bis*-allylic dihydroperoxide pathway to HNE-related aldehydes. **2** exhibits a UV chromophore (λmax 218 nm) similar in character to the spectrum of HPNE. Treatment of the extracts with triphenylphosphine converted **2** to a slightly more polar derivative (λmax 221 nm) consistent with reduction of the hydroperoxy analogue to its hydroxy counterpart. The hydroxy analogue of **2** was analyzed by GC-MS as the methyl ester TMS ether methoxime derivative, **Figure 53A**. Structurally diagnostic ions were observed at m/z values of 327 ($M^{+\bullet}$, 1% abundance), 312 (M-15, 2%), 296 (M-31, 2%), 186 (C_8-C_{11}, 100%) and 155 (16%), compatible with the methyl ester of a C_{11} fatty acid containing an 8-hydroxyl and C_{11} aldehyde. The proton NMR spectrum of the parent **2** defined the structure, **Figure 53B**. Thus, the doublet at 9.6 ppm in **Figure 53B** represents the aldehyde proton ($J_{10,11}$ = 7.7 Hz), with coupling to the doublet of doublets at 6.3 ppm (H10, J = 7.7 and 16.0 Hz), the 16.0 Hz J value indicating a *trans* double bond with H9 (dd at 6.8 ppm, J = 16.0 and 6.0 Hz), next to the C8 proton geminal with the hydroperoxide (C8, q, J = 6 Hz), with further clear couplings through to H2. Consistent with the conjugated enone chromophore and GC-MS analysis, and taking into account its formation from 8*R*-HPETE, the **2** was identified as 8*R*-hydroperoxy-11-oxo-undeca-5*Z*,9*E*-dienoic acid. This HPNE-like aldehyde is formed by cleavage of the C_{20} precursor between C11 and C12. The yield of **2**, estimated from an experiment using [1-^{14}C]8*R*-HPETE as substrate, was approximately 8% of the recovered radioactive products.

Other prominent products shown in **Figure 50** are outlined as follows: the several compounds with UV spectra characteristic of all-*trans* or *trans-cis-trans* conjugated trienes were readily identified as 8,15-diHETEs or 8,15-diHPETEs based on the

availability of synthetic standards, and the change in chromatographic mobility of the hydroperoxides on reduction with triphenylphosphine;. Peak **3** eluting at 15 min with λmax at 272 nm exhibits a conjugated dienone chromophore, and was identified by GC-MS and ^{1}H-NMR as the C_{11} aldehyde 6-hydroperoxy-(2*E*,4*E*)-undecadienal. Peak **4** at 24 min retention time has the UV absorbance characteristic of a conjugated trienone (λmax 316 nm), and was identified as the C_{13} aldehyde, 8-hydroperoxy-(2,4,6)-tridecatrienal. Experiments using [1-^{14}C]arachidonic acid as 8*R*-LOX substrate confirmed that the C_7 keto and aldehyde acids in peak **1** and the HPNE-related **2** retain the 1-^{14}C label, and for example, that the C_{11} and C_{13} aldehydes from the methyl end of the fatty acid were unlabeled. The radioactivity also facilitated the detection of two additional polar products that are resolved using RP-HPLC solvent containing 90% water. LC-MS analysis indicated that these extra products, which absorb very weakly near 200 nm in the UV are C_7 hydroxy acids (M-H ion at m/z 143), likely 5-hydroxy-hept-6-enoic acid and 7-hydroxy-hept-5-enoic acid, expected as α-cleavage products from 8-HPETE or 8,15-diHPETE.

Trapping the intermediate to the HNE-like aldehyde

To aid in the isolation of unstable or rapidly metabolized intermediates, the incubation of arachidonic acid with 8*R*-LOX was repeated at ice-cold temperature. RP-HPLC of the on-ice incubation showed a relative decrease in formation of all cleavage products, including those in peaks **1** - **4**, with increased recovery of the 8,15-diH(P)ETEs and, eluting just after the 8,15-diHPETEs, a prominent new peak that was hardly detected in the incubation at room temperature (**Figure 54**).

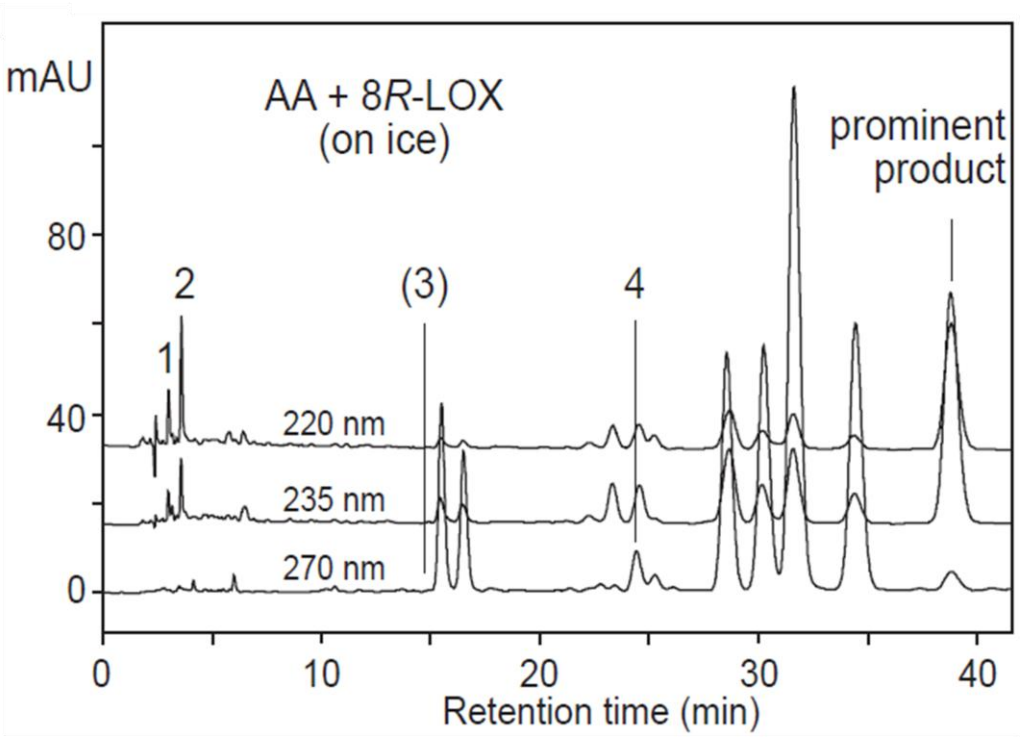

Figure 54: RP-HPLC analysis of on-ice incubation of arachidonic acid with 8*R*-LOX Recombinant 8*R*-LOX (10 μg/ ml) was reacted with arachidonic acid (50 μM) in 50 mM Tris pH 8 containing 500 mM NaCl, 2 mM $CaCl_2$ plus 0.01% Emulphogene detergent for 15 min at the ice-cold temperature. An aliquot of the reaction was analyzed by RP-HPLC using a Waters Symmetry column (25 x 0.46 cm), a solvent of CH_3CN/H_2O/HAc (45/55/0.01, by volume), at a flow rate of 1 ml/min, with diode array detection. The peaks labeled 1-4 correspond to those in **Figure 50**. The different wavelengths are on the same scale and are offset for clarity.

The new peak showed an unfamiliar UV chromophore with a smooth profile (as opposed to the angular shoulders on a typical conjugated diene) and a relatively high λ_{max} at 242 nm (**Figure 55**).

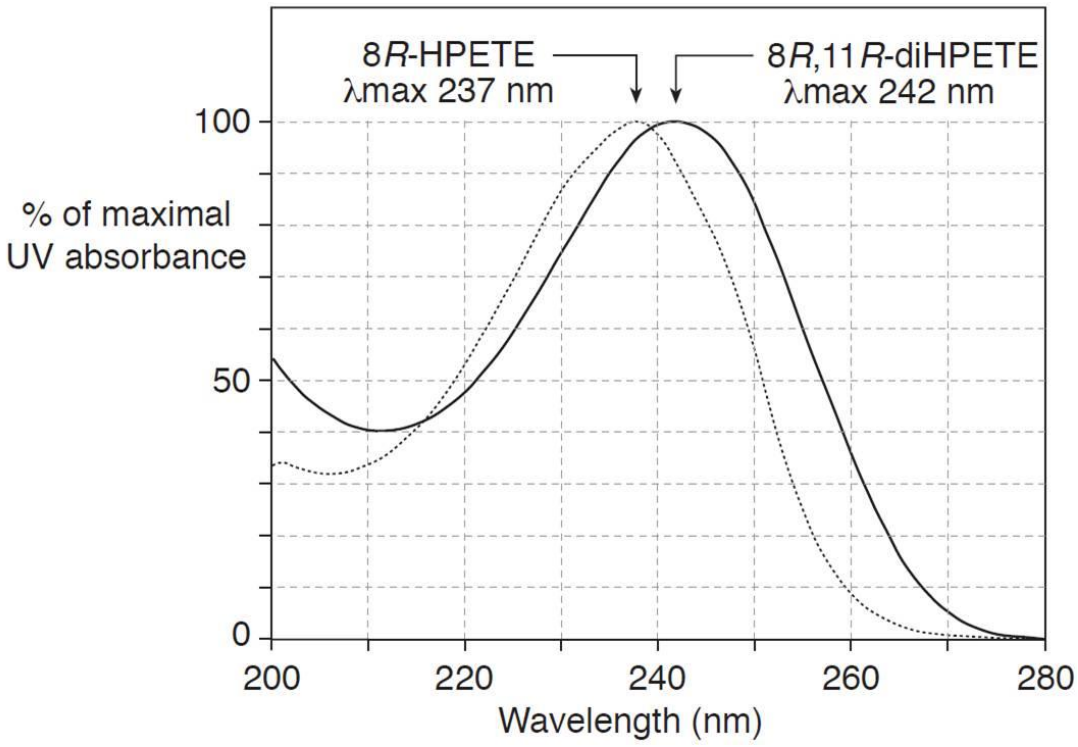

Figure 55: Overlay of the UV spectra of 8*R*-HPETE and 8,11-diHPETE.

After hydrogenation to remove the double bonds, GC-MS analysis of the TMS ester TMS ether derivative showed diagnostic ions at m/z values of 545 (M-15, 1% abundance), 455 (M-90, 1%), 359 (C8-C20, 7%), 343 ([C1-C11]-90, 92%), 303 (C1-C8, 97%), 269 ([C8-C20]-90, 89%) and 229 (C11-C20, 73%) (**Figure 56**). The major α-cleavage fragment ions define the position of the two hydroxyl groups at C8 and C11. The parent 8,11-diHPETE (5*Z*,9*E*,12*E*,14*Z*) exhibits a distinctive conjugated diene chromophore (12*E*,14*Z*) modulated mainly by the presence of the nearby 9*E* double bond.

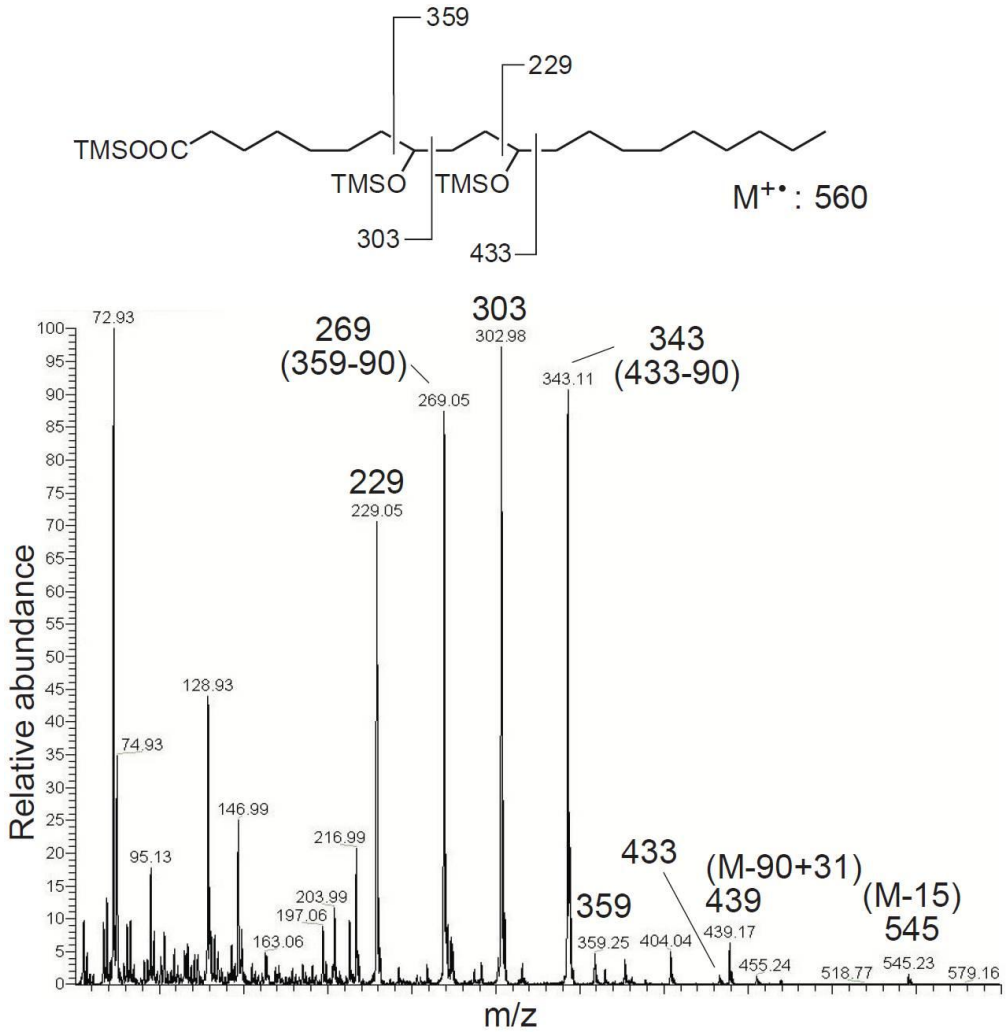

Figure 56: GC-MS analysis of the TMS ester TMS ether derivative of the TPP-reduced hydrogenated 8,11-diHPETE.

Conversion of purified 8,11-diHPETE to the aldehydes in peaks **1** and **2**

To examine the relationship between 8,11-diHPETE and the secondary cleavage products, purified 8,11-diHPETE was incubated with 8*R*-LOX and formation of the cleavage products was checked by RP-HPLC (**Figure 57**). The conversion was minimal using 8*R*-LOX alone, but upon co-incubation with NDGA, a reductant of the LOX iron, 8,11-diHPETE was completely consumed, and accompanied by production of the C_7 aldehyde acid of peak **1** and the HPNE-related C_{11} acid **2**. Control experiments examining the conversions of 8,15-diHPETEs by 8*R*-LOX with or without added NDGA established that neither condition produced peaks **1** and **2**.

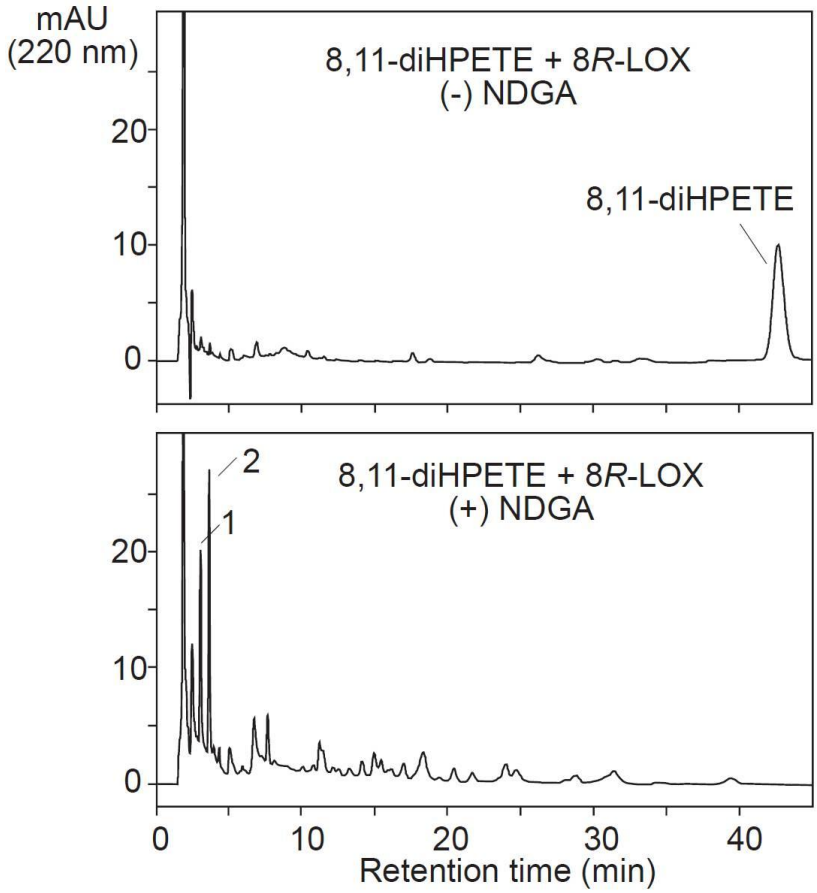

Figure 57: Conversion of purified 8,11-diHPETE to peaks 1 and 2
Reactions of recombinant 8*R*-LOX (10 μg/ml) with purified 8,11-diHPETE (5 μg/ml) were conducted in 50 mM Tris pH 8 containing 500 mM NaCl, 2 mM $CaCl_2$ plus 0.01%

Emulphogene detergent for 15 min at room temperature without (top) or with (below) adding 5 μM NDGA. Aliquots of the reaction were analyzed by RP-HPLC with diode array detection as outlined above. The UV profiles at 220 nm are illustrated.

Determination of the C11-hydroperoxyl configuration

Formation of 8,11-diHPETE by 8*R*-LOX appears to involve a secondary oxygenation via a "frame-shift" along the carbon chain of the 8*R*-HPETE substrate, in which case formation of an 11*R* hydroperoxy moiety is predicted. To provide support for this proposed biosynthetic mechanism, I examined the 8*R*-LOX metabolism of 9*E*,11*Z*,14*Z*-eicosatrienoic acid, a synthetic C20 fatty acid containing a conjugated diene in the same position as in 8-HPETE, but lacking the 8-hydroperoxyl (**Figure 58**).

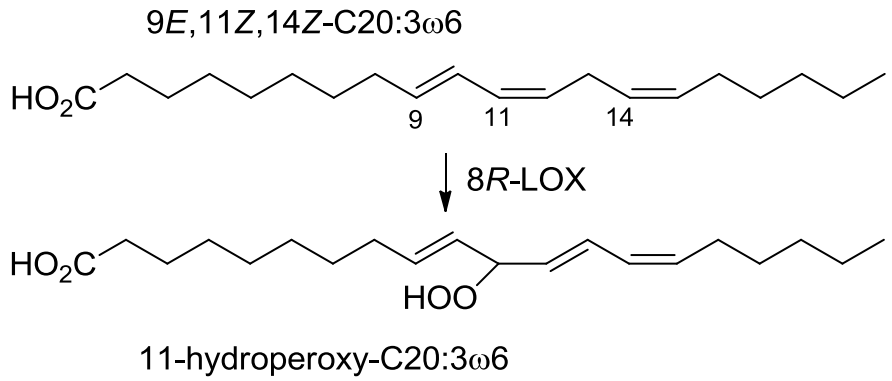

Figure 58: Scheme of 8*R*-LOX reactions with 9*E*,11*Z*,14*Z*-C20:3.

The incubation of 9*E*,11*Z*,14*Z*-eicosatrienoic acid with 8*R*-LOX was conducted at the ice-cold temperature. RP-HPLC analysis of the reaction products demonstrated, in addition to the formation of two conjugated triene-containing products (presumably oxygenated at C9, thus extending the conjugation to 10,12,14), a more prominent product

exhibiting a UV chromophore similar in profile to that of 8,11-diHPETE, except with the λ_{max} 4 nm lower, at 239 nm. GC-MS analysis of the TPP-reduced and hydrogenated product as the TMS ester TMS ether derivative unequivocally established the position of the hydroxy at C11 (**Figure 59**). The parent is therefore 11-hydroperoxy-eicosa-9,12,14-trienoic acid.

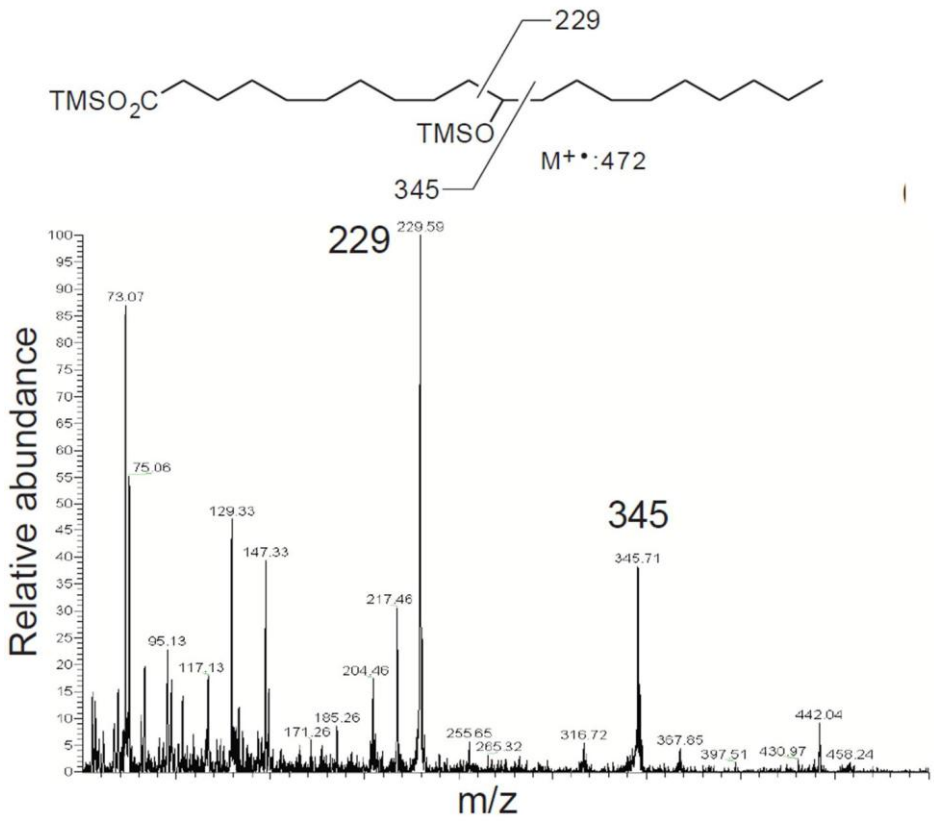

Figure 59: GC-MS analysis of TMS ether TMS ester of TPP-reduced hydrogenated 11-hydroperoxy-C20:3

To determine the stereochemistry at C11, the hydrogenated derivative was converted to the PFB ester and compared by chiral column HPLC with the PFB esters of hydrogenated 11*R*-HETE and 11*RS*-HETE. The chiral phase-HPLC analysis showed

mainly the 11*R* enantiomer (**Figure 60**), and therefore by direct analogy, the structure of the 8,11-diHPETE generated from arachidonic acid is expected to be 8*R*,11*R*-diHPETE.

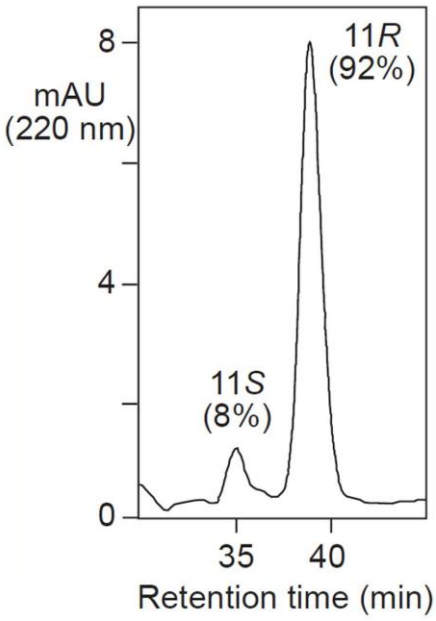

Figure 60: Chiral phase-HPLC analysis of PFB ester of TPP-reduced hydrogenated 11-hydroperoxyl C20:3 using a Chiralpak AD column with a solvent system of hexane/methanol (100/2, by volume) at a flow rate of 1 ml/min. The UV profile at 205 nm is illustrated.

Formation of bis-allylic dihydroperoxides and HPNE from the reactions of 15*S*-HPETE with mammalian 15-LOX

Since detection of such bis-allylic dihydroperoxides is uncommon, I investigated the capability of mammalian lipoxygenase enzymes in producing this type of compounds. Mouse platelet-type 12*S*-LOX and human 15-LOX-1 are chosen because they are capable of oxygenating both C12 and C15 with arachidonic acid as substrate. The concept is that if these two enzymes can oxygenate C12 at 15*S*-HPETE, which is the mono-oxygenation product of human 15-LOX-1 from arachidonic acid, bis-allylic 12,15-diHPETE can be produced. Although 12,15-diHPETE has not been reported as a lipoxygenase product, it could be simply because it is not looked for in lipoxygenase reactions. In addition, the instability of bis-allylic hydroperoxides during typical acid extraction conditions limits the prospects of their detection by chance.

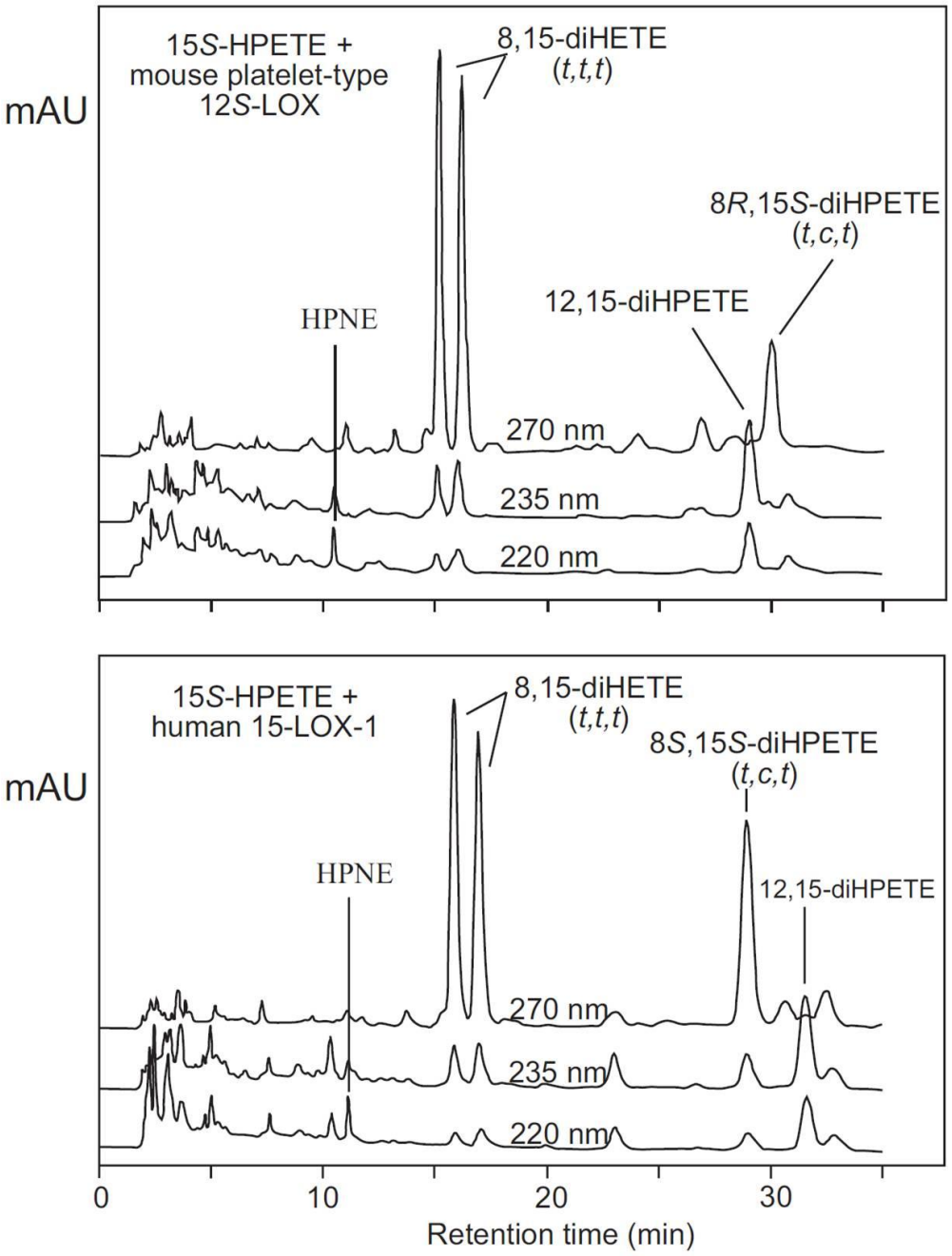

Figure 61: RP-HPLC analyses of room temperature reactions of 15*S*-HPETE with mouse platelet-type 12*S*-LOX (top) and human 15-LOX-1 (below). Column: Waters Symmetry C18, 25 x 0.46 cm; solvent, CH_3CN/H_2O/HAc (45/55/0.01, by volume); flow rate, 1 ml/min; on-line diode array detection. (The retention time difference between the two chromatograms is due to the use of different columns).

Figure 61 demonstrated the product profile of room temperature reactions of 15*S*-HPETE with mouse platelet-type 12*S*-LOX and human 15-LOX-1. The peak, which has a very similar UV chromophore with 8,11-diHPETE (**Figure 62**), was detected within the region of diHPETEs from both reactions. Based on these observations and the understanding of the catalytic properties of these two lipoxygenases, this peak was assigned as 12*S*,15*S*-diHPETE. Interestingly, HPNE was detected as a significant product from both reactions. It is very likely that in these reactions HPNE is formed via 12,15-diHPETE as an intermediate.

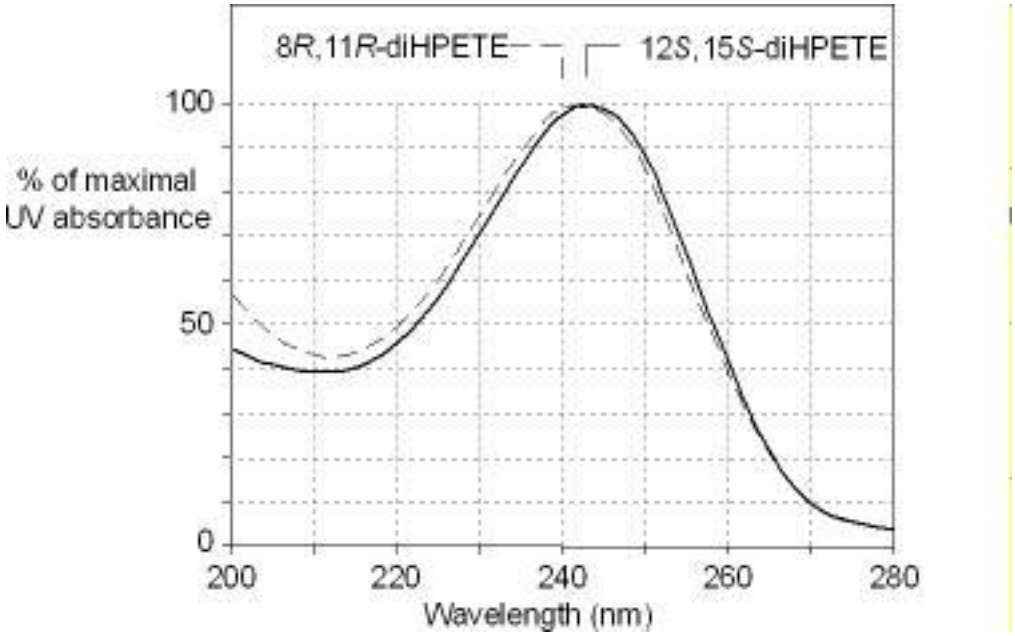

Figure 62: Overlay of the UV spectra of 8*R*,11*R*-diHPETE and 12*S*,15*S*-diHPETE

Discussion

Herein we establish that 8*R*-LOX forms 8*R*,11*R*-diHPETE as one of the transformation products of 8*R*-HPETE, and that this bis-allylic dihydroperoxide is further converted in the course of the ongoing enzymatic reactions, forming the 4-hydro(pero)xy-alkenals, compounds **1** and **2**, as products of this pathway. Considering initially the generation of 8,11-diHPETE, it is notable that detection of such bis-allylic fatty acid hydroperoxides is uncommon, for several reasons. At the top of the list is that, until the year 2000, bis-allylic hydroperoxides remained undiscovered as products of lipid peroxidation (154) and therefore they were simply not looked for in lipoxygenase reactions. Secondly, the instability of bis-allylic hydroperoxides during typical acid extraction conditions, (most extensively studied with the corresponding bis-allylic hydroxy derivatives e.g. refs.(155,156)), limits the prospects of their detection by chance. Thirdly, aside from the fungal enzyme manganese-lipoxygenase that forms 11-hydroperoxy-linoleate as a major product (157), the initial reaction of lipoxygenases with polyunsaturated fatty acids forms the bis-allylic hydroperoxides as very minor products (≤1% abundance) (61,158). By comparison, bis-allylic dihydroperoxides are more prominent products of lipoxygenase secondary reactions, as evidenced here by their detection using the *P. homomalla* 8*R*-LOX (**Figure 54**), the mouse platelet-type 12*S*-LOX, and human 15-LOX-1 (**Figure 61**).

The transformation from arachidonic acid to the aldehyde fragments involves a dual catalytic activity of the lipoxygenase active site iron. The dioxygenase activity by the ferric iron oxygenates C8 and C11 in a sequential manner and produces 8*R*,11*R*-diHPETE. (While 8*R*-HPETE is the prominent mono-oxygenation product from

arachidonic acid by 8*R*-LOX, 11*R*-HPETE is not detected as a product from the reaction.) If the oxygenation proceeded efficiently, then ferric iron would be regenerated in each catalytic cycle and free ferrous iron would not become available. Although the first oxygenation to 8*R*-HPETE is fast and efficient, the secondary reactions by 8*R*-LOX are slow, and they produce a complex mixture of products. Therefore, the primary product, 8*R*-HPETE, can be considered as a poor substrate of the 8*R*-LOX, and the weak secondary reactions may not be well controlled. For instance, with 8*R*-HPETE in the enzyme active site there may be, in effect, a low concentration of suitably-positioned molecular oxygen available to intercept the LOX-generated radicals (cf. refs.(13,27,30)), and/or radical intermediates may escape the active site (13,27). Either possibility will leave the non-heme iron in the ferrous state, now available to catalyze reductive transformations. Indeed there is ample evidence from our product analyses to establish that reduction to alkoxyl radicals is catalyzed by the 8*R*-LOX enzyme. This reaction is involved in synthesis of each of the aldehydic products detected (cf.(159)). Using 8*R*,11*R*-diHPETE as substrate, the ferrous iron catalyzes a homolytic cleavage of the 11-hydroperoxide and generates an alkoxyl radical at C11. The subsequent carbon chain cleavage between C11 and C12 is promoted by β-cleavage of the alkoxyl radical and gives the HPNE-like aldehyde, peak **2** (**Figure 63**). These reductive reactions were inhibited significantly by the use of ice-cold temperatures during the enzyme incubation, likely by improving the efficiency of the oxygenation reactions, allowing recovery of the bis-allylic dihydroperoxide.

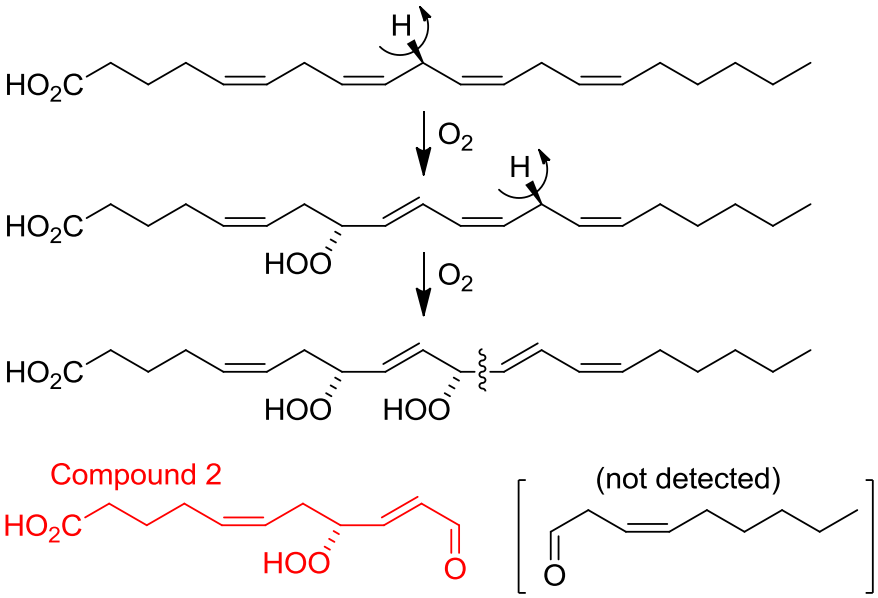

Figure 63: Proposed routes of formation of compound 2

As noted in **Figure 63**, the C11-C12 carbon chain cleavage should also produce 3*Z*-nonenal, although this fragment was not detected in our experiments. Our prior experience with 3*Z*-nonenal is that it chromatographs very poorly on RP-HPLC, and with its weak UV absorbance (end absorbance only) such a product is difficult to detect. Although it might isomerize to 2*E*-nonenal or oxidize to HPNE, which chromatograph nicely and are more readily detectable, I checked using authentic standards for comparison and neither was present on the chromatograms.

The use of NDGA in the 8*R*-LOX-catalyzed transformation from 8,11-diHPETE to HNE-related aldehydes is required. The reduction from the bis-allylic dihydroperoxide to the alkoxyl radical leaves the LOX iron in the oxidized state, and addition of NDGA helps promote ferric-to-ferrous recycling and thus is required for the accumulation of

HNE-related aldehydes. By contrast, as noted above, the cycling occurs fairly efficiently in the complex mixture of reactions starting from arachidonic acid.

Carbon chain cleavage leading to aldehydes was recognized four decades ago as a secondary lipoxygenase activity (promoted under anaerobic conditions) (160). This well-recognized reaction occurs via alkoxyl radical formation then carbon chain cleavage at the C(O•)-CH_2 bond distal to the conjugated diene. The resulting products are akin to the C11 and C13 aldehydes from the methyl end of the molecule identified in the present study. A similar cleavage activity by lipoxygenase that is not reliant on anaerobic conditions was established more recently (161), although mechanistic studies postulate a lack of oxygen availability in the LOX active site as a predisposing factor (27). The formation of a bis-allylic dihydroperoxide as observed here appears to offer an alternative option for carbon chain cleavage. Formation of compounds **1** and **2** occurs with fragmentation at the C(O•)-conjugated diene bond, thus creating the 4-hydro(pero)xy-alkenal.

One property that makes the current reaction plausible in a physiological context is the fast enzymatic turnover via the bis-allylic dihydroperoxide intermediate. 8*R*,11*R*-diHPETE was almost not detected in the room-temperature incubation but accumulated when the secondary cleavage reaction was intercepted by the on-ice incubation. Based on our proposed mechanism, the bis-allylic hydroperoxyl group at C11, but not the hydroxyl, is required for the secondary cleavage reaction to proceed. The fast enzymatic turnover ensures that the secondary cleavage reaction occurs once the dihydroperoxide intermediate is formed and minimizes the possibility that the dihydroperoxide diffuses out of the active site and exposes to the peroxidases which are abundant *in vivo*.

CHAPTER VII

PARTIALLY RESOLVED ISSUES AND OPEN QUESTIONS

1. Dimeric peroxides and novel pathways of lipid peroxidation

Lipid peroxidation is the process in which the starting lipids, usually the polyunsaturated fatty acids (PUFAs), undergo a series of free radical chain reactions and result in various hazards to the host cells. Free radicals generated in lipid peroxidation form not only lipid hydroperoxides as primary products but also reactive aldehydes as secondary products. The formation of reactive aldehydes is of wide research interest because of their toxicity as well as their implication in lipid peroxidation mechanisms.

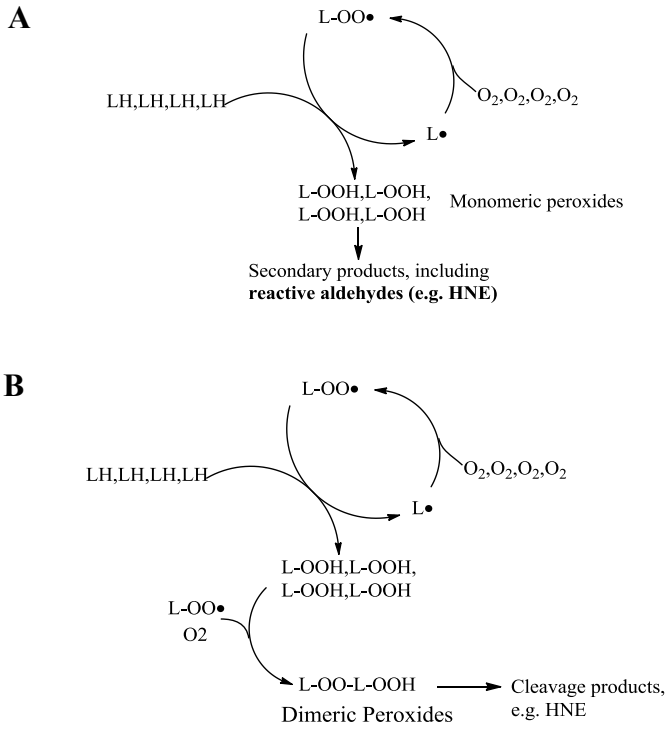

Figure 64: Reactive aldehyde formation in lipid peroxidation. (A) the monomeric lipid hydroperoxides directly give aldehyde formation; (B) the dimeric peroxides are formed and generate aldehyde products.

Figure 64 shows the reactive aldehyde formation in lipid peroxidation. **Figure 64A** shows the classic view of lipid peroxidation in which the monomeric lipid hydroperoxides directly give aldehyde formation; **Figure 64B** shows a proposed view of lipid peroxidation in which the dimeric peroxides are formed and generate aldehyde products. To test the hypothesis in **Figure 64B** is the major aim of this project.

Preparation of dimers

For each preparation, 5 mg of 13*S*-HPODE is placed in a 1.5 ml Eppendorf tube and blown to dryness under a stream of nitrogen. The resulting thin lipid film is subjected to autoxidation under O_2 atmosphere at 37 °C for 2 hr. The autoxidation sample is subsequently analyzed by thin layer chromatography (TLC) and gel filtration separation (**Figure 65**).

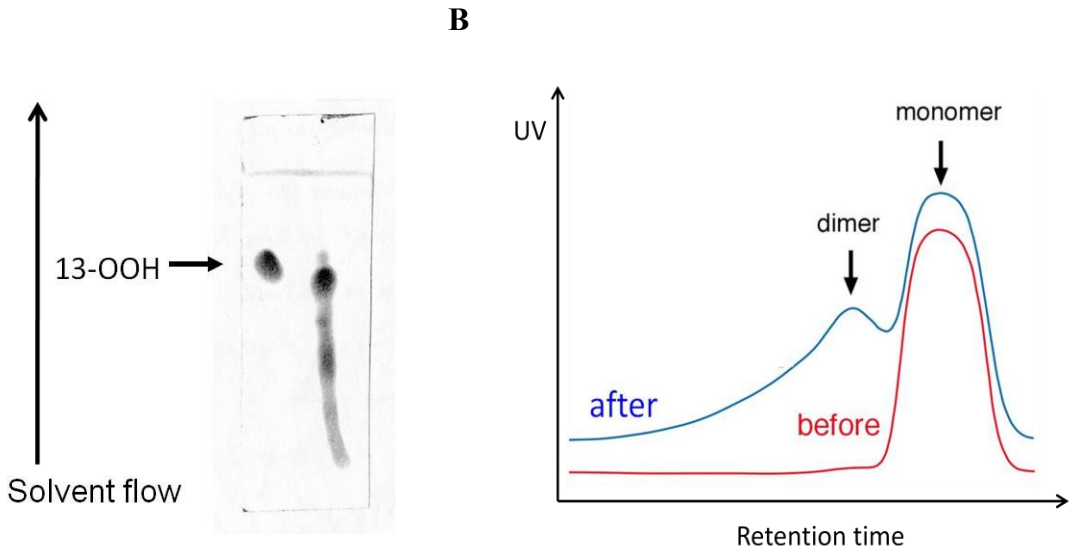

Figure 65: Dimer formation in lipid autoxidation. **A**, Thin layer chromatography analysis before and after autoxidation of 13*S*-HPODE at 37 °C for 2 hr. Solvent: Hex/EtOAc/HAc:60/40/0.1; **B**, Gel filtration analysis before and after autoxidation of 13*S*-HPODE at 37 °C for 2 hr. Column: LH 20 column, 1.5 x 100 cm. Solvent: MeOH.

Identification of dimers

A

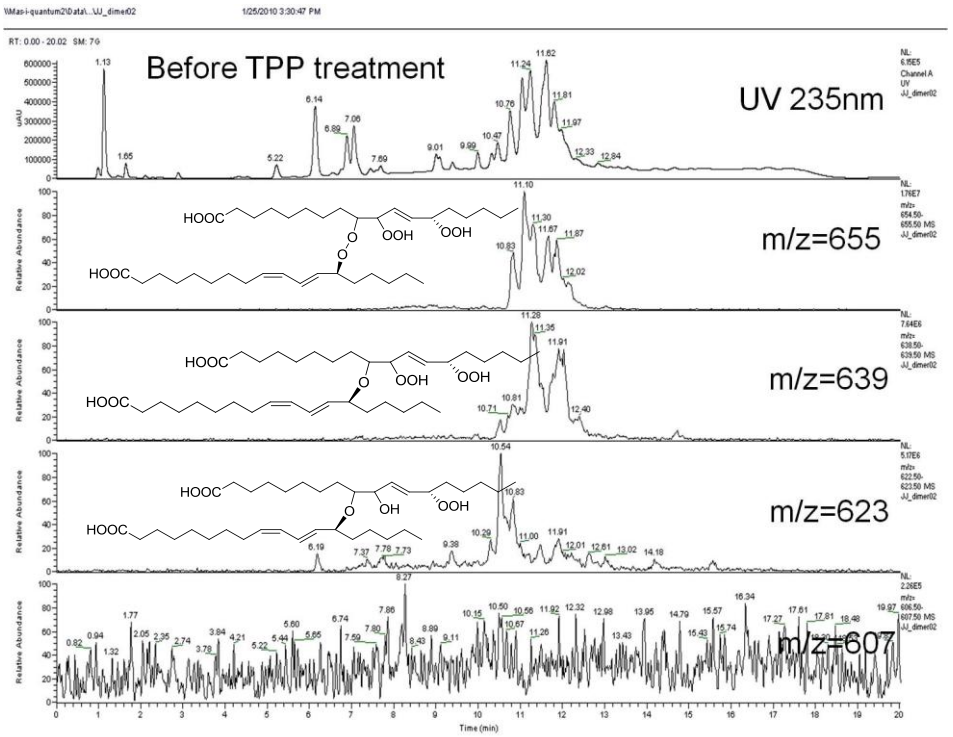

B

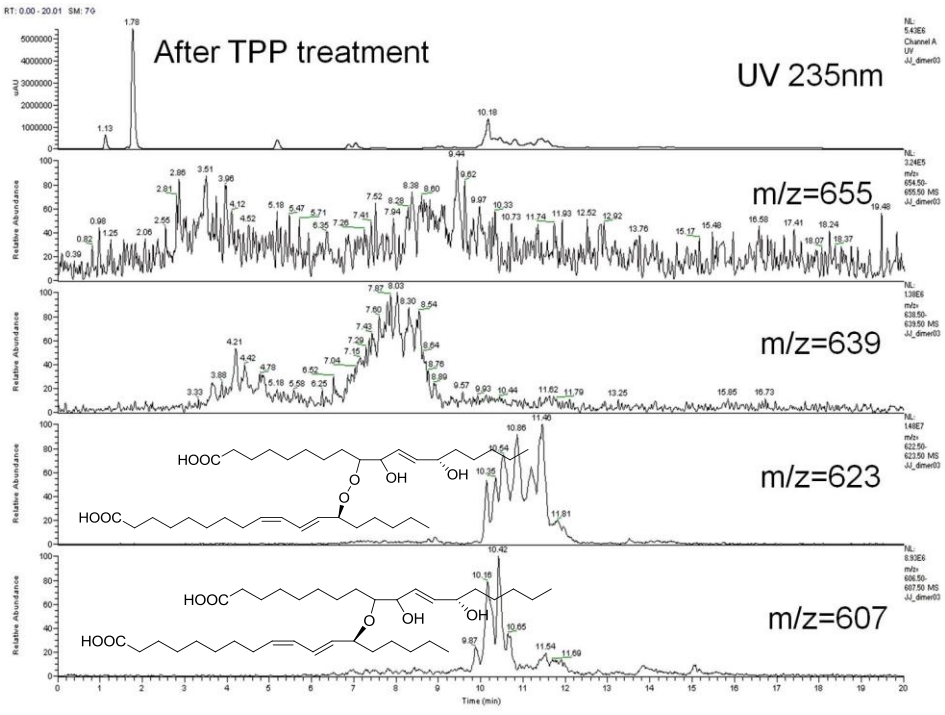

Figure 66: LC-MS analyses of dimeric fractions of LH 20 column separation of 13*S*-HPODE autoxidation sample (**A**) before and (**B**) after TPP treatment.

Figure 66 demonstrated the LC-MS analysis of the dimeric fractions collected from gel filtration separation. The dimers formed in lipid peroxidation consist of a series of compounds with similar structures. The selective ion chromatograms indicate that the different species in dimeric fractions vary in the oxidation states of the hydroxyl/hydroperoxyl groups as well as the type of linkage that bridges the two monomers (-O- or –O-O-).

Production of H(P)NE from dimeric fractions and pure 13*S*-HPODE

In order to investigate whether the dimers function as intermediate in the conversion from the polyunsaturated fatty acid to H(P)NE, I used LC-MS to quantitatively compare the H(P)NE production from the dimers and the pure 13*S*-HPODE.

(1) Development of quantification methods

To develop the H(P)NE quantification method using LC-MS, d3-HNE was added to the sample as the internal standard and HNE (or HPNE after TPP treatment) was derivatized using 2,4-Dinitrophenylhydrazine (DNPH) to improve the detection by mass spectrometry.

To generate the standard curve relating the signal intensities with the HNE amount in the sample, 100 ng of d3-HNE were added to 10 ng, 20 ng, 30 ng, 40 ng, 50 ng of HNE standards (or 10 ng, 20 ng, 30 ng, 40 ng, 50 ng HPNE after TPP treatment). After conversion to HNE-DNP derivatives, the samples were analyzed by LC-MS. The ratios of the peak areas of HNE standard (or HPNE after TPP treatment) over d3-HNE standard

were obtained and plotted against the amount of HNE (or HPNE after TPP treatment) (**Figure 67**).

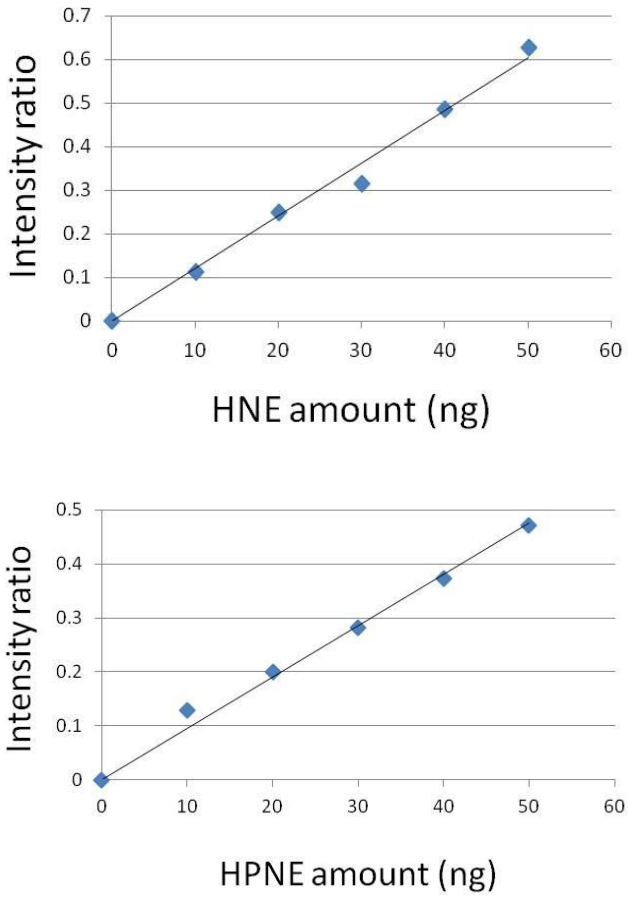

Figure 67: Standard curve of HNE/HPNE quantification by LC-MS

(2) Comparison of H(P)NE production from dimers and pure 13*S*-HPODE

13*S*-HPODE was prepared by the soybean lipoxygenase reaction with linoleic acid followed by SP-HPLC purification. Dimers were prepared by autoxidation of 13*S*-HPODE followed by gel filtration separation. The same amount of dimers and 13*S*-HPODE (based on UV absorbance at 237 nm) were subjected to autoxidation at 37 °C for 0, 20, 40, 60 and 120 min. After addition of d3-HNE, the autoxidation samples were

reduced with TPP and derivatized using DNPH. The H(P)NE (HNE+HPNE) amount in the autoxidation samples was obtained by comparing the ion intensities with the standard curves generated in **Figure 67**.

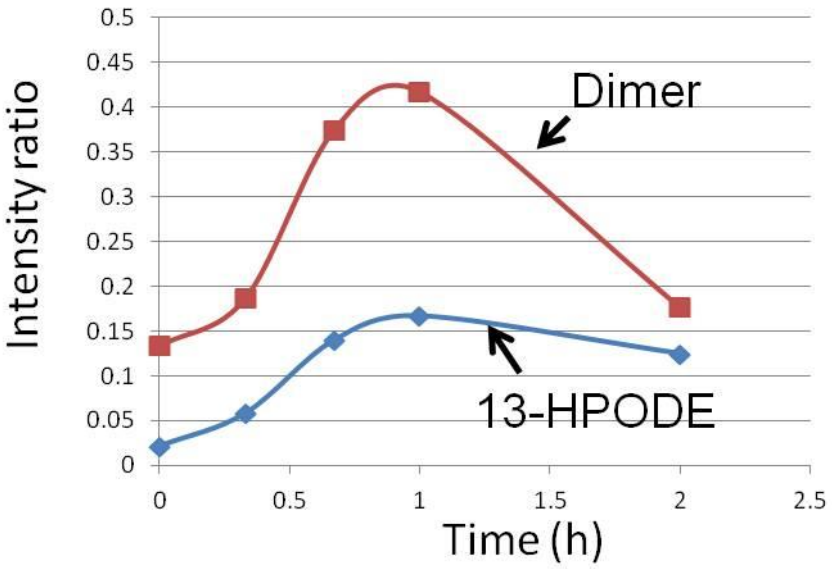

Figure 68: H(P)NE production from autoxidation of dimers and pure 13*S*-HPODE

Figure 68 demonstrates that the H(P)NE formation during autoxidation of both dimers and 13*S*-HPODE reach the highest amount at ~1 hr and diminished afterwards. Dimers have a higher amount of H(P)NE at the starting time point but do not show a significantly higher H(P)NE generation rate than that of 13*S*-HPODE during autoxidation.

To further test the role of dimers in H(P)NE formation during lipid autoxidation, assays using the diluted lipids were performed. These assays use the same protocol as what were performed in **Figure 68** except that the starting dimers and 13*S*-HPODE are mixed with an excess amount of oleic acid. The concept is that by being diluted with

excess other lipids, 13*S*-HPODE cannot generate dimers and thus cannot make H(P)NE if the dimers are the intermediate to H(P)NE. On the other hand, the H(P)NE formation initiated from dimers will not be affected by the dilution with oleate.

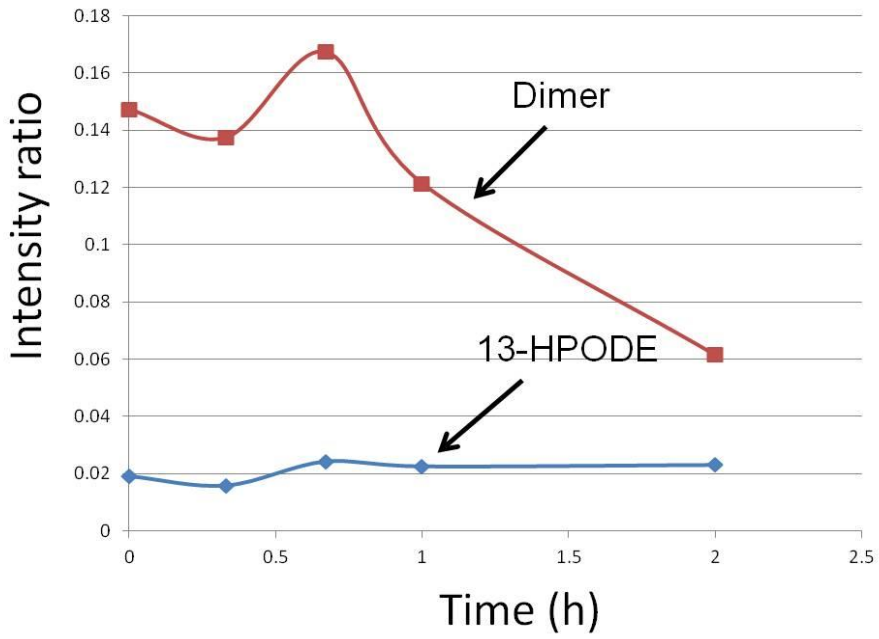

Figure 69: H(P)NE production from autoxidation of dimers and pure 13*S*-HPODE in the presence of excess oleic acid.

Figure 69 shows the time course of H(P)NE production from autoxidation of the dimers and the pure 13*S*-HPODE in the presence of excess oleic acid. Under these conditions the H(P)NE production from both starting substrates was inhibited.

HPNE distribution in LH20 column fractions

In **Figure 68 and 69**, the dimer samples started with a significantly higher amount of H(P)NE than the pure 13*S*-HPODE (0.15 versus 0.02, mass spectrometry peak area ratios of H(P)NE over d3-HNE). In **Figure 66** it was shown that the dimer fractions collected from LH20 column separation consist of a series of compounds with similar

structures. To explain the higher starting HPNE detection in the dimer samples as well as the autoxidation results that the dimers do not show a higher HPNE generation capacity than monomer, I propose that the "unstable" dimers degrade to HPNE during the LH20 column separation, while the left-over dimers degrade to monomers during autoxidation, thus showing the same HPNE generation ability as that of monomer. To test this, the concentration of HPNE was determined in the LH20 fractions collected across the dimer and monomer peaks from the 13*S*-HPODE autoxidation (**Figure 70**).

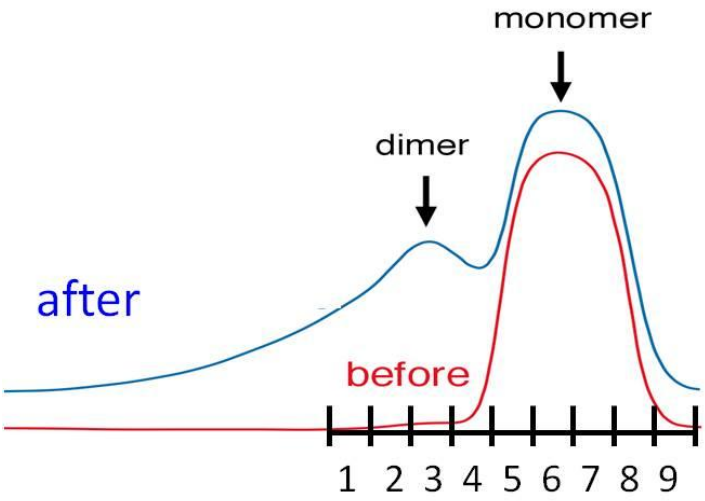

BLUE: UV220nm of HPNE
RED: UV270nm of 13-HPODE

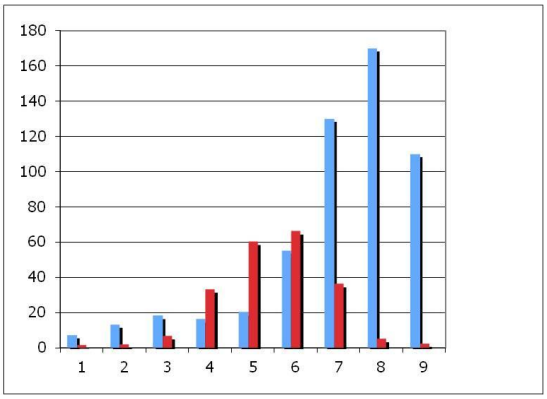

Figure 70: HPNE and 13*S*-HPODE distribution on LH20 column

The dimer and monomer-eluting region on the LH20 column was divided into 9 fractions. Each fraction was injected on HPLC to determine the amounts of HPNE and 13*S*-HPODE. 13*S*-HPODE (monomer) exhibited a symmetrical distribution with the peak center between fractions 5 and 6. The HPNE peak center was located at fraction 8. However, there is a significant increase in HPNE detection in fractions 1, 2, 3 and 4 which correspond to the dimer-eluting region of the chromatogram. This distribution of HPNE with a higher abundance in the dimer fractions provides strong evidence that during the LH20 column separation the "unstable" dimers degrade to HPNE.

In summary, in this part a method of quantitatively analyzing HNE production has been developed. The hypothesis that during lipid peroxidation dimeric peroxides are formed and serve as the intermediate to H(P)NE production was tested. My data showed that dimer fractions from LH20 column do not show a significantly higher H(P)NE generation rate than that of the fatty acid hydroperoxide monomer during autoxidation. However, further analyses on HPNE distribution in the dimer fractions of LH20 column led to another hypothesis that there exist two types of dimers, "stable" and "unstable" dimers, and during the LH20 column separation the "unstable" dimers degrade to HPNE.

2. 15-lipoxygenase as a 5,6-LTA_4 synthase

15-LOX was first demonstrated to have a 5,6-LTA_4 synthase activity by the Dr. Robert C. Murphy laboratory. They showed that inhibition of cytosolic 5-lipoxygenase from human blood granulocytes inhibited the LTA_4 synthase activity by only 47%. Incubation of 5*S*-HPETE with the recombinant mammalian 15-LOX resulted in the formation of 6-*trans*-LTB_4 and 6-*trans*-12-*epi*-LTB_4, the LTA_4 non-enzymatic hydrolysis products. They proposed that the formation of LTA_4 by 15-LOX involves removing the pro-*R* hydrogen atom at C10 of 5*S*-HPETE which is antarafacial to the hydroperoxy group (120).

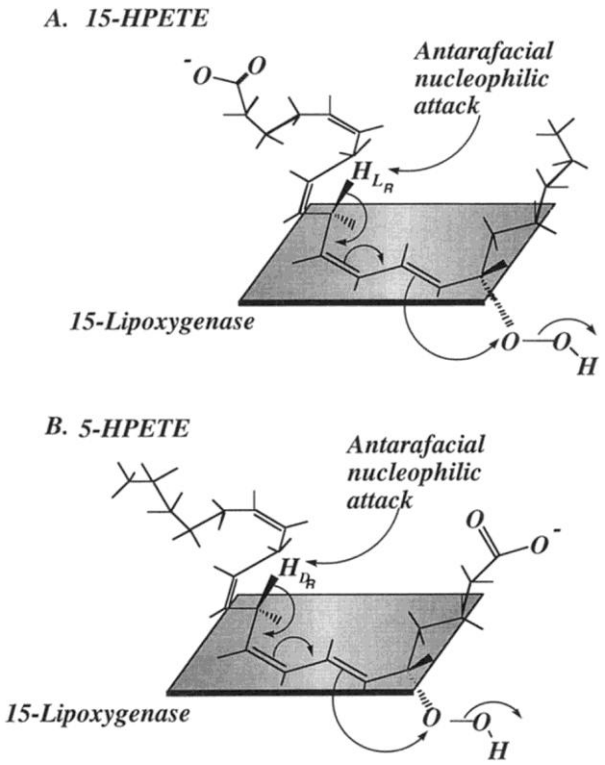

Figure 71: LTA synthase activity of 15-LOX proposed by R. C. Murphy. (A) 14,15-LTA_4 formation. (B) 5,6-LTA_4 formation.
This figure was originally published in Journal of Biological Chemistry. MacMillan et al. Eosinophil 15-lipoxygenase is a leukotriene A_4 synthase. J. Biol. Chem.. 1994; 269:26663-8. © the American Society for Biochemistry and Molecular Biology.

The mechanisms presented in **Figure 71** differ from our proposed mechanisms of LTA epoxide formation (Chapter 3). In **Figure 71A**, 15*S*-HPETE binds to 15-LOX with the abstracted 10L hydrogen antarafacial to the 15*S*-hydroperoxide. The carbon chain at C13-16 thus adopts a *cis* conformation, which should lead to formation of a *cis*-epoxide product. By contrast, our proposal invokes a suprafacial relationship of the abstracted hydrogen and hydroperoxide moieties, correctly predicting *trans*-epoxy 14,15-LTA_4 as product (**Figure 12**). In **Figure 71B**, 5*S*-HPETE is drawn to bind the enzyme in the reversed orientation and the above argument applies to the antarafacial relationship of the 10D hydrogen abstraction and 5*S*-hydroperoxide. The predicted outcome gives *cis*-LTA_4 as product, whereas LTA_4 is a *trans*-epoxide (**Figure 29**).

Our proposed mechanisms of LTA epoxide formation predict the reactions of 5-HPETE with 12/15-LOX to proceed as follows:

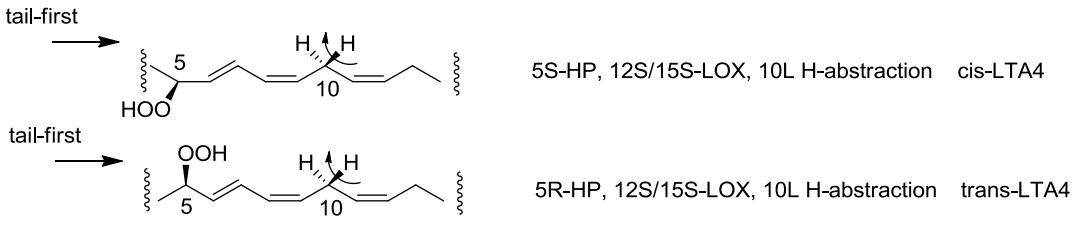

As illustrated, the suprafacial relationship of the hydrogen abstraction and the hydroperoxide moiety leads to the conclusion that 12/15-LOX will convert 5*S*-HPETE to *cis*-LTA_4 (top) and the enantiomeric 5*R*-HPETE to (5*R*) *trans*-LTA_4 (below). This prediction is not incompatible with the earlier experimental results, which based the synthesis of LTA epoxide on detection of the characteristic products of LTA-type

epoxide hydrolysis. *cis*-LTA_4 is hydrolyzed to the same major 5,12-dihydroxy products as *trans*-LTA_4 (58).

Using the biphasic synthesis and simultaneous extraction methods developed in Chapter 2, I was able to directly analyze the LTA epoxide products from the reactions of the enantiomeric 5-HPETEs with human 15-LOX-1. The optimal pH for the recombinant human 15-LOX-1 activity is ~7.5. Here I lowered the aqueous phase pH to 6.5 based on two concepts: (1) the ionic form of the carboxyl group would hurt the stability of the LTA type epoxides especially 5,6-LTA_4; (2) acidic pH would help the back extraction of the LTA epoxide products to the organic phase. Another problem with 5-HPETE, which was also met in Chapter 3, is the lactone formation after it is stored in alcohol solvents for a period of time. To avoid the lactone formation, purified enantiomeric 5-HPETEs are stored in acetonitrile before further usage.

A

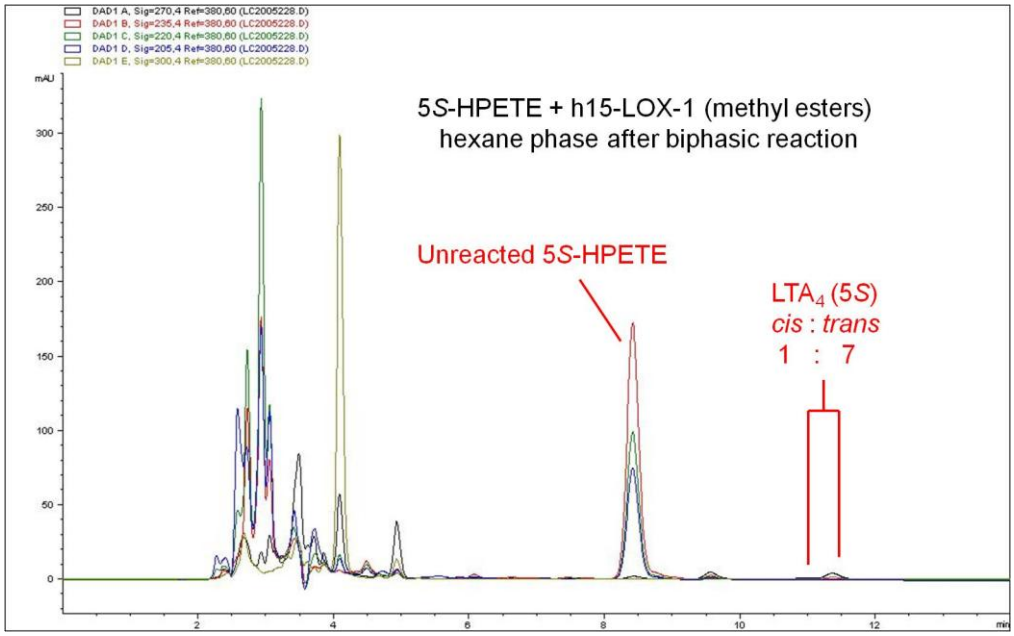

B

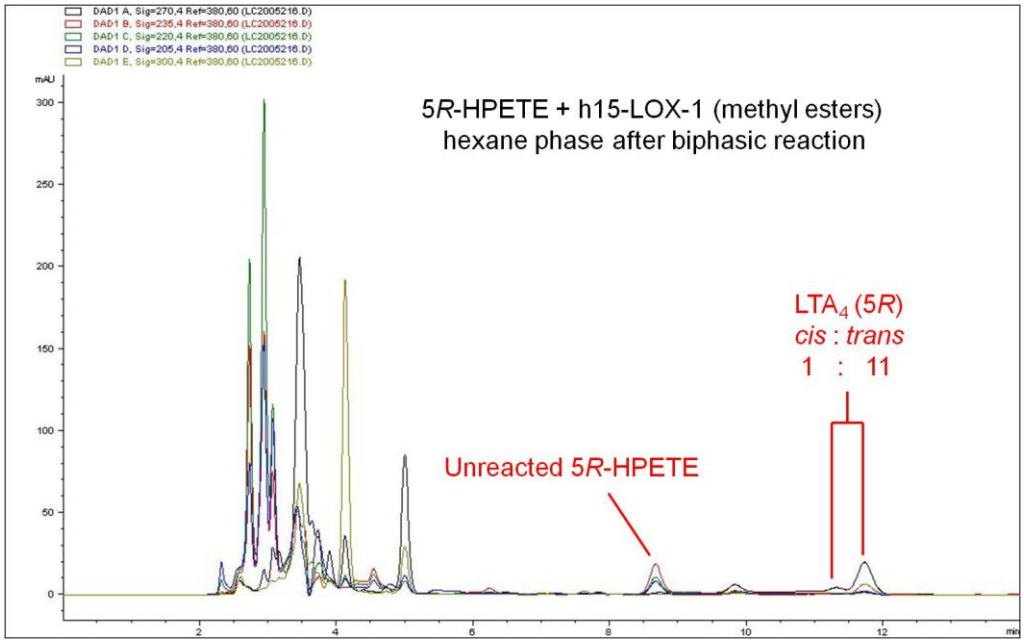

Figure 72: RP-HPLC analyses of the organic phase of biphasic reactions of enantiomeric 5-HPETEs with human 15-LOX-1. **A**, 5*S*-HPETE; **B**, 5*R*-HPETE.

The composition of LTA products (*cis*/*trans*-LTA ratio) is analyzed by comparing the areas underneath individual LTA product peaks on RP-HPLC (**Figure 72**). With human 15-LOX-1 as catalyst, by comparison with the authentic standards 5*S*-HPETE generated *cis*- and *trans*- LTA_4 in a ratio of 1:7 (**Figure 72A**) and 5*R*-HPETE generated *cis*- and *trans*-LTA_4 (5*R*) in a ratio of 1:11 (**Figure 72B**). Based on our proposed LTA formation mechanisms, 5*S*-HPETE metabolism by 15-lipoxygenase is predicted to generate *cis*-LTA_4 and 5*R*- to generate *trans*-LTA_4 (5*R*). The former is out of line with our hypothesis. The inconsistency in the case of 5*S*-HPETE metabolism may be due to the following two reasons: (1) The recovery of LTA_4 was low in these experiments (especially from 5*S*-HPETE). The low yield may indicate that the enzymatic control of LTA formation in these reactions is poor and the product pattern might be modified by the non-enzymatic synthesis (2) Secondly, the LTA_4 epoxides are converted by human 15-LOX-1 to lipoxin-like products (which are not extracted into the hexane phase), and the relative efficiency of conversion of *cis*- and *trans*-LTA_4 is unknown. It is possible that a higher conversion of *cis*-LTA results in its lower detection.

CHAPTER VIII

SUMMARY

Around 1980, the structural elucidation of LTB_4 and LTC_4 and an appreciation of their biosynthesis through the epoxide LTA_4 established the importance of this pathway of arachidonic acid metabolism in inflammation research. The relationship between the leukotriene formation and the lipoxygenase catalysis was then established when it was appreciated that 5-lipoxygenase (5-LOX) catalyzes not only the conversion of arachidonic acid to 5*S*-HPETE but also the further transformation to the pivotal epoxide in the pathway, LTA_4.

Our understanding of lipoxygenase biochemistry took a great leap in the ensuing years, yet the mechanistic basis of the LOX-catalyzed LTA epoxide synthesis has not been completely understood. Currently there is no proper understanding of the relationships between the fatty acid hydroperoxide structure and the LTA epoxide produced, no understanding of why some LOX enzymes form an LTA epoxide, others not, and very little experimental basis for understanding the metabolism of these unstable intermediates. My Ph.D. projects aim to clarify these issues and put the synthesis of leukotriene-related products on a more solid conceptual foundation.

The first breakthrough in my Ph.D. study is the successful development of methods for the biosynthesis, isolation and NMR structural analysis of the LTA-type epoxides. The elegant “biphasic synthesis and simultaneous extraction” system allows the LTA product, once formed, instantly extracted out of the aqueous phase, therefore getting

protected against hydrolysis. By applying the methods first on the reaction of 15*S*-HPETE with human 15-LOX-1, 14,15-LTA_4, the proposed intermediate to the pro-inflammatory eoxin family, was isolated in the amount sufficient for NMR analysis. This is the first time the LTA-type intermediate was isolated and subjected to a structural analysis directly from a lipoxygenase reaction.

Critical to my Ph.D. projects is a paper of E. J. Corey's group published in Journal of the American Chemical Society in 1989. They used two different sources of LOX enzyme to demonstrate (1) the existence of a *cis*-LTA epoxide from a biological source and (2) a relationship between the hydrogen abstraction from 5*S*-HPETE and the configuration of the resulting LTA epoxide. We proposed to follow up and extend Corey's work on LTA epoxide biosynthesis and hypothesized a mechanism illustrating the relationships between the fatty acid hydroperoxide structure, the lipoxygenase catalyst and the LTA epoxide produced. Central to our hypothesis is that transformation of the fatty acid hydroperoxide to LTA epoxide depends on participation of the lipoxygenase non-heme iron in catalyzing both the initial hydrogen abstraction and in facilitating cleavage of the hydroperoxide moiety.

In order to test our hypothesis, the biphasic reaction system was applied on reactions of different combinations of the fatty acid hydroperoxide substrates and the lipoxygenase enzymes. It was successfully demonstrated that the enantiomeric 5-HPETEs, when reacting with *Arabidopsis* LOX1, are transformed separately to the LTA product with either *trans*- or *cis*-epoxy. The results are consistent with what our hypothesis predicts, thus providing strong experimental support.

The establishment of mechanistic basis of the classical leukotriene pathway is also directly relevant to the understanding of related transformations that are biochemically less well defined, namely biosynthesis of the resolvin, (neuro)protectin and maresin anti-inflammatory mediators, all of which are derived from omega-3 fatty acids. By applying the biphasic reaction system on the omega-3 fatty acid metabolism, two LTA-type epoxides in the omega-3 fatty acid pathways, 16,17-LTA_6 from DHA and 14,15-LTA_5 from EPA, were isolated and analyzed structurally. Further *in vitro* metabolism using recombinant LOX enzymes and *ex vivo* metabolism using cells helped to substantiate the enzymatic basis of these novel pathways.

Another research focus of my Ph.D. study is the mechanistic origin of HNE and the related 4-hydroxy-alkenals, i.e. the mechanism of the carbon chain cleavage reaction leading to the aldehyde fragment. The carbon chain cleavage is not a chemically facile step and needs to be promoted by extra activation. Multiple mechanistic proposals have appeared over the years to account for this activation, two of which were tested in my Ph.D. study. One of the very first projects after I joined the Brash lab was to test the intermediate role of the dimeric peroxides in HNE formation during lipid peroxidation. The formation of dimeric peroxides were demonstrated by different analytical approaches and preliminary experimental data support there exist two types of dimers, "stable" and "unstable" dimers, and the "unstable" dimers degrade to HPNE. A more complete and rigorous investigation was conducted on the bis-allylic dihydroperoxide pathway. Through a series of unequivocal chemical studies, I demonstrated the HNE-related aldehyde formation via lipoxygenase-catalyzed synthesis of a bis-allylic dihydroperoxide intermediate. The transformation was first discovered in the coral 8*R*-LOX reaction and

then extended to the reactions with mouse platelet-type 12*S*-LOX, and human 15-LOX-1, indicating its possible application in different species.

In sum, in my Ph.D. study I investigated lipoxygenase reactions catalyzing the transformations from polyunsaturated fatty acids to their various types of primary and secondary oxidation products. The unique and precise control of the lipoxygenase enzymes ensures the production of biological important lipids with their specific structures and stereochemistry.

REFERENCES

1. Brash, A. R. (1999) *J. Biol. Chem.* **274**, 23679-23682

2. Grechkin, A. N. (1998) *Prog. Lipid Res.* **37**, 317-352

3. Samuelsson, B., Dahlen, S. E., Lindgren, J. A., Rouzer, C. A., and Serhan, C. N. (1987) *Science* **237**, 1171-1176

4. Funk, C. D. (2001) *Science* **294**, 1871-1875

5. Smith, W. L., and Lands, W. E. (1972) *J. Biol. Chem.* **247**, 1038-1047

6. Schilstra, M. J., Veldink, G. A., Verhagen, J., and Vliegenthart, J. F. G. (1992) *Biochemistry* **31**, 7692-7799

7. Solomon, E. I., Brunold, T. C., Davis, M. I., Kemsley, J. N., Lee, S. K., Lehnert, N., Neese, F., Skulan, A. J., Yang, Y. S., and Zhou, J. (2000) *Chem. Rev.* **100**, 235-350

8. Schneider, C., Pratt, D. A., Porter, N. A., and Brash, A. R. (2007) *Chem. Biol.* **14**, 473-488

9. Egmond, M. R., Vliegenthart, J. F. G., and Boldingh, J. (1972) *Biochem. Biophys. Res. Commun.* **48**, 1055-1060

10. Bryant, R. W., Bailey, J. M., Schewe, T., and Rapoport, S. M. (1982) *J. Biol. Chem.* **257**, 6050-6055

11. Saam, J., Ivanov, I., Walther, M., Holzhutter, H. G., and Kuhn, H. (2007) *Proc. Natl. Acad. Sci. USA* **104**, 13319-13324

12. Knapp, M. J., Seebeck, F. P., and Klinman, J. P. (2001) *J. Am. Chem. Soc.* **123**, 2931-2932

13. Zheng, Y., and Brash, A. R. (2010) *J. Biol. Chem.* **285**, 39876-39887

14. Yu, Z., Schneider, C., Boeglin, W. E., Marnett, L. J., and Brash, A. R. (2003) *Proc. Natl. Acad. Sci. USA* **100**, 9162-9167

15. Yu, Z., Schneider, C., Boeglin, W. E., and Brash, A. R. (2007) *Lipids* **42**, 491-497

16. Newman, J. W., Morisseau, C., and Hammock, B. D. (2005) *Prog. Lipid Res.* **44**, 1-51

17. Samuelsson, B. (1997) *Adv. Exp. Med. Biol.* **433**, 1-7

18. Serhan, C. N. (1997) *Prostaglandins* **53**, 107-137

19. Wurzenberger, M., and Grosch, W. (1984) *Biochim. Biophys. Acta* **794**, 18-24

20. Wurzenberger, M., and Grosch, W. (1984) *Biochim. Biophys. Acta* **794**, 25-30

21. Glasgow, W. C., Harris, T. M., and Brash, A. R. (1986) *J. Biol. Chem.* **261**, 200-204

22. Serhan, C. N., Hamberg, M., and Samuelsson, B. (1984) *Proc. Natl. Acad. Sci. USA* **81**, 5335-5339

23. Powell, W. S., Gravelle, F., and Gravel, S. (1992) *J. Biol. Chem.* **267**, 19233-19241

24. Powell, W. S., Gravel, S., Halwani, F., Hii, C. S., Huang, Z. H., Tan, A. M., and Ferrante, A. (1997) *J. Immunol.* **159**, 2952-2959

25. Groeger, A. L., Cipollina, C., Cole, M. P., Woodcock, S. R., Bonacci, G., Rudolph, T. K., Rudolph, V., Freeman, B. A., and Schopfer, F. J. (2010) *Nat. Chem. Biol.* **6**, 433-441

26. Jacobs, A. T., and Marnett, L. J. (2010) *Acc. Chem. Res.* **43**, 673-683

27. Zheng, Y., and Brash, A. R. (2010) *J. Biol. Chem.* **285**, 39866-39875

28. Ivanov, I., Saam, J., Kuhn, H., and Holzhutter, H. G. (2005) *FEBS J.* **272**, 2523-2535

29. Veldink, G. A., Vliegenthart, J. F. G., and Boldingh, J. (1970) *Biochim. Biophys. Acta*, 198-199

30. Zheng, Y., and Brash, A. R. (2010) *J. Biol. Chem.* **285**, 13427-13436

31. Samuelsson, B. (1983) *Biosci. Rep.* **3**, 791-813

32. Samuelsson, B. (1983) *Science* **220**, 568-575

33. Borgeat, P., Hamberg, M., and Samuelsson, B. (1976) *J. Biol. Chem.* **251**, 7816-7820

34. Borgeat, P., and Samuelsson, B. (1979) *J. Biol. Chem.* **254**, 2643-2646

35. Borgeat, P., and Samuelsson, B. (1979) *J. Biol. Chem.* **254**, 7865-7869

36. Borgeat, P., and Samuelsson, B. (1979) *Proc. Natl. Acad. Sci. USA* **76**, 2148-2152

37. Dahlen, S. E., Bjork, J., Hedqvist, P., Arfors, K. E., Hammarstrom, S., Lindgren, J. A., and Samuelsson, B. (1981) *Proc. Natl. Acad. Sci. USA* **78**, 3887-3891

38. Murphy, R. C., Hammarstrom, S., and Samuelsson, B. (1979) *Proc. Natl. Acad. Sci. USA* **76**, 4275-4279

39. Hammarstrom, S., Murphy, R. C., Samuelsson, B., Clark, D. A., Mioskowski, C., and Corey, E. J. (1979) *Biochem. Biophys. Res. Commun.* **91**, 1266-1272

40. Rådmark, O., Malmsten, C., Samuelsson, B., Clark, D. A., Goto, G., Marfat, A., and Corey, E. J. (1980) *Biochem. Biophys. Res. Commun.* **92**, 954-961

41. Lewis, R. A., Austen, K. F., Drazen, J. M., Clark, D. A., Marfat, A., and Corey, E. J. (1980) *Proc. Natl. Acad. Sci. USA* **77**, 3710-3714

42. Borgeat, P., and Samuelsson, B. (1979) *Proc. Natl. Acad. Sci. USA* **76**, 3213-3217

43. Fitzpatrick, F. A., Morton, D. R., and Wynalda, M. A. (1982) *J. Biol. Chem.* **257**, 4680-4683

44. Radmark, O., Malmsten, C., Samuelsson, B., Goto, G., Marfat, A., and Corey, E. J. (1980) *J. Biol. Chem.* **255**, 11828-11831

45. Marfat, A., and Corey, E. J. (1985) *Adv. Prostaglandin Thromboxane Leukot. Res.* **14**, 155-228

46. Rokach, J., and Adams, J. (1985) *Accounts Chem. Res.* **18**, 87-93

47. Maas, R. L., and Brash, A. R. (1983) *Proc. Natl. Acad. Sci. USA* **80**, 2884-2888

48. Shimizu, T., Rådmark, O., and Samuelsson, B. (1984) *Proc. Natl. Acad. Sci. USA* **81**, 689-693

49. Maas, R. L., Ingram, C. D., Taber, D. F., Oates, J. A., and Brash, A. R. (1982) *J. Biol. Chem.* **257**, 13515-13519

50. Hamberg, M., and Hamberg, G. (1980) *Biochem. Biophys. Res. Commun.* **95**, 1090-1097

51. Rouzer, C. A., Matsumoto, T., and Samuelsson, B. (1986) *Proc. Natl. Acad. Sci. USA* **83**, 857-861

52. Shimizu, T., Izumi, T., Seyama, Y., Tadokoro, K., Radmark, O., and Samuelsson, B. (1986) *Proc. Natl. Acad. Sci. USA* **83**, 4175-4179

53. Rouzer, C. A., Rands, E., Kargman, S., Jones, R. E., Register, R. B., and Dixon, R. A. (1988) *J. Biol. Chem.* **263**, 10135-10140

54. Maas, R. L., Brash, A. R., and Oates, J. A. (1981) *Proc. Natl. Acad. Sci. USA* **78**, 5523-5527

55. Bryant, R. W., Schewe, T., Rapoport, S. M., and Bailey, J. M. (1985) *J. Biol. Chem.* **260**, 3548-3555

56. Feltenmark, S., Gautam, N., Brunnstrom, A., Griffiths, W., Backman, L., Edenius, C., Lindbom, L., Bjorkholm, M., and Claesson, H. E. (2008) *Proc. Natl. Acad. Sci. USA* **105**, 680-685

57. Sachs-Olsen, C., Sanak, M., Lang, A. M., Gielicz, A., Mowinckel, P., Lodrup Carlsen, K. C., Carlsen, K. H., and Szczeklik, A. (2010) *J. Allergy Clin. Immunol.* **126**, 859-867 e859

58. Corey, E. J., Wright, S. W., and Matsuda, S. P. T. (1989) *J. Am. Chem. Soc.* **111**, 1452-1455

59. Bundy, G. L., Nidy, E. G., Epps, D. E., Mizsak, S. A., and Wnuk, R. J. (1986) *J. Biol. Chem.* **261**, 747-751

60. Brash, A. R., Boeglin, W. E., Chang, M. S., and Shieh, B.-H. (1996) *J. Biol. Chem.* **271**, 20949-20957

61. Boutaud, O., and Brash, A. R. (1999) *J. Biol. Chem.* **274**, 33764-33770

62. Hamberg, M. (1983) *Biochim. Biophys. Acta* **752**, 353-356

63. Hamberg, M. (1983) *Biochim. Biophys. Acta* **752**, 191-197

64. Sok, D. E., Chung, T., and Sih, C. J. (1983) *Biochem. Biophys. Res. Commun.* **110**, 273-279

65. Ueda, N., Yamamoto, S., Oates, J. A., and Brash, A. R. (1986) *Prostaglandins* **32**, 43-48

66. Panossian, A., Hamberg, M., and Samuelsson, B. (1982) *FEBS Lett.* **150**, 511-513

67. Kemal, C., Louis-Flamberg, P., Krupinski-Olsen, R., and Shorter, A. L. (1987) *Biochemistry* **26**, 7064-7072

68. Majno, G., and Joris, I. (2004) *Cells, tissues, and disease : principles of general pathology*, 2nd ed., Oxford University Press, New York

69. Serhan, C. N., Chiang, N., and Van Dyke, T. E. (2008) *Nat. Rev. Immunol.* **8**, 349-361

70. Serhan, C. N. (2011) *FASEB J.* **25**, 1441-1448

71. Serhan, C. N. (2010) *Am. J. Pathol.* **177**, 1576-1591

72. Yokomizo, T., Izumi, T., Chang, K., Takuwa, Y., and Shimizu, T. (1997) *Nature* **387**, 620-624

73. Fiore, S., Maddox, J. F., Perez, H. D., and Serhan, C. N. (1994) *J. Exp. Med.* **180**, 253-260

74. Chiang, N., Serhan, C. N., Dahlen, S. E., Drazen, J. M., Hay, D. W., Rovati, G. E., Shimizu, T., Yokomizo, T., and Brink, C. (2006) *Pharmacol. Rev.* **58**, 463-487

75. Arita, M., Bianchini, F., Aliberti, J., Sher, A., Chiang, N., Hong, S., Yang, R., Petasis, N. A., and Serhan, C. N. (2005) *J. Exp. Med.* **201**, 713-722

76. Arita, M., Ohira, T., Sun, Y. P., Elangovan, S., Chiang, N., and Serhan, C. N. (2007) *J. Immunol.* **178**, 3912-3917

77. Serhan, C. N., Hong, S., Gronert, K., Colgan, S. P., Devchand, P. R., Mirick, G., and Moussignac, R. L. (2002) *J. Exp. Med.* **196**, 1025-1037

78. Mukherjee, P. K., Marcheselli, V. L., Serhan, C. N., and Bazan, N. G. (2004) *Proc. Natl. Acad. Sci. USA* **101**, 8491-8496

79. Serhan, C. N., Yang, R., Martinod, K., Kasuga, K., Pillai, P. S., Porter, T. F., Oh, S. F., and Spite, M. (2009) *J. Exp. Med.* **206**, 15-23

80. Neuringer, M., Anderson, G. J., and Connor, W. E. (1988) *Annu. Rev. Nutr.* **8**, 517-541

81. Oldham, M. L., Brash, A. R., and Newcomer, M. E. (2005) *J. Biol. Chem.* **39**, 39545-39552

82. Brash, A. R., Baertschi, S. W., Ingram, C. D., and Harris, T. M. (1988) *Proc. Natl. Acad. Sci. USA* **85**, 3382-3386

83. Gao, B., Boeglin, W. E., Zheng, Y., Schneider, C., and Brash, A. R. (2009) *J. Biol. Chem.* **284**, 22087-22098

84. Schneider, C., Niisuke, K., Boeglin, W. E., Voehler, M., Stec, D. F., Porter, N. A., and Brash, A. R. (2007) *Proc. Natl. Acad. Sci. USA* **104**, 18941-18945

85. Niisuke, K., Boeglin, W. E., Murray, J. J., Schneider, C., and Brash, A. R. (2009) *J. Lipid Res.* **50**, 1448-1455

86. Schewe, T., Halangk, W., Hiebsch, C., and Rapoport, S. M. (1975) *FEBS Lett.* **60**, 149-153

87. Sigal, E., Craik, C. S., Highland, E., Grunberger, D., Costello, L. L., Dixon, R. A. F., and Nadel, J. A. (1988) *Biochem. Biophys. Res. Commun.* **157**, 457-464

88. Chen, X.-S., Kurre, U., Jenkins, N. A., Copeland, N. G., and Funk, C. D. (1994) *J. Biol. Chem.* **269**, 13979-13987

89. Brash, A. R., Boeglin, W. E., and Chang, M. S. (1997) *Proc. Natl. Acad. Sci. USA* **94**, 6148-6152

90. Brash, A. R., Jisaka, M., Boeglin, W. E., and Chang, M. S. (1997) Molecular cloning of a second human 15*S*-lipoxygenase and its murine homologue, an 8*S*-lipoxygenase: Their relationship to other mammalian lipoxygenases. in *Lipoxygenases and their products: biological functions* (Pace-Asciak, C. R., and Nigam, S. eds.), Plenum Press, New York. pp 29-36

91. Maas, R. L., Ingram, C. D., Porter, A. T., Oates, J. A., Taber, D. F., and Brash, A. R. (1985) *J. Biol. Chem.* **260**, 4217-4228

92. Newcomer, M. E., and Gilbert, N. C. (2010) *J. Biol. Chem.* **285**, 25109-25114

93. Tang, Z., Martin, M. V., and Guengerich, F. P. (2009) *Anal. Chem.* **81**, 3071-3078

94. Zheng, Y., Yin, H., Boeglin, W. E., Elias, P. M., Crumrine, D., Beier, D. R., and Brash, A. R. (2011) *J. Biol. Chem.* **286**, 24046-24056

95. Bild, G. S., Ramadoss, C. S., and Axelrod, B. (1977) *Lipids* **12**, 732-735

96. Glickman, M. H., and Klinman, J. P. (1995) *Biochemistry* **34**, 14077-14092

97. Gilbert, N. C., Bartlett, S. G., Waight, M. T., Neau, D. B., Boeglin, W. E., Brash, A. R., and Newcomer, M. E. (2011) *Science* **331**, 217-219

98. Radmark, O., and Samuelsson, B. (2010) *Biochem. Biophys. Res. Commun.* **396**, 105-110

99. Chen, X., Reddanna, P., Reddy, G. R., Kidd, R., Hildenbrandt, G., and Reddy, C. C. (1998) *Biochem. Biophys. Res. Commun.* **243**, 438-443

100. Boeglin, W. E., Itoh, A., Zheng, Y., Coffa, G., Howe, G. A., and Brash, A. R. (2008) *Lipids* **43**, 979-987

101. Corey, E. J., and Lansbury, P. T., Jr. (1983) *J. Am. Chem. Soc.* **105**, 4093-4094

102. Brash, A. R., Baertschi, S. W., Ingram, C. D., and Harris, T. M. (1987) *J. Biol. Chem.* **262**, 15829-15839

103. Boeglin, W. E., Kim, R. B., and Brash, A. R. (1998) *Proc. Natl. Acad. Sci. USA* **95**, 6744-6749

104. Coffa, G., Schneider, C., and Brash, A. R. (2005) *Biochem. Biophys. Res. Commun.* **338**, 87-92

105. Van Os, C. P. A., Rijke-Schilder, G. P. M., Van Halbeek, H., Verhagen, J., and Vliegenthart, J. F. G. (1981) *Biochim. Biophys. Acta.* **663**, 177-193

106. Boyington, J. C., Gaffney, B. J., and Amzel, L. M. (1993) *Science* **260**, 1482-1486

107. Boyington, J. C., Gaffney, B. J., and Amzel, L. M. (1993) *Biochem. Soc. Trans.* **21 (Pt 3)**, 744-748

108. Coffa, G., Imber, A. N., Maguire, B. C., Laxmikanthan, G., Schneider, C., Gaffney, B. J., and Brash, A. R. (2005) *J. Biol. Chem.* **280**, 38756-38766

109. Peers, K. E., and Coxon, D. T. (1983) *Chem. Phys. Lipids* **32**, 49-56

110. Schneider, C., Yu, Z., Boeglin, W. E., Zheng, Y., and Brash, A. R. (2007) *Methods Enzymol.* **433**, 145-157

111. Tavazzi, L., Maggioni, A. P., Marchioli, R., Barlera, S., Franzosi, M. G., Latini, R., Lucci, D., Nicolosi, G. L., Porcu, M., and Tognoni, G. (2008) *Lancet* **372**, 1223-1230

112. Rizos, E. C., Ntzani, E. E., Bika, E., Kostapanos, M. S., and Elisaf, M. S. (2012) *JAMA : the journal of the American Medical Association* **308**, 1024-1033

113. Serhan, C. N., Clish, C. B., Brannon, J., Colgan, S. P., Chiang, N., and Gronert, K. (2000) *J. Exp. Med.* **192**, 1197-1204

114. Tjonahen, E., Oh, S. F., Siegelman, J., Elangovan, S., Percarpio, K. B., Hong, S., Arita, M., and Serhan, C. N. (2006) *Chem. Biol.* **13**, 1193-1202

115. Oh, S. F., Pillai, P. S., Recchiuti, A., Yang, R., and Serhan, C. N. (2011) *J. Clin. Invest.* **121**, 569-581

116. Hong, S., Gronert, K., Devchand, P. R., Moussignac, R. L., and Serhan, C. N. (2003) *J. Biol. Chem.* **278**, 14677-14687

117. Butovich, I. A., Lukyanova, S. M., and Bachmann, C. (2006) *J. Lipid Res.* **47**, 2462-2474

118. Kuhn, H., and O'Donnell, V. B. (2006) *Prog. Lipid Res.* **45**, 334-356

119. Nadel, J. A., Conrad, D. J., Ueki, I. F., Schuster, A., and Sigal, E. (1991) *J. Clin. Invest.* **87**, 1139-1145

120. MacMillan, D. K., Hill, E., Sala, A., Sigal, E., Shuman, T., Henson, P. M., and Murphy, R. C. (1994) *J. Biol. Chem.* **269**, 26663-26668

121. Kuhn, H., Walther, M., and Kuban, R. J. (2002) *Prostaglandins Other. Lipid Mediat.* **68-69**, 263-290

122. Conrad, D. J., Kühn, H., Mulkins, M., Highland, E., and Sigal, E. (1992) *Proc. Natl. Acad. Sci. USA* **89**, 217-221

123. Heydeck, D., Thomas, L., Schnurr, K., Trebus, F., Thierfelder, W. E., Ihle, J. N., and Kuhn, H. (1998) *Blood* **92**, 2503-2510

124. Levy, B. D., Clish, C. B., Schmidt, B., Gronert, K., and Serhan, C. N. (2001) *Nat. Immunol.* **2**, 612-619

125. Weiner, T. W., and Sprecher, H. (1984) *Biochim. Biophys. Acta* **792**, 293-303

126. Hammarstrom, S. (1981) *Biochim. Biophys. Acta* **663**, 575-577

127. Lam, B. K., Hirai, A., Yoshida, S., Tamura, Y., and Wong, P. Y. (1987) *Biochim. Biophys. Acta* **917**, 398-405

128. Ferreri, C., Samadi, A., Sassatelli, F., Landi, L., and Chatgilialoglu, C. (2004) *J. Am. Chem. Soc.* **126**, 1063-1072

129. Zhang, X., Goncalves, R., and Mosser, D. M. (2008) *Curr. Protoc. Immunol.* **Chapter 14**, Unit 14 11

130. Dalli, J., Zhu, M., Vlasenko, N. A., Deng, B., Haeggstrom, J. Z., Petasis, N. A., and Serhan, C. N. (2013) *FASEB J.*

131. Weinheimer, A. J., and Spraggins, R. L. (1969) *Tetrahedron Lett.* **59**, 5185-5188

132. Valmsen, K., Järving, I., Boeglin, W. E., Varvas, K., Koljak, R., Pehk, T., Brash, A. R., and Samel, N. (2001) *Proc. Natl. Acad. Sci. USA* **98**, 7700-7705

133. Schneider, C., and Brash, A. R. (2002) *Prostaglandins Other Lipid Mediat.* **68-69**, 291-301

134. Brash, A. R., Baertschi, S. W., Ingram, C. D., and Harris, T. M. (1987) *J. Biol. Chem.* **262**, 15829-15839

135. Corey, E. J., Washburn, W. N., and Chen, J. C. (1973) *J. Am. Chem. Soc.* **95**, 2054-2055

136. Jin, J., Boeglin, W. E., Cha, J. K., and Brash, A. R. (2012) *J. Lipid Res.* **53**, 292-299

137. Song, W.-C., Baertschi, S. W., Boeglin, W. E., Harris, T. M., and Brash, A. R. (1993) *J. Biol. Chem.* **268**, 6293-6298

138. Lee, D. S., Nioche, P., Hamberg, M., and Raman, C. S. (2008) *Nature* **455**, 363-368

139. Esterbauer, H., Schaur, R. J., and Zollner, H. (1991) *Free Radic. Biol. Med.* **11**, 81-128

140. Lee, S. H., Oe, T., and Blair, I. A. (2001) *Science* **292**, 2083-2086

141. Sayre, L. M., Lin, D., Yuan, Q., Zhu, X., and Tang, X. (2006) *Drug Metab. Rev.* **38**, 651-675

142. Salomon, R. G., and Gu, X. (2011) *Chem. Res. Toxicol.* **24**, 1791-1802

143. Ullery, J. C., and Marnett, L. J. (2012) *Biochim. Biophys. Acta* **1818**, 2424-2435

144. Pryor, W. A., and Porter, N. A. (1990) *Free Radic. Biol. Med.* **8**, 541-543

145. Gu, X., and Salomon, R. G. (2012) *Free Radic. Biol. Med.* **52**, 601-606

146. Schneider, C., Porter, N. A., and Brash, A. R. (2008) *J. Biol. Chem.* **283**, 15539-15543

147. Liu, W., Porter, N. A., Schneider, C., Brash, A. R., and Yin, H. (2011) *Free Radic. Biol. Med.* **50**, 166-178

148. Griesser, M., Boeglin, W. E., Suzuki, T., and Schneider, C. (2009) *J. Lipid Res.* **50**, 2455-2462

149. Schneider, C., Tallman, K. A., Porter, N. A., and Brash, A. R. (2001) *J. Biol. Chem.* **276**, 20831-20838

150. Schneider, C., Porter, N. A., and Brash, A. R. (2004) *Chem. Res. Toxicol.* **17**, 937-941

151. Uchida, K. (2003) *Prog. Lipid Res.* **42**, 318-343

152. Jian, W., Lee, S. H., Arora, J. S., Silva Elipe, M. V., and Blair, I. A. (2005) *Chem. Res. Toxicol.* **18**, 599-610

153. Schneider, C., Boeglin, W. E., Yin, H., Stec, D. F., Hachey, D. L., Porter, N. A., and Brash, A. R. (2005) *Lipids* **40**, 1155-1162

154. Brash, A. R. (2000) *Lipids* **35**, 947-952

155. Hamberg, M., Gerwick, W. H., and Åsen, P. A. (1992) *Lipids* **27**, 487-493

156. Brash, A. R., Boeglin, W. E., Capdevila, J. H., Suresh, Y., and Blair, I. A. (1995) *Arch. Biochem. Biophys.* **321**, 485-492

157. Hamberg, M., Su, C., and Oliw, E. (1998) *J. Biol. Chem.* **273**, 13080-13088

158. Oliw, E. H., Cristea, M., and Hamberg, M. (2004) *Lipids* **39**, 319-323

159. Gardner, H. W. (1989) *Free Radical Biol. Med.* **7**, 65-86

160. Garssen, G. J., Vliegenthart, J. F. G., and Boldingh, J. (1971) *Biochem. J.* **122**, 327-332

161. Senger, T., Wichard, T., Kunze, S., Gobel, C., Lerchl, J., Pohnert, G., and Feussner, I. (2005) *J. Biol. Chem.* **280**, 7588-7596